Summer 2019

Periodic Orbit Analytic Construction In The Circular Restricted Three-Body Problem

Jay Shriram Suryawanshi
Old Dominion University

PERIODIC ORBIT ANALYTIC CONSTRUCTION IN THE CIRCULAR RESTRICTED THREE-BODY PROBLEM

by

Jay Shriram Suryawanshi
B. Tech. June 2013, College of Engineering Pune

A Thesis Submitted to the Faculty of
Old Dominion University in Partial Fulfillment of the
Requirements for the Degree of

MASTER OF SCIENCE

AEROSPACE ENGINEERING

OLD DOMINION UNIVERSITY
August 2019

Approved by:

Brett Newman (Director)

Colin Britcher (Member)

Gordon Melrose (Member)

ABSTRACT

PERIODIC ORBIT ANALYTIC CONSTRUCTION IN THE CIRCULAR RESTRICTED THREE-BODY PROBLEM

Jay Shriram Suryawanshi
Old Dominion University, 2019
Director: Dr. Brett Newman

This thesis investigates an approximate analytic construction of halo-type periodic orbits about the collinear equilibrium points in the circular restricted three-body problem. The research follows a parallel approach to the one used by Ghazy and Newman, but the initial assumptions and utilized functions are unique to this thesis. A suppositional base solution constructed using Jacobi elliptic functions and satisfying Jacobi's integral equation is at the core of the analytic construction framework. The locus of this solution is a circle lying in the plane perpendicular to the line joining the primaries. The base solution elicits a closed-form expression for the period in terms of the elliptic integral of the first kind and a frequency-like parameter. The base solution satisfies a combination of third body equations of motion in the y and z axes, and the equation of motion in the x axis is satisfied in an averaged and bounded sense when the vertical plane is located at one of the collinear Lagrange points.

Because the third body cannot traverse this type of path naturally, an analytic correction process is pursued to recover accuracy. An iterated perturbation process is used whereby corrections to the base solution along the axis connecting the primaries is considered first, followed by correction in the other two directions. The iterated approach is followed to exploit the coupling structure inherent in the three-body system to simplify calculations. Linear assumptions are also used in these calculations for simplifying reasons. The non-homogeneous solution excitations for

the x and y corrections are in the form of Fourier series expansions of the Jacobi elliptic functions in terms of the nome function. The development assumes the suppositional plane passes through one of the collinear Lagrange points. Only homogeneous correction is needed for the z axis. The modified solution then consists of the base solution plus first order corrections which can be further developed to include second and higher order corrections.

The base solution is compared with a L_1 halo orbit example and somewhat rough similarity is observed; the period of the base solution being approximately half of the true orbit. An interesting result is obtained when the truncated version of the correction forcing signal is compared with the exact one. When the frequency-like parameter is greater than or equal to unity, the full and truncated forcing signals become almost identical which justifies the use of the truncated forcing function for the L_1 halo orbit test case. The initial conditions for the true orbit are substituted in the truncated series solution and a new value of the frequency-like parameter is obtained using numerical computation depending in which axis is sought. For the test case, a unique value of the parameter is obtained from the y axis velocity initial conditions, which when employed in the x, y, and z solutions gives improved motion compared to the base one, and the corrected orbit reaches closer to the true orbit. The error in the period of this corrected orbit is reduced to zero when compared to the true orbit.

Dedicated to my parents Asha and Shriram Suryawanshi
and younger brother Vijay Suryawanshi.

ACKNOWLEDGMENTS

Many people have contributed to the successful completion of this thesis. My major advisor Dr. Brett Newman who has always guided me through this process deserves special recognition. I also extend many thanks to my committee members Dr. Colin Britcher and Dr. Gordon Melrose for their patience and hours of guidance on my research and editing of this manuscript. I express my gratitude to my father, Aba, for his constant support and encouragement.

TABLE OF CONTENTS

LIST OF TABLES

Table Page

LIST OF FIGURES

Figure Page

CHAPTER 1

INTRODUCTION

1.1 Problem Motivation

The three-body problem is a classic setting in celestial mechanics (natural bodies) and astrodynamics (artificial satellites) dealing with the motion of three bodies under their mutual gravitation. The objective of this problem is to predict positions and velocities of all three bodies at any given future time when their initial positions and velocities are provided. Examples include the combined motion of the Moon and Earth around the Sun, satellite motion in the vicinity of the Earth and Moon, or comet-asteroid motion in the Sun-Jupiter system. Although the three-body problem has been examined extensively over many decades,[1-3] the problem and its solution remain of high interest for scientific and engineering purposes.

Spacecraft for solar observation have been launched and placed around the L_1 point of the Sun-Earth system which lies about 1.5 million kilometers from the Earth. The International Sun-Earth Explorer 3 (ISEE 3) launched in 1978 and Solar and Heliocentric Observatory (SOHO) launched in 1995 are examples of such missions.[4,5] In 2001, to measure cosmic microwave background radiation, the Wilkinson Microwave Anisotropy Probe (WMAP) was launched aboard a Delta II rocket on a three month journey to the Sun-Earth Lagrange point L_2, which also lies 1.5 million kilometers from the Earth in the opposite direction from L_1.[6] The 6200 kg James Webb Space Telescope (JWST), which is the successor of the Hubble Space Telescope (HST), is scheduled to launch in 2018 aboard an Arianne 5 and will be flown to an orbit around L_2.[7] JSWT will use a 6.5 m mirror to gather data in the infrared spectrum over a period of 5-10 years. The advantage of such missions is that the spacecraft is placed in an almost stable periodic orbit around any of the collinear Lagrange points, so that a minimal amount of station-keeping is required, and less fuel is expended. In the case of JWST, another advantage is the L_2 region provides a better environment

for deep space observation due to reduced solar intensity and geo albedo. In studies related to exploring the far side of the Moon, Farquhar (1968-1970) found a family of three-dimensional almost periodic orbits around the equilibrium point L_2 in the Earth-Moon system: the translunar collinear libration point. A satellite or space station placed in this orbit has the advantage of continuous contact with both the far side of the Moon and the Earth. With control, this type of orbiting platform is never blocked from view by the Moon, hence the term "halo" was coined.[8]

Several particular analytic solutions to the three-body problem exist and include Lagrange's equilateral triangle solution and libration point solutions. However, the vast majority of situations involving time dependent orbits in two or three dimensions do not have analytic solutions. Obtaining closed-form periodic solutions, even in an approximate sense for particular cases, is of high importance for improved understanding of the evolving motion, orbit determination, maneuver planning, and communication tracking. Therefore, this thesis explores an approximate analytic construction for the three-body motion problem using Jacobi elliptic functions, which is inspired from Ghazy and Newman's [9] analytical theory for high inclination halo orbits, but with potential enhancement to the framework.

1.2 Literature Review

Reference 10 provides a thorough discussion of the general and restricted three-body problems, with historical and technical aspects. In the general problem, all three bodies are considered to have appreciable mass. In the restricted problem, one of the three bodies is treated with negligible mass in comparison with the other two bodies. Any review of the three-body problem literature must mention the Szebehely text.[3] This book gives a large database of knowledge on the three-body problem subject regarding formulation, reduction, regularization, transformation, equilibria,

disturbances, and periodicity, with many extensions and refinements to the assumptions and framework.

In 1778, Lagrange discovered the first special solution of the general three-body problem, the "equilateral triangle solution." He also developed the second and third special solutions denoted as the "straight line solution" and the "conic section solution," respectively. Lunar theory was studied in the eighteenth century by Euler using the restricted problem of three bodies where the Earth and Sun primaries are assumed to revolve in circular orbits around each other. The theory of the restricted three-body problem was further developed by Jacobi (1836) and reached its peak in the later nineteenth century with the work of Hill (1878) and Poincaré (1892–1899).[11]

For the general three-body problem, eighteen integrals of the motion are required to solve for the position coordinates in time, but only ten are known to exist.[11] Also, there are no known coordinate transformations which would simplify the general problem greatly. For this reason, much of the literature focuses on the restricted problem where one of the three masses is regarded as negligible in comparison with the other two primaries, which revolve in a circular orbit around each other. This problem becomes one of determining the motion of a single body after restricting the motion of the other two. Six integrals leading to algebraic relations are needed to solve the three second order scalar differential equations to obtain rectangular coordinates in time, but only one integral of the motion is known to exist. After introducing a rotating coordinate system moving with the primaries and reformulating the governing expressions, the problem is simplified and Jacobi's integral equation is derivable. Note this conversion to a rotating frame is a form of transformation on the problem variables. With this integral, particular solutions and concepts are facilitated like libration points, zero velocity curves, and the rectilinear oscillation solution.

Numerical solutions to the three-body governing relations are often considered in analysis. These solutions can be for periodic conditions or general transient orbits that do not repeat. The primary strength of numerical solutions is their high level of accuracy, but they can be more costly to construct, especially in real-time applications, and they often do not provide a means to better understand the dynamic characteristics of the motion. Analytically framed periodic and non-periodic solutions can complement numerical solutions by giving insights to qualitative and quantitative aspects of the motion of the third body.[3] For example, any relationship originating from an exact integral of the governing equations can be used to characterize boundaries on the motion or constraints between the dynamic variables. Pursuits of this type lie within the field of dynamical systems theory. To facilitate analytic computations, approximations in the form of series expansions are commonly employed. This approach can lead to complete solutions for the position and velocity components over time due to initial conditions by trading accuracy for solvability. These approaches lie in the field of system dynamics and control. Orbits in the neighborhood of approximate analytical solutions are of primary interest in this thesis.

Jacobi was the first to find an energy-like integral of the circular restricted problem, namely Jacobi's integral equation and the specific "energy" of the third body, which is a constant called Jacobi's constant. Jacobi's integral equation was used by Hill and Moulton to create zero velocity curves which are bounding curves that decide the permissible two-dimensional motion of the third body with a specific initial "energy" level (i.e., the Jacobi constant). Surfaces of zero velocity in three dimensions using numerical computation can be found in References 12 and 13. A special solution by MacMillan in Reference 14 is the rectilinear oscillation of the third body along a line passing through the system mass center and perpendicular to the plane of rotation of the primaries (i.e., xy plane), where primaries are of equal mass. In this problem, equations of motion in the x

and y axes are satisfied in a trivial manner while the z axis equation becomes the governing equation of motion, which can be solved using elliptic functions and the period is also obtained in closed-form. Another approach by Battin[10] to this solution is to start from Jacobi's integral equation and to use elliptic functions which gives the same motion but with different mathematical structure.

Periodic solutions are important for multiple reasons.[3] Moulton,[1] using linear analysis, initiated the analytical basis for classifying the periodic orbits about the collinear libration points and solving them. Original periodic orbit classes included two-dimensional horizontal orbits, one-dimensional vertical orbits, and three-dimensional orbits. These orbits classes were further studied and became known as Lyapunov periodic orbits, nearly vertical out-of-plane periodic orbits, and three-dimensional periodic but unstable halo orbits.[15] These halo orbits were analytically studied by Farquhar and Kamel[16] using higher order perturbation techniques.

Since 1960 with the advent of numerical computational tools, construction of such periodic orbits is achieved by investigating appropriate initial conditions such that after propagation through a finite time, the orbit closes on itself. Barden and Howell[17] have used manifold theory for numerical computation. Valtonen and Karttunen [11] discuss both analytical and statistical numerical approaches. Richardson[18] used the linearized motion equations and their solution about collinear libration points as a generating orbit to produce halo orbits through a successive analytical approximation technique applied to the full nonlinear equations of motion in which the origin is the collinear equilibrium point. A correction in frequency and restriction on the amplitudes of coordinates is required. Ghazy and Newman[9] used a similar approach as Richardson[18] except a nonlinear base solution is constructed using the origin of the rotating coordinate system at the barycenter. The base solution motion satisfies Jacobi's integral equation. The period and

coordinates in time are obtained in closed-form. Successive approximate higher order techniques are employed to improve solution accuracy.

1.3 Research Statement

This thesis investigates an iterative analytical procedure for constructing approximate solutions for three-dimensional periodic orbits about the collinear libration points in the circular restricted three-body problem. The research follows a parallel approach to Reference 9, but the initial assumptions and utilized functions are unique to this thesis. The methodology is similar to that used to construct the rectilinear oscillation solution in Sitnikov,[19] where a certain motion is hypothesized and then confirmed or altered for correctness. A base solution is constructed using Jacobi elliptic functions in the first step motivated by the observation that the speed of the third body along halo orbits is non-uniform. Utilization of Jacobi elliptic functions is one distinguishing difference between the thesis research and Reference 9, which utilized regular harmonic functions. By exploiting Jacobi elliptic function identities, the base solution is shown to exactly satisfy the Jacobi integral equation and the tangential equation of motion, but only approximately satisfies the other motion equations. The base solution also elicits a closed-form expression for the period in terms of the elliptic integral of the first kind and a constant parameter. This parameter acts like the frequency of motion as in the Richardson[18] procedure. Two formulations of the base solution are possible. The Jacobi $sn(\tau, k)$ and $cn(\tau, k)$ functions can be used but require the modulus k to be an imaginary number. In these functions, variable τ is the temporal argument. Alternatively, the Jacobi $sd(\tau, k)$ and $cd(\tau, k)$ functions can be used and require k to be real. Both sets of functions with imaginary and real modulus are used throughout the thesis.

Because the base solution does not solve the restricted three-body system exactly, an analytic correction process is pursued to recover accuracy. An iterated perturbation process is used whereby

corrections to the base solution along the axis connecting the primaries is considered first, followed by correction in the other two directions. The iterated approach is followed to exploit the coupling structure inherent in the three-body system to simplify calculations. Linear assumptions are also used in these calculations for simplifying reasons. The procedure whereby an unknown constant in these corrections is determined is another distinguishing difference between the thesis research and Reference 9.

Objectives of the thesis research include 1) investigation of the iterative analytic solution procedure for periodic halo orbits in the restricted three-body problem under new base assumptions, 2) evaluation of the solution accuracy for orbit period when using two different base assumptions, and 3) evaluation of the solution accuracy for orbit motion when using two different base assumptions. The first objective addresses the closed-form solvability of the restricted three-body problem using an iterative analytic construction procedure with the base solutions founded on Jacobi elliptic functions. The primary point is to determine whether or not the procedure remains analytically tractable when using more complex functions in the base solution as compared to Reference 9. The second and third objectives examine and compare period and orbit solution accuracies and characteristics when using more complex functions in the base solution as compared to Reference 9. The hypothesis is that initiation of the analytic solution process with a more accurate representation of the non-uniform speed along the orbital path will produce improved accuracy, or at least solution design freedom to achieve improved accuracy.

1.4 Thesis Outline

Chapter 2 discusses briefly the fundamental theories regarding the gravitational n-body problem, the general three-body problem, and the circular restricted three-body problem (CRTBP). The third body equations of motion in the CRTBP are derived, Lagrangian and Hamiltonians are

then written, followed by discussion of Lagrange points which are also calculated numerically for the Earth-Moon system. The Jacobi constant is derived and curves of zero velocity are plotted for the Earth-Moon configuration. At the end, the equations of motion are written in dimensionless form.

The main content of the thesis starts with Chapter 3, which discusses the hypothesized base solution and how it satisfies Jacobi's integral equation. A modified but equivalent base solution and its derivatives are also written. The period of this suppositional motion is derived and determination of the constant parameters of the base solution from initial conditions is worked out. Constraints on initial conditions and on the parameters are discussed. The base solution is substituted into the third body equations of motion and the extent of the accuracy is checked.

Chapter 4 covers the higher order perturbation technique to correct the base solution. Third body differential equations are set up in terms of corrections for each axis. The homogeneous and non-homogeneous solutions for the corrections are obtained. The development assumes the suppositional plane passes through one of the collinear Lagrange points. The complete solution for the x, y, and z axes are written.

In Chapter 5, the base solution is compared with a L_1 halo orbit example and results are discussed. Initial conditions for the true orbit are substituted in the modified series solution and new values of the frequency-like parameter are obtained using numerical computation. Motions in all three axes are obtained using a unique updated parameter value. These analytical motions along with the periods are compared with the exact numerical true orbit and the results obtained from the original harmonic base solution assumption in Reference 9.

Chapter 6 briefly summarizes the work completed in Chapters 3, 4, and 5.

CHAPTER 2

MULTI-BODY PROBLEM

2.1 n-Body Problem Equations of Motion

Newton's law of gravity indicates that any two bodies in nature having masses m_1 and m_2 attract each other with a force F proportional to the product of their masses and inversely proportional to the square of distance R between them. This law is expressed as

$$F = \frac{Gm_1m_2}{R^2} \tag{2.1.1}$$

where G is the universal gravitational constant. This Newtonian model uses a pseudo-inertial coordinate system in local flat space-time. The more complex and accurate model based on general relativity, where gravity manifests as curvature of space-time and bodies follow each other on a space-time geodesic, is not considered or required in this thesis.

Let XYZ be the inertial coordinate system, with origin located at point O. Assume there are n point bodies with corresponding masses m_i and position vectors $\mathbf{R}_i(X_i, Y_i, Z_i)$ where i = 1, 2, 3,…n. From Newton's second law, and using the gravitational force model in Equation (2.1.1), the equation of motion in time t for mass "i" is[11]

$$m_i \frac{d^2X_i}{dt^2} = -G\, m_i \sum_{j=1,j\neq i}^{n} m_j \frac{X_i - X_j}{R_{ij}^3} \tag{2.1.2}$$

$$m_i \frac{d^2Y_i}{dt^2} = -G\, m_i \sum_{j=1,j\neq i}^{n} m_j \frac{Y_i - Y_j}{R_{ij}^3} \tag{2.1.3}$$

$$m_i \frac{d^2Z_i}{dt^2} = -G\, m_i \sum_{j=1,j\neq i}^{n} m_j \frac{Z_i - Z_j}{R_{ij}^3} \tag{2.1.4}$$

In the above motion equations, the range R_{ij} between body "i" and body "j" is

$$R_{ij} = \left\{ (X_i - X_j)^2 + (Y_i - Y_j)^2 + (Z_i - Z_j)^2 \right\}^{1/2} \tag{2.1.5}$$

In vector form, the above equations of motion for mass i are represented as

$$m_i \ddot{\mathbf{R}}_i = -G\, m_i \sum_{j=1, j\neq i}^{n} m_j \frac{\mathbf{R}_{ij}}{R_{ij}^3} \tag{2.1.6}$$

where position vector of body i with respect to body j is

$$\mathbf{R}_{ij} = \mathbf{R}_i - \mathbf{R}_j \tag{2.1.7}$$

Summing all equations of motion for all n bodies gives

$$\sum_{i=1}^{n} m_i \ddot{\mathbf{R}}_i = -G \sum_{i=1}^{n} \sum_{j=1, j\neq i}^{n} m_i m_j \frac{\mathbf{R}_{ij}}{R_{ij}^3} \tag{2.1.8}$$

The right-hand side of Equation (2.1.8) represents all system gravitational forces which are acting in pairs with opposite directions and equal magnitudes ($\mathbf{R}_{ij} = -\mathbf{R}_{ji}$), hence all force pairs cancel out giving

$$\sum_{i=1}^{n} m_i \ddot{\mathbf{R}}_i = \mathbf{0} \tag{2.1.9}$$

The above equation, when integrated twice with respect to time, gives

$$\sum_{i=1}^{n} m_i \mathbf{R}_i = \mathbf{A}t + \mathbf{B} \tag{2.1.10}$$

where **A** and **B** are vector integration constants. According to the definition of center of mass, individual position vectors are related by

$$\sum_{i=1}^{n} m_i \mathbf{R}_i = m\mathbf{R}_c \tag{2.1.11}$$

$$m = \sum_{i=1}^{n} m_i \tag{2.1.12}$$

where $\mathbf{R}_c$ is the position vector of the system mass center and m is the system mass. Thus,

$$\mathbf{R}_c = \frac{1}{m}(\mathbf{A}t + \mathbf{B}) \tag{2.1.13}$$

Equation (2.1.13) indicates the center of mass or barycenter moves with a constant velocity along a straight line. This behavior is a consequence of no external forces being applied to the n-body system. Also, a non-rotating coordinate system with its origin at the barycenter can be used as an inertial frame of reference.

The potential energy V of the system is

$$V = -\frac{1}{2} G \sum_{i=1}^{n} \sum_{j=1}^{n} \frac{m_i m_j}{R_{ij}} \tag{2.1.14}$$

The net gravitational force acting on the i^{th} mass is the negative gradient ($-\boldsymbol{\nabla}_i$) of the potential energy of the system, leading to

$$m_i \ddot{\mathbf{R}}_i = -\boldsymbol{\nabla}_i V \tag{2.1.15}$$

or

$$m_i \frac{d^2 X_i}{dt^2} = -\frac{\partial V}{\partial X_i} \tag{2.1.16}$$

$$m_i \frac{d^2 Y_i}{dt^2} = -\frac{\partial V}{\partial Y_i} \tag{2.1.17}$$

$$m_i \frac{d^2 Z_i}{dt^2} = - \frac{\partial V}{\partial Z_i} \tag{2.1.18}$$

Taking the dot product on both sides of Equation (2.1.15) with $\dot{\mathbf{R}}_i$, and summing for all masses i = 1, 2, 3,…n, yields

$$\sum_{i=1}^{n} m_i \ddot{\mathbf{R}}_i \cdot \dot{\mathbf{R}}_i = - \sum_{i=1}^{n} \nabla_i V \cdot \dot{\mathbf{R}}_i \tag{2.1.19}$$

$$= - \sum_{i=1}^{n} \frac{dX_i}{dt} \frac{\partial V}{\partial X_i} + \frac{dY_i}{dt} \frac{\partial V}{\partial Y_i} + \frac{dZ_i}{dt} \frac{\partial V}{\partial Z_i} \tag{2.1.20}$$

$$= - \frac{dV}{dt} \tag{2.1.21}$$

Integrating on both sides with respect to time gives

$$\frac{1}{2} \sum_{i=1}^{n} m_i \dot{\mathbf{R}}_i \cdot \dot{\mathbf{R}}_i = -V + C \tag{2.1.22}$$

where C is the integration constant. Note the left-hand side of this equation is the kinetic energy of the system, which is denoted here by T, giving

$$T + V = C \tag{2.1.23}$$

Thus, the total energy is conserved in the n-body system.

The total angular momentum of the system **L** is

$$\mathbf{L} = \sum_{i=1}^{n} m_i \mathbf{R}_i \times \dot{\mathbf{R}}_i \tag{2.1.24}$$

Taking the time derivative gives

$$\dot{\mathbf{L}} = \frac{d}{dt}\left(\sum_{i=1}^{n} m_i \mathbf{R}_i \times \dot{\mathbf{R}}_i\right) \tag{2.1.25}$$

$$= \sum_{i=1}^{n} m_i \dot{\mathbf{R}}_i \times \dot{\mathbf{R}}_i + \sum_{i=1}^{n} m_i \mathbf{R}_i \times \ddot{\mathbf{R}}_i \tag{2.1.26}$$

$$= \sum_{i=1}^{n} m_i \mathbf{R}_i \times \ddot{\mathbf{R}}_i \tag{2.1.27}$$

Using the relation in Equation (2.1.6),

$$\dot{\mathbf{L}} = -G \sum_{i=1}^{n} \sum_{j=1,\, j\neq i}^{n} m_i m_j \frac{\mathbf{R}_i \times (\mathbf{R}_i - \mathbf{R}_j)}{R_{ij}^3} \tag{2.1.28}$$

$$= G \sum_{i=1}^{n} \sum_{j=1,\, j\neq i}^{n} m_i m_j \frac{\mathbf{R}_i \times \mathbf{R}_j}{R_{ij}^3} \tag{2.1.29}$$

Since a vector product is anticommutative and vector products occur in Equation (2.1.29) occur in pairs, the right-hand side of Equation (2.1.29) becomes zero. Thus,

$$\dot{\mathbf{L}} = \mathbf{0} \tag{2.1.30}$$

This result indicates total angular momentum is conserved in the n-body system and is a constant vector denoted by **D**.

$$\mathbf{L} = \mathbf{D} \tag{2.1.31}$$

Summarizing the above discussion on the n-body system, there are three second order differential equations for the motion of the i^{th} body given by Equations (2.1.2), (2.1.3), and (2.1.4), which requires six integration constants. So, for n bodies, 6n integration constants are required and are typically called integrals of the motion. Ten integrals are known beforehand, specifically, one energy integral giving constant C from Equation (2.1.23), six integrals representing rectilinear motion of the barycenter giving constants **A** and **B** from Equation (2.1.10), and three integrals

denoting constant angular momentum giving constant vector **D** from Equation (2.1.31). With 6n unknowns and only 10 available integrals, the under determined condition implies the closed-form insolvability of the n-body problem. For the complete solution, 6n-10 additional constants are required. The missing constants are easily found when n = 2 but for n > 2, no additional independent constants are known. In the case of the three- body problem where n = 3, some of the special solutions with special initial conditions like Lagrange's equilateral triangle solution are available, but there is no general analytic solution which can give the coordinates and velocities of any of the three bodies at future times when provided with arbitrary initial conditions.

2.2 Circular Restricted Three-Body Problem

The circular restricted three-body problem is a special case of the general three-body problem. In the CRTBP, one of the three masses is negligibly small compared to the other two, so that the gravitational influence from the small body on the two primaries is neglected. The primaries move in a circular coplanar orbit around each other about their common center of mass. Given the initial coordinates and velocities of the third body, the primary objectives are finding its path over time, investigating the periodicity of orbits, analyzing the stability of the orbits, and determining forbidden and allowed regions of existence. Before proceeding to the geometry of the CRTBP, the fundamentals of vector kinematics are discussed next.

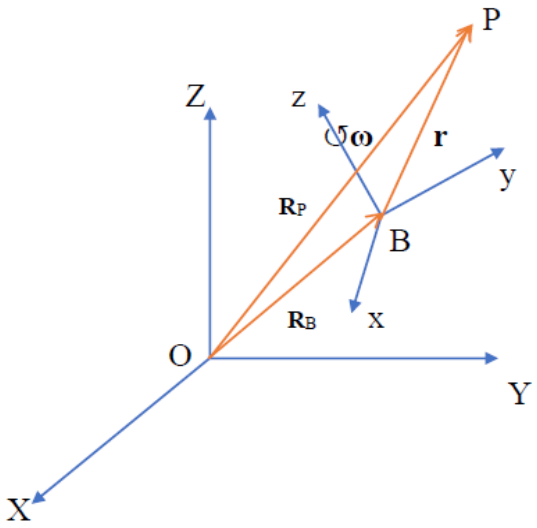

Figure 1 Coordinate Frames of Reference

As shown in Figure 1, XYZ is an inertial coordinate system with origin O. Also, xyz is a rotating coordinate system attached to the point B which is also the origin. This frame rotates with angular velocity vector **ω**. The position vector of point P is given by

$$\mathbf{R}_p = \mathbf{R}_B + \mathbf{r} \tag{2.2.1}$$

where vectors $\mathbf{R}_P$, $\mathbf{R}_B$ and **r** can all be expressed in the inertial coordinate system or the rotating coordinate system. Denote **I, J, K** as unit vectors in the X, Y, Z inertial coordinate directions, and **i, j, k** as unit vectors in the x, y, z rotating coordinate system directions. The inertial velocity of point P, expressed in the two frames, is given by

$$\mathbf{V}_p = V_{XP}\mathbf{I} + V_{YP}\mathbf{J} + V_{ZP}\mathbf{K} \tag{2.2.2}$$

$$= V_{xP}\mathbf{i} + V_{yP}\mathbf{j} + V_{zP}\mathbf{k} \tag{2.2.3}$$

$$= \frac{d\mathbf{R}_P}{dt}_{XYZ} \tag{2.2.4}$$

Also, the velocity of point B can be expressed as

$$\mathbf{V}_B = V_{XB}\mathbf{I} + V_{YB}\mathbf{J} + V_{ZB}\mathbf{K} \tag{2.2.5}$$

$$= V_{xB}\mathbf{i} + V_{yB}\mathbf{j} + V_{zB}\mathbf{k} \tag{2.2.6}$$

$$= \frac{d\mathbf{R}_B}{dt}_{XYZ} \tag{2.2.7}$$

Now, the velocities of point P and point B can also be shown to relate as

$$\mathbf{V}_P = \mathbf{V}_B + \boldsymbol{\omega}\times\mathbf{r} + \mathbf{v} \tag{2.2.8}$$

where

$$\mathbf{v} = \frac{d\mathbf{r}}{dt}_{xyz} \tag{2.2.9}$$

Further, the accelerations of point P and point B are related as

$$\mathbf{A}_P = \mathbf{A}_B + \dot{\boldsymbol{\omega}}\times\mathbf{r} + \boldsymbol{\omega}\times(\boldsymbol{\omega}\times\mathbf{r}) + 2(\boldsymbol{\omega}\times\mathbf{v}) + \mathbf{a} \tag{2.2.10}$$

where

$$\mathbf{a} = \frac{d\mathbf{v}}{dt}_{xyz} \tag{2.2.11}$$

An important item to note is all vector quantities on both sides of these expressions should be expressed in the same coordinate system, i.e., either in the inertial or rotating systems.

Consider the geometry for the CRTBP illustrated in Figure 2. Masses m_1 and m_2 are the two primary bodies moving in circular coplanar orbits around each other. Their common center of mass or barycenter is denoted as "cm" in Figure 2. Each of the masses m_1 and m_2 also traverse in circular orbits about the mass center. The third body having mass m_3 is inertially negligible, e.g., a spacecraft or an asteroid. Mathematically, this means

$$m_1 \gg m_3 \quad , \quad m_2 \gg m_3 \tag{2.2.12}$$

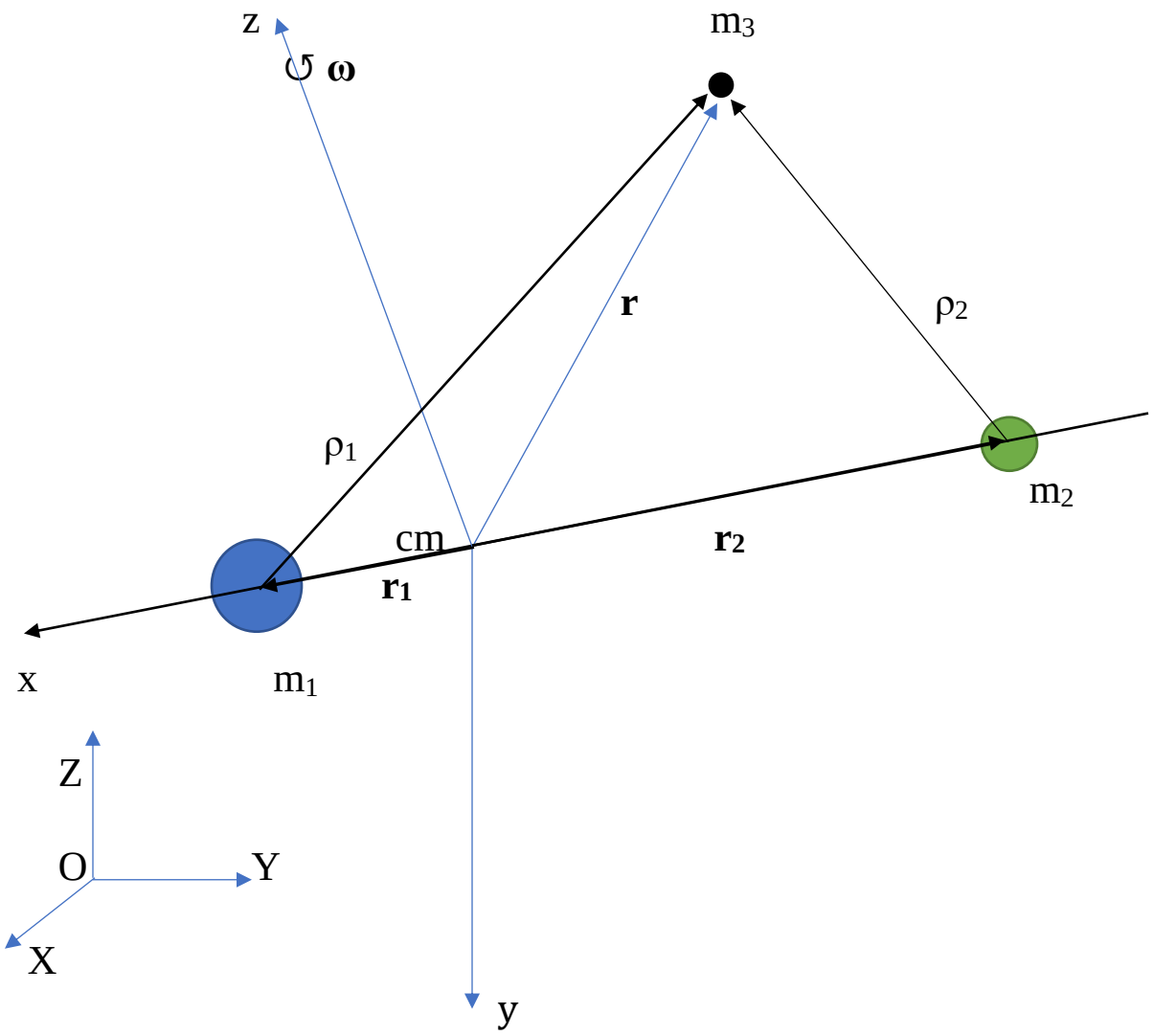

Figure 2 Geometry of the Restricted Problem

Frame XYZ is the inertial frame of reference. The rotating coordinate system xyz is attached to the system mass center and is rotating with angular velocity **ω** which is also the rate with which masses m_1 and m_2 revolve around each other. Frame xyz forms a right-handed coordinate system and masses m_1 and m_2 and the cm are aligned along the x axis. Mass m_1 is situated in the positive direction of the x axis. The xy plane is the plane of rotation of the primaries where angular velocity vector **ω** is directed along the positive z axis. Vectors $\mathbf{r}_1$, $\mathbf{r}_2$, and **r** are the position vectors of m_1, m_2, and m_3 relative to the cm, respectively. Variables ρ_1 and ρ_2 are the scalar distances of the third

body from m_1 and m_2, respectively. Finally, **i, j, k** are the unit vectors in the x, y, z directions. These various vectors and distances are defined as

$$\boldsymbol{\omega} = \omega \mathbf{k} \tag{2.2.13}$$

$$\mathbf{r}_1 = x_1 \mathbf{i} \quad , x_1 > 0 \tag{2.2.14}$$

$$\mathbf{r}_2 = x_2 \mathbf{i} \quad , x_2 < 0 \tag{2.2.15}$$

$$\mathbf{r} = x\mathbf{i} + y\mathbf{j} + z\mathbf{k} \tag{2.2.16}$$

$$\rho_1 = \{(x-x_1)^2+y^2+z^2\}^{\frac{1}{2}} \tag{2.2.17}$$

$$\rho_2 = \{(x-x_2)^2+y^2+z^2\}^{\frac{1}{2}} \tag{2.2.18}$$

Several relations involving the system period, rotation frequency, and primary coordinates are developed next. The distance r_{12} between the two primaries is denoted as

$$r_{12} = x_1 - x_2 \tag{2.2.19}$$

The angular velocity ω can also be written as

$$\omega = \frac{2\pi}{T} \tag{2.2.20}$$

where T denotes period for one revolution of the primaries.

Period is given by Kepler's law for the two-body problem, or

$$T = \frac{2\pi}{\sqrt{\mu}} r_{12}^{3/2} \tag{2.2.21}$$

where

$$\mu = G\,(m_1+m_2) \tag{2.2.22}$$

From Equations (2.2.20), (2.2.21), and (2.2.22),

$$\omega^2 = \frac{G(m_1+m_2)}{r_{12}^3} \tag{2.2.23}$$

Now, the mass center of the system, which is also the origin of the xyz frame, is governed by

$$0 = m_1 x_1 + m_2 x_2 \tag{2.2.24}$$

Also introduce parameters π_1 and π_2 defined as follows,

$$\pi_1 = \frac{m_1}{m_1+m_2} \tag{2.2.25}$$

$$\pi_2 = \frac{m_2}{m_1+m_2} \tag{2.2.26}$$

Thus, from Equations (2.2.24), (2.2.25), and (2.2.26)

$$x_1 = \pi_2 r_{12}\ ,\ \ x_2 = -\pi_1 r_{12} \tag{2.2.27}$$

The velocity of the third body can be written as

$$\mathbf{V}_{m_3} = \mathbf{V}_{cm} + \boldsymbol{\omega}\times\mathbf{r} + \mathbf{V}_{m_3/cm} \tag{2.2.28}$$

and the acceleration of the third body is thus given by

$$\mathbf{A}_{m_3} = \mathbf{A}_{cm} + \dot{\boldsymbol{\omega}}\times\mathbf{r} + \boldsymbol{\omega}\times(\boldsymbol{\omega}\times\mathbf{r}) + 2(\boldsymbol{\omega}\times\mathbf{V}_{m_3/cm}) + \mathbf{A}_{m_3/cm} \tag{2.2.29}$$

The quantities on the right side of above equation are now evaluated term by term. The velocity $\mathbf{V}_{cm}$ of the mass center is a constant vector, leading to

$$\mathbf{A}_{cm} = \mathbf{0} \tag{2.2.30}$$

In other words, $\mathbf{A}_{cm}$ is zero and drops out from Equation (2.2.29). The relative velocity of the third body with respect to the mass center is

$$\mathbf{V}_{m_3/cm} = \dot{x}\mathbf{i} + \dot{y}\mathbf{j} + \dot{z}\mathbf{k} \tag{2.2.31}$$

Consequently, $\mathbf{A}_{m_3/cm}$ is the relative acceleration of the third body with respect to the center of mass and is given by

$$\mathbf{A}_{m_3/cm} = \ddot{x}\mathbf{i} + \ddot{y}\mathbf{j} + \ddot{z}\mathbf{k} \tag{2.2.32}$$

The angular velocity $\boldsymbol{\omega}$ is a constant vector always directed along positive z axis having constant magnitude given by Equation (2.2.13). This invariance is because of the exact circular motion of the primaries. Therefore,

$$\dot{\boldsymbol{\omega}} = \mathbf{0} \tag{2.2.33}$$

The quantity $\boldsymbol{\omega}\times(\boldsymbol{\omega}\times\mathbf{r})$ is evaluated as

$$\begin{aligned}\boldsymbol{\omega}\times(\boldsymbol{\omega}\times\mathbf{r}) &= \boldsymbol{\omega}\,(\boldsymbol{\omega}\cdot\mathbf{r}) - \mathbf{r}\,(\boldsymbol{\omega}\cdot\boldsymbol{\omega}) \\ &= \omega\mathbf{k}\,(\omega z) - \omega^2\,(x\mathbf{i}+y\mathbf{j}+z\mathbf{k}) \\ &= -\omega^2(\,x\mathbf{i}+y\mathbf{j}\,)\end{aligned} \tag{2.2.34}$$

Also,

$$\begin{aligned}2\,(\boldsymbol{\omega}\times\mathbf{V}_{m_{3/CM}}) &= 2\,\{\omega\mathbf{k}\times(\dot{x}\mathbf{i}+\dot{y}\mathbf{j}+\dot{z}\mathbf{k})\} \\ &= 2\dot{x}\omega\mathbf{j} - 2\dot{y}\omega\mathbf{i}\end{aligned} \tag{2.2.35}$$

Collecting all the terms on the right-hand side of Equation (2.2.29) and separating **i, j**, **k** components, the absolute (inertial) acceleration of the third body can now be written in terms of the components of the non-inertial rotating frame as follows

$$\mathbf{A}_{m_3} = (\ddot{x}-\omega^2 x-2\omega\dot{y})\mathbf{i}+(\ddot{y}-\omega^2 y+2\omega\dot{x})\mathbf{j}+\ddot{z}\mathbf{k} \tag{2.2.36}$$

The external forces acting on the third body are the gravitational forces due to masses m_1 and m_2. If the forces are written in the rotating coordinate system, then from Newton's second law,

$$m_3\mathbf{A}_{m_3} = -\frac{Gm_3m_1}{\rho_1^3}\boldsymbol{\rho}_1 - \frac{Gm_3m_2}{\rho_2^3}\boldsymbol{\rho}_2 \tag{2.2.37}$$

where

$$\boldsymbol{\rho}_1 = (x-x_1)\mathbf{i}+y\mathbf{j}+z\mathbf{k}\ ,\quad \boldsymbol{\rho}_2 = (x-x_2)\mathbf{i}+y\mathbf{j}+z\mathbf{k} \tag{2.2.38}$$

The vectors $\boldsymbol{\rho}_1$ and $\boldsymbol{\rho}_2$ are the position vectors of the third body with respect to the masses m_1 and m_2 and directed towards m_3 itself, but gravity being an attractive force, the negative (-) signs are introduced in Equation (2.2.37).

Introduce gravitational parameters μ_1 and μ_2 , or

$$\mu_1 = Gm_1 \text{ and } \mu_2 = Gm_2 \tag{2.2.39}$$

Equation (2.3.37) can now be written as

$$\mathbf{A}_{m_3} = -\frac{\mu_1}{\rho_1^3}\boldsymbol{\rho}_1 - \frac{\mu_2}{\rho_2^3}\boldsymbol{\rho}_2 \tag{2.2.40}$$

Equating **i, j, k** components on both sides of Equation (2.2.40), three scalar equations of motion of the third body are obtained as

$$\ddot{x}-\omega^2 x-2\omega\dot{y}+\frac{\mu_1}{\rho_1^3}(x-x_1)+\frac{\mu_2}{\rho_2^3}(x-x_2)=0 \tag{2.2.41}$$

$$\ddot{y}-\omega^2 y+2\omega\dot{x}+\frac{\mu_1}{\rho_1^3}y+\frac{\mu_2}{\rho_2^3}y=0 \tag{2.2.42}$$

$$\ddot{z}+\frac{\mu_1}{\rho_1^3}z+\frac{\mu_2}{\rho_2^3}z=0 \tag{2.2.43}$$

Equations (2.2.41)-(2.2.43) are the second order nonlinear coupled ordinary differential equations of motion which govern the dynamics of the third body.

Introduce the specific gravitational potential function U

$$U=\frac{Gm_1}{\rho_1}+\frac{Gm_2}{\rho_2}=\frac{\mu_1}{\rho_1}+\frac{\mu_2}{\rho_2} \tag{2.2.44}$$

Partially differentiating the function U with respect to x, y, and z positions yields

$$\frac{\partial U}{\partial x}=-\frac{\mu_1}{\rho_1^2}\frac{\partial \rho_1}{\partial x}-\frac{\mu_2}{\rho_2^2}\frac{\partial \rho_2}{\partial x} \tag{2.2.45}$$

$$\frac{\partial U}{\partial y} = -\frac{\mu_1}{\rho_1^2}\frac{\partial \rho_1}{\partial y} - \frac{\mu_2}{\rho_2^2}\frac{\partial \rho_2}{\partial y} \tag{2.2.46}$$

$$\frac{\partial U}{\partial z} = -\frac{\mu_1}{\rho_1^2}\frac{\partial \rho_1}{\partial z} - \frac{\mu_2}{\rho_2^2}\frac{\partial \rho_2}{\partial z} \tag{2.2.47}$$

Hence, from Equations (2.2.41)-(2.2.43) and Equations (2.2.45)-(2.2.47) one can rewrite the third body equations of motion as

$$\ddot{x} - \omega^2 x - 2\omega\dot{y} = \frac{\partial U}{\partial x} \tag{2.2.48}$$

$$\ddot{y} - \omega^2 y + 2\omega\dot{x} = \frac{\partial U}{\partial y} \tag{2.2.49}$$

$$\ddot{z} = \frac{\partial U}{\partial z} \tag{2.2.50}$$

The specific Lagrangian and Hamiltonian functions L and H for the third body can be written as

$$L = \frac{1}{2}\left[\left(\dot{q}_1^2 + \dot{q}_2^2 + \dot{q}_3^2\right) + 2\omega\left(q_1\dot{q}_2 - q_2\dot{q}_1\right) + \omega^2\left(q_1^2 + q_2^2\right)\right] + U \tag{2.2.51}$$

$$H = \frac{1}{2}\left(p_1^2 + p_2^2 + p_3^2\right) + \omega\left(p_1 q_2 - p_2 q_1\right) - U \tag{2.2.52}$$

where

$$q_1 = x, \quad q_2 = y, \quad q_3 = z \tag{2.2.53}$$

Also, the specific momenta p_1, p_2, p_3 are given by

$$p_1 = \frac{\partial L}{\partial \dot{q}_1}, \quad p_2 = \frac{\partial L}{\partial \dot{q}_2}, \quad p_3 = \frac{\partial L}{\partial \dot{q}_3} \tag{2.2.54}$$

Hamilton's canonical equations are

$$\frac{dq_1}{dt} = p_1 + \omega q_2 \qquad \frac{dp_1}{dt} = \omega p_2 + \frac{\partial U}{\partial q_1}$$

$$\frac{dq_2}{dt} = p_2 - \omega q_1 \qquad \frac{dp_2}{dt} = -\omega p_1 + \frac{\partial U}{\partial q_2}$$

$$\frac{dq_3}{dt} = p_3 \qquad \frac{dp_3}{dt} = \frac{\partial U}{\partial q_3} \tag{2.2.55}$$

This first order differential equation model is equivalent to the second order model in Equations (2.2.41)-(2.2.43)

2.3 Lagrange Points

Equations (2.2.41)-(2.2.43), which govern the motion of the third body, have no general closed-form analytical solution. But five particular solutions exist in the form of Lagrange points which are also called libration or equilibrium points. These points are the locations in space where the third body would have zero relative velocity and zero relative acceleration. Therefore, all three bodies would appear to be at rest with respect to the rotating coordinate system. A body initially at one of the Lagrangian points would remain there forever, unless and until disturbed by some external force.

Therefore, for Lagrangian points,

$$\dot{x} = \dot{y} = \dot{z} = 0 \text{ and } \ddot{x} = \ddot{y} = \ddot{z} = 0 \tag{2.3.1}$$

Substituting the conditions mentioned in Equation (2.3.1), into Equations (2.2.41)-(2.2.43), yields

$$-\omega^2 x + \frac{\mu_1}{\rho_1^3}(x - x_1) + \frac{\mu_2}{\rho_2^3}(x - x_2) = 0 \tag{2.3.2}$$

$$-\omega^2 y + \frac{\mu_1}{\rho_1^3} y + \frac{\mu_2}{\rho_2^3} y = 0 \tag{2.3.3}$$

$$\frac{\mu_1}{\rho_1^3} z + \frac{\mu_2}{\rho_2^3} z = 0 \tag{2.3.4}$$

Equations (2.3.2)-(2.3.4) can also be written in terms of the gravitational potential function U. Hence, for libration points,

$$-\omega^2 x = \frac{\partial U}{\partial x} \tag{2.3.5}$$

$$-\omega^2 y = \frac{\partial U}{\partial y} \tag{2.3.6}$$

$$0 = \frac{\partial U}{\partial z} \tag{2.3.7}$$

From Equation (2.3.4), it is clear that $z = 0$ because the quantity $\frac{\mu_1}{\rho_1^3} + \frac{\mu_2}{\rho_2^3}$ is always positive. So, all libration points lie in the xy plane or in the plane of the rotation of the primaries. Obvious relations include,

$$\pi_1 + \pi_2 = 1, \qquad \pi_1 \mu = \mu_1, \qquad \pi_2 \mu = \mu_2 \tag{2.3.8}$$

Also, from Equation (2.2.23)

$$\frac{\omega^2}{\mu} = \frac{1}{r_{12}^3} \tag{2.3.9}$$

Now, dividing Equation (2.3.2) and (2.3.3) throughout by μ and using Equations (2.3.8) and (2.3.9), and doing some algebraic manipulations with case $y \neq 0$, yields

$$\rho_1 = \rho_2 = r_{12} \tag{2.3.10}$$

Using Equation (2.3.10) along with $z = 0$ gives

$$x = \left(\pi_2 - \frac{1}{2}\right) r_{12} \tag{2.3.11}$$

$$y = \pm \frac{\sqrt{3}}{2} r_{12} \tag{2.3.12}$$

Thus, the coordinates of the Lagrangian points L_4 and L_5 are

$$L_4 \equiv \left(\left(\pi_2 - \frac{1}{2}\right) r_{12} , + \frac{\sqrt{3}}{2} r_{12} , 0 \right) \tag{2.3.13}$$

$$L_5 \equiv \left(\left(\pi_2 - \frac{1}{2}\right) r_{12} , - \frac{\sqrt{3}}{2} r_{12} , 0 \right) \tag{2.3.14}$$

Observe that, both L_4 and L_5 form an equilateral triangle with the two primary masses. The other case of $y = 0$ with $z = 0$ allows the remaining Lagrange points to be found. In that case $\rho_1 = |x - x_1|$ and $\rho_2 = |x - x_2|$. Also, Equations (2.3.3) and (2.3.4) vanish and substituting values of ρ_1 and ρ_2 in the only remaining Equation (2.3.2), yields

$$-\omega^2 x + \frac{\mu_1}{|x-x_1|^3}(x-x_1) + \frac{\mu_2}{|x-x_2|^3}(x-x_2) = 0 \tag{2.3.15}$$

Three values of the x coordinate that will satisfy Equation (2.3.15) can be obtained. These roots are denoted by (ξ_1, ξ_2, ξ_3). These three values correspond to Lagrange points L_1, L_2 and L_3.

$$\begin{aligned} L_1 &= (\xi_1, 0 , 0) \\ L_2 &= (\xi_2, 0 , 0) \\ L_3 &= (\xi_3 , 0 , 0) \end{aligned} \tag{2.3.16}$$

L_1, L_2 and L_3 lie along the x axis or along the line joining the primaries.

If the third body is initially situated at one of the equilibrium points and is given a small disturbance or nudged out of its position, one primary question is whether it will drift away forever or return to its equilibrium position. This outcome is determined by whether the Lagrange point is stable or unstable.[20] If the third body is initially at a stable Lagrange point, then a small perturbation

will result in oscillation (small orbit) of the body about the equilibrium point. But, if the point is unstable then the third body initially oscillates in the divergent fashion, then it permanently drifts away. L_1, L_2 and L_3 are always unstable for any CRTBP configuration. L_4 and L_5 can be stable or unstable depending upon the CRTBP configuration. If the ratio $\frac{m_1}{m_2}+\frac{m_2}{m_1}$ exceeds 25, then the points are stable. For the Earth-Moon configuration this ratio is around 81.3, but L_4 and L_5 are destabilized by the Sun's gravity.

An example which calculates the libration points for the Earth-Moon configuration is discussed next. First, the primary masses are defined.

$$\text{Earth mass} = m_1 = 5.974\times10^{24} \quad \text{kg}$$

$$\text{Moon mass} = m_2 = 7.348\times10^{22} \quad \text{kg}$$

Next, the distance between the Earth and the Moon is defined.

$$\text{Earth-Moon distance} = r_{12} = 3.844*10^5 \text{ km}$$

Various parameters of the system are then computed.

$$\pi_2 = \frac{m_2}{m_1+m_2} = 0.01215 \qquad x_1 = \pi_2 r_{12} = 4670 \text{ km}$$

$$x_2 = -\pi_1 r_{12} = -(1-\pi_2) r_{12} = -379730 \text{ km} \qquad x_{cm}=0$$

$$\left(\pi_2-\frac{1}{2}\right) r_{12} = -187530 \text{ km} \qquad \frac{\sqrt{3}}{2} r_{12}=332900 \text{ km}$$

Lagrange points L_4 and L_5 are computed next.

$$L_4 \equiv \left(r_{12}\pi_2-\frac{r_{12}}{2} , +\frac{\sqrt{3}}{2} r_{12} , 0 \right) \equiv (-187530, 332900 , 0) \text{ km}$$

$$L_5 \equiv \left(r_{12}\pi_2-\frac{r_{12}}{2} , -\frac{\sqrt{3}}{2} r_{12} , 0 \right) \equiv (-187530,- 332900 , 0) \text{ km}$$

To get L_1, L_2, L_3 requires finding the roots of Equation (2.3.15)

$L_1 \equiv (-321711, 0, 0)$ km

$L_2 \equiv (-444243, 0, 0)$ km

$L_3 \equiv (386345, 0, 0)$ km

Figure 3 illustrates these Lagrange point results for the Earth-Moon system.

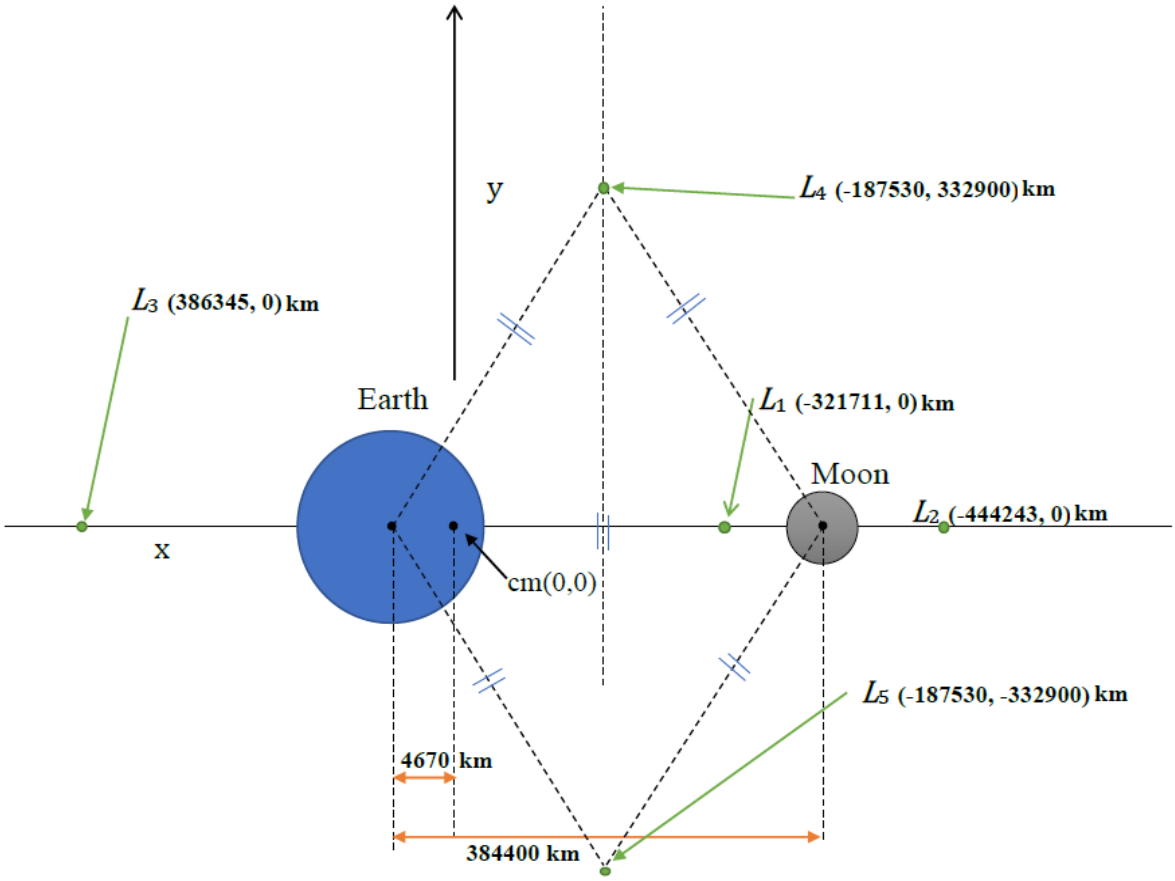

Figure 3 Lagrange Points of the Earth-Moon System

2.4 Jacobi Constant

The specific energy of the third body is constant in the CRTBP problem,[20] given by

$$C^* = \frac{1}{2}V^2 - \frac{1}{2}\omega^2(x^2+y^2) - \frac{\mu_1}{\rho_1} - \frac{\mu_2}{\rho_2} \qquad (2.4.1)$$

where V is the magnitude of velocity of m_3 in the rotating coordinate system.

$$V^2 = \left|\mathbf{V}_{m_3/cm}\right|^2 = \dot{x}^2+\dot{y}^2+\dot{z}^2 \tag{2.4.2}$$

The term $\frac{1}{2}V^2$ represents kinetic energy, and $-\frac{1}{2}\omega^2(x^2+y^2)$ can be thought of as potential energy induced by rotation of the reference frame, while $-\frac{\mu_1}{\rho_1}-\frac{\mu_2}{\rho_2}$ is the gravitational potential energy, all being energies per unit mass of the third body.

If the Jacobi function J is defined as

$$J = \frac{1}{2}\omega^2(x^2+y^2)+\frac{\mu_1}{\rho_1}+\frac{\mu_2}{\rho_2} \tag{2.4.3}$$

then it is obvious that

$$C^* = \frac{1}{2}V^2 - J \tag{2.4.4}$$

Multiplying both sides of this relation by -2 gives

$$-2C^* = 2J - V^2 = C \tag{2.4.5}$$

Parameter C is called the Jacobi constant. Note the equations of motion of the third body can be represented in terms of the Jacobi function as follows.

$$\ddot{x} - 2\omega\dot{y} = \frac{\partial J}{\partial x} \tag{2.4.6}$$

$$\ddot{y} + 2\omega\dot{x} = \frac{\partial J}{\partial y} \tag{2.4.7}$$

$$\ddot{z} = \frac{\partial J}{\partial z} \tag{2.4.8}$$

2.5 Curves of Zero Velocity

From Equation (2.4.5)

$$2J - C = V^2 \tag{2.5.1}$$

which upon expanding gives

$$\omega^2(x^2+y^2)+\frac{2\mu_1}{\rho_1}+\frac{2\mu_2}{\rho_2}-C = V^2 \tag{2.5.2}$$

or

$$\omega^2(x^2+y^2)+\frac{2\mu_1}{\{(x-x_1)^2+y^2+z^2\}^{\frac{1}{2}}}+\frac{2\mu_2}{\{(x-x_2)^2+y^2+z^2\}^{\frac{1}{2}}}-C = V^2 \tag{2.5.3}$$

If the motion of the third body is restricted to lie in the plane of the primaries, i.e., substituting $z = 0$ in Equation (2.5.3), the expression becomes

$$\omega^2(x^2+y^2)+\frac{2\mu_1}{\{(x-x_1)^2+y^2\}^{\frac{1}{2}}}+\frac{2\mu_2}{\{(x-x_2)^2+y^2\}^{\frac{1}{2}}}-C = V^2 \tag{2.5.4}$$

The quantity on the right-hand side of Equation (2.5.4) is the velocity squared, which is always positive. So, the quantity on the left-side when equated to zero renders the zero velocity curves. For a particular value of C, these curves create a region where the third body motion would cease to exist. For the third body possessing a specific energy in the CRTBP system corresponding to C, the body will not enter the forbidden regions lying on the other side of the zero velocity curve boundary.

Figure 4 shows the zero velocity curves for the Earth-Moon system. Starting from the Jacobi constant C = 3.6 and gradually reducing its value, interesting patterns are observed for the allowed and forbidden regions of motion. For C = 3.6, the allowable regions are essentially circles surrounding both the Earth and the Moon. Spacecraft possessing this specific energy located near the Earth cannot reach the Moon because of the large annular shaped forbidden region lying between the two attractors. For C = 3.347, the regions meet exactly at the Lagrange point L_1, and it becomes just possible to reach the Moon through a narrow corridor. Similarly, for C = 3.3298,

escape from Earth-Moon system can be just achieved. For C = 3.1624, a lot of freedom exists for the spacecraft around the moon and the points L_1 and L_2, but L_3 become just possible to reach with zero velocity while forbidden region still exists around L_4 and L_5. Around C = 3.14 almost the entire space is available except narrow regions around L_4 and L_5. For C = 3.136, spacecraft can now reach the L_4 and L_5, and there is no forbidden region for this energy level. Here, the decrease in the value of the Jacobi constant C means an increase in the value of C* which is the actual specific energy, as they are related by $-2C^* = C$ according to Equation (2.4.5). Here, it should be remembered that the larger mass m_1, i.e., the center of the Earth is in the positive x direction. The Lagrange point L_1 is defined to lie in between the Earth and the Moon, L_2 being on the far side of the Moon, and L_3 on the far side of the Earth. L_4 and L_5 of course lie in between the two primaries, L_4 defined to have positive y coordinate. The mass center or barycenter is located at the origin.

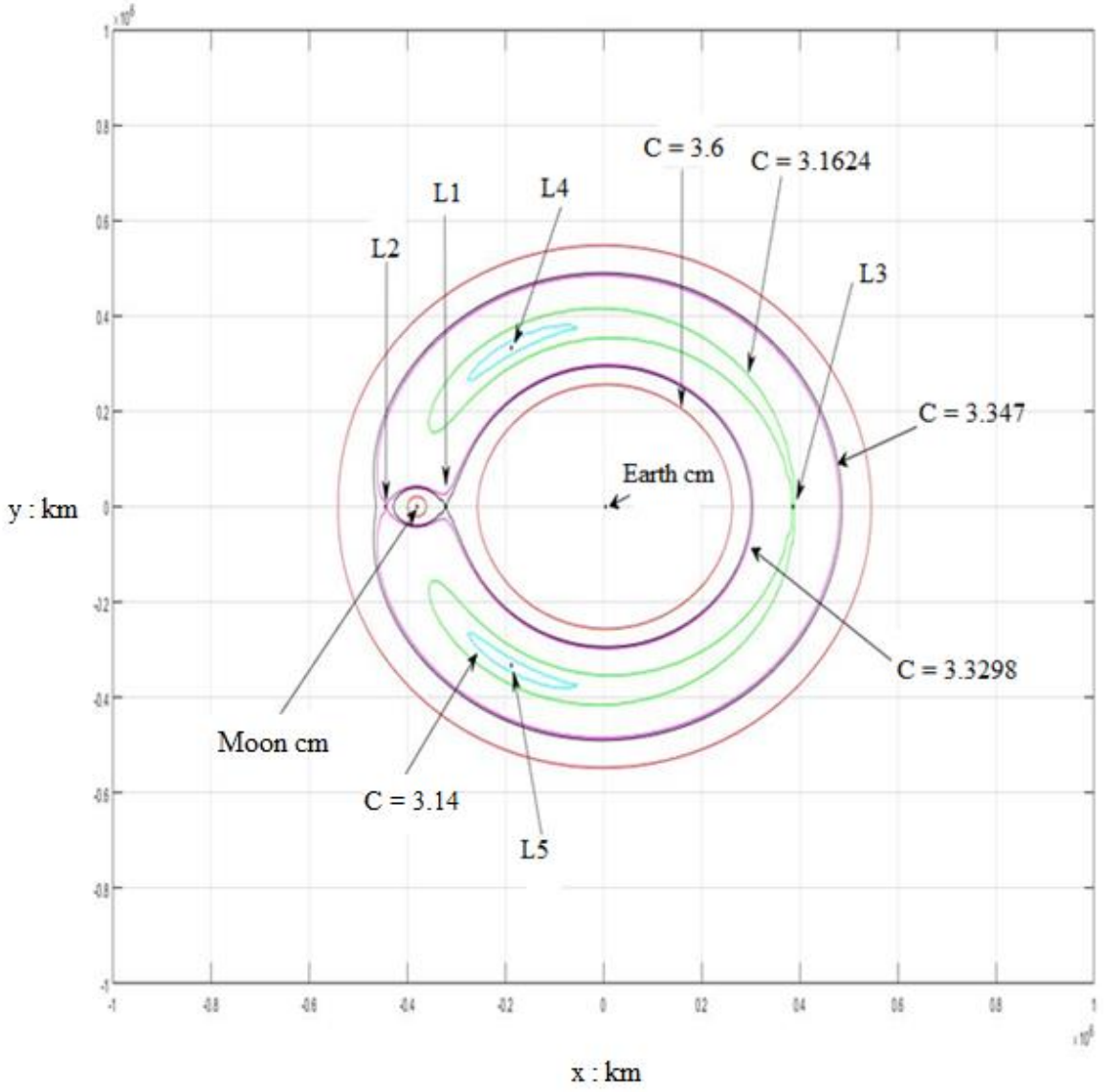

Figure 4 Zero Velocity Curves for the Earth-Moon System

2.6 Equations of Motion in Dimensionless Form

The circular restricted three-body problem and the equations of motion discussed so far can also be put in the dimensionless form for simplicity. Non-dimensional units are chosen such that the following quantities are equal to unity: the universal gravitational constant G, the angular velocity of the rotating frame ω, the distance between the primaries r_{12}, and the sum of the masses of the primaries m_1+m_2.

$$\omega^2 = \frac{G(m_1+m_2)}{r_{12}^3} \Rightarrow 1=1 \tag{2.6.1}$$

Also, renaming the quantity π_2 as μ gives

$$\mu = \frac{m_2}{m_1+m_2} = m_2$$

$$m_1 = 1-\mu = \pi_1 \tag{2.6.2}$$

Then, the Jacobi function is

$$J = \frac{1}{2}(x^2+y^2) + \frac{1-\mu}{\rho_1} + \frac{\mu}{\rho_2} \tag{2.6.3}$$

where

$$\rho_1 = \{ (x-\mu)^2+y^2+z^2 \}^{\frac{1}{2}}$$

$$\rho_2 = \{(x+1-\mu)^2+y^2+z^2\}^{\frac{1}{2}} \tag{2.6.4}$$

Note in these expressions, coordinates x, y, z are now dimensionless having been normalized by r_{12}. Likewise velocities $\dot{x}, \dot{y}, \dot{z}$ and accelerations $\ddot{x}, \ddot{y}, \ddot{z}$ are now dimensionless, having been normalized by $r_{12}\omega$ and $r_{12}\omega^2$, respectively. Hence, the dimensionless equations of motion of the third body can be represented in the terms of the Jacobi function as follows.

$$\ddot{x}-2\dot{y}=\frac{\partial J}{\partial x} \qquad \ddot{y}+2\dot{x}=\frac{\partial J}{\partial y} \qquad \ddot{z}=\frac{\partial J}{\partial z} \tag{2.6.5}$$

or the general dimensionless form is

$$\ddot{x}-x-2\dot{y}+\frac{1-\mu}{\rho_1^3}(x-\mu)+\frac{\mu}{\rho_2^3}(x+1-\mu)=0 \tag{2.6.6}$$

$$\ddot{y}-y+2\dot{x}+\frac{1-\mu}{\rho_1^3}y+\frac{\mu}{\rho_2^3}y=0 \tag{2.6.7}$$

$$\ddot{z}+\frac{1-\mu}{\rho_1^3}z+\frac{\mu}{\rho_2^3}z=0 \tag{2.6.8}$$

2.7 Halo Orbits

The three-body problem periodic halo orbit is geometrically more complex than the two-body problem periodic elliptic orbit. Halo orbits are closed three-dimensional, twisted curves that do not lie in a single fixed plane. These orbits can be described as "egg" shaped ovals that are three-dimensionally distorted. Although the curves are not describable by simple elementary functions like harmonic sine and cosine, the curves do exhibit symmetry about the xz plane. In Figure 5, suppose times $t = t_+$ and $t = t_-$ represent points along the orbit positioned on opposing sides of the xz plane. If position, velocity, and acceleration values $x(t_+), y(t_+), z(t_+)$; $\dot{x}(t_+)$, $\dot{y}(t_+)$, $\dot{z}(t_+)$; and $\ddot{x}(t_+), \ddot{y}(t_+), \ddot{z}(t_+)$ solve the three-body problem equations of motion in Equations (2.2.41)-(2.2.43), then corresponding values indicated below

$$x(t_-) = +x(t_+)\,,\ y(t_-) = -y(t_+),\ z(t_-) = +z(t_+)$$

$$\dot{x}(t_-) = -\dot{x}(t_+)\,,\ \dot{y}(t_-) = +\dot{y}(t_+),\ \dot{z}(t_-) = -\dot{z}(t_+) \tag{2.7.1}$$

$$\ddot{x}(t_-) = +\ddot{x}(t_+),\ \ddot{y}(t_-) = -\ddot{y}(t_+), \qquad \ddot{z}(t_-) = +\ddot{z}(t_-)$$

also satisfy the equations of motion, confirming the symmetric nature of halo orbits.

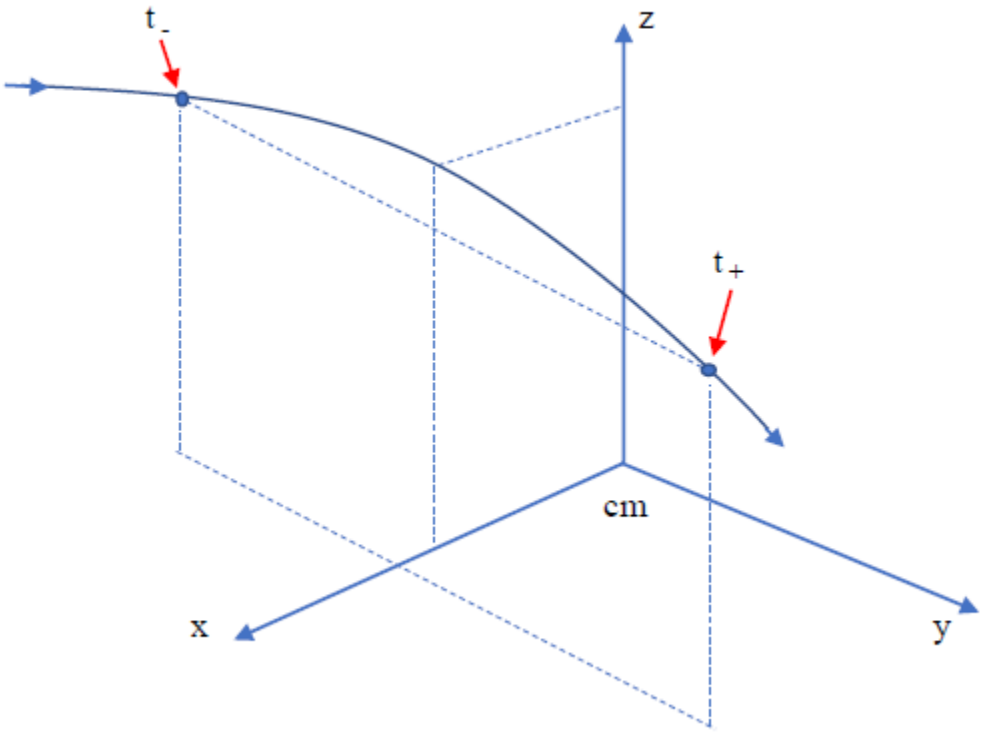

Figure 5 Symmetric Halo Orbit Geometry

Reference 15 contains a large database of initial condition triples $\{x(t_0), \dot{y}(t_0), z(t_0)\} = \{x_0, \dot{y}_0, z_0\}$ and corresponding periods T for various families of halo orbits about the L_1, L_2, and L_3 Lagrange points for a generic three-body system that approximates the Earth-Moon system where t_0 denotes initial time. One specific L_1 halo orbit from Reference 15, also used by Ghazy and Newman in Reference 9, is generated from non-dimensional initial condition and period values of

$$x_0 = 0.723268,\ \dot{y}_0 = 0.198019,\ z_0 = 0.040000$$
$$T = 2(1.300177),\ t_0 = 0,\ \mu = 0.04 \qquad (2.7.2)$$

This orbit will be used in an example in this thesis also, and will represent the true halo orbit to compare analytic approximations with.

After solving the non-dimensional equations of motion with nonlinear simulation using the fourth order Runge-Kutta numerical integration algorithm with a time step of $\Delta t = 0.0001$, the position and velocity error in exact periodicity is

$$\begin{aligned}
\Delta x &= x(T) - x(0) = -5.568454057873762e\text{-}04 \\
\Delta y &= y(T) - y(0) = 1.670398000067595e\text{-}04 \\
\Delta z &= z(T) - z(0) = 2.488929981720595e\text{-}05 \\
\Delta \dot{x} &= \dot{x}(T) - \dot{x}(0) = -0.001629620221659 \\
\Delta \dot{y} &= \dot{y}(T) - \dot{y}(0) = 6.381568099895763e\text{-}04 \\
\Delta \dot{z} &= \dot{z}(T) - \dot{z}(0) = 1.479102133680319e\text{-}04
\end{aligned} \tag{2.7.3}$$

Values at t = T were obtained by linear interpolation between the simulation output values. Initial condition precision of 10^{-8} (see Equation (2.7.2)) and position-velocity periodicity error of only 10^{-3} (see Equation (2.7.3)) is inconsistent. Discrepancies could be due to different computational resources available in 1984[15] vs. today, truncation in reported initial condition values ($z_0 = 0.04$),[15] typographical error in published literature ($\mu = 0.04$),[15] or some other reason. Therefore, initial condition values in Equation (2.7.2) were updated with a differential correction process[15] whereby x_0 is fixed at Equation (2.7.2) value and $\dot{y}_0$, z_0 , T are allowed to vary until 10^{-8} periodicity error is achieved. Updated initial condition values are

$$\begin{aligned}
&x_0 = 0.723268,\ \dot{y}_0 = 0.198019,\ z_0 = 0.039993891964 \\
&T = 2(1.300177),\ t_0 = 0,\ \ \mu = 0.04
\end{aligned} \tag{2.7.4}$$

Corresponding position and velocity errors after one period are now

$$\begin{aligned}
\Delta x &= x(T) - x(0) = 8.906621662418957e\text{-}09 \\
\Delta y &= y(T) - y(0) = -1.092678937368887e\text{-}05 \\
\Delta z &= z(T) - z(0) = 4.799122386989208e\text{-}08
\end{aligned}$$

(2.7.5)

$$\Delta\dot{x} = \dot{x}(T) - \dot{x}(0) = -9.000247425235077e\text{-}06$$

$$\Delta\dot{y} = \dot{y}(T) - \dot{y}(0) = -6.104191499489708e\text{-}08$$

$$\Delta\dot{z} = \dot{z}(T) - \dot{z}(0) = 1.008889975478254e\text{-}05$$

Figures 6-9 show the resulting halo orbit and typical characteristics of this type of orbit. A three-dimensional perspective view and three sectional views are provided in Figures 6-9. The xy and yz sectional views illustrate the symmetric nature of the halo orbit and the "egg" shaped oval characteristic. The xz sectional view exhibits the distortion of motion within a single plane to a fully three-dimensional motion behavior. The orbit in Figures 6-9 and described by Equations (2.6.6)-(2.6.8) is an exact solution to the three-body problem and will be used as a truth reference to compare against.

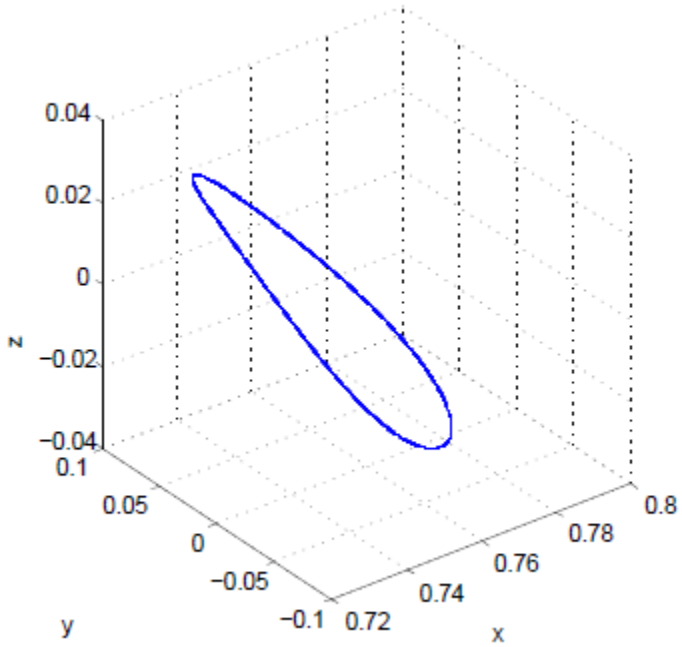

Figure 6 Three-Dimensional Perspective View of Halo Orbit

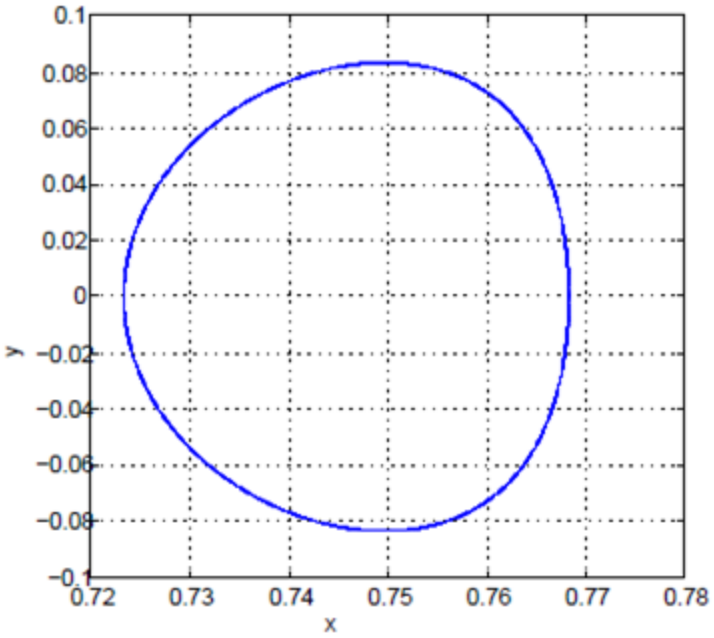

Figure 7 xy Sectional View of Halo Orbit

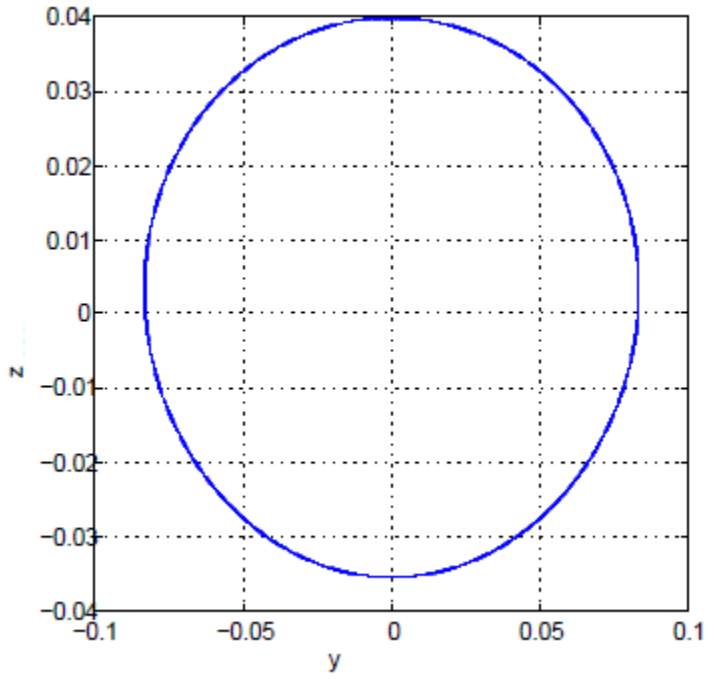

Figure 8 yz Sectional View of Halo Orbit

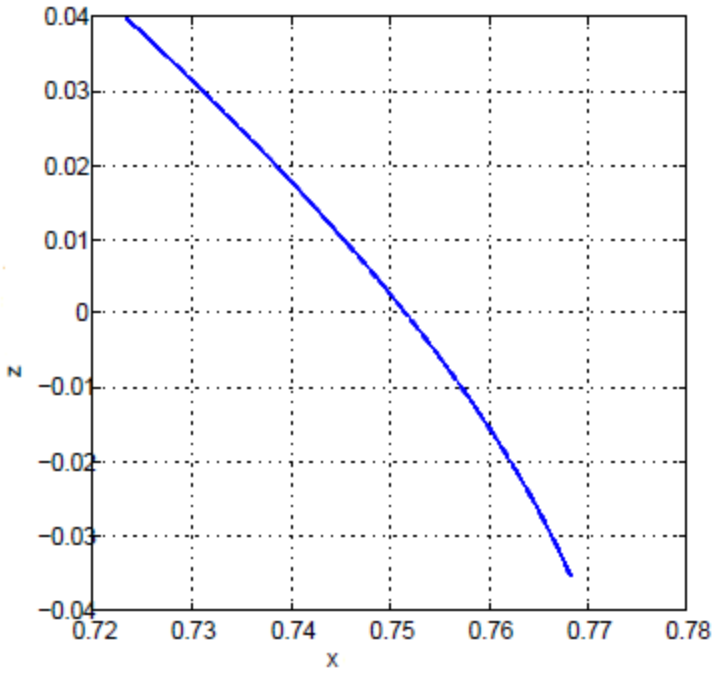

Figure 9 xz Sectional View of Halo Orbit

CHAPTER 3

SUPPOSITIONAL CIRCULAR MOTION

3.1 Introduction

The third body equations of motion given by Equations (2.2.41)-(2.2.43) are second order coupled nonlinear ordinary differential equations whose closed-form analytic solution is not known to exist. Some special solutions are available like Lagrange points, the Jacobi integral equation, and the zero velocity curves which were discussed in the previous chapter. Another special solution is the rectilinear oscillation of the third body along a line passing through the mass center and perpendicular to the plane of the rotation of the primaries (i.e., xy plane), where primaries are of equal mass. In this problem, equations of motion in the x axis and y axis are satisfied in a trivial manner while the z axis equation becomes the governing equation of motion, which can be solved using elliptic functions and the period is obtained in closed-form.[14] Another approach by Battin[10] is to start from Jacobi's integral equation and to use elliptic functions which gives the same motion but with different mathematical structure. In this chapter, an attempt to analytically construct a periodic orbit around collinear Lagrange points is investigated. A suppositional or base solution is constructed using Jacobi elliptic functions and following a similar approach as conducted in the case of the rectilinear oscillation solution, this base solution is employed into the Jacobi integral equation.

Ghazy and Newman[9] proposed a suppositional vertical circular orbit for the third body in a plane which is perpendicular to the line joining the primaries and is offset by a constant distance d_x from the yz plane of the rotating coordinate frame. The y coordinate and the z coordinate of the base solution were selected as the sin and cosine functions of the angle the radius vector to the third body makes with the "vertical" axis. Note this selection leaves the time variation of angular coordinate undetermined. The base solution from Reference 9 was

$$x(t) = d_x \tag{3.1.1}$$

$$y(t) = a\,\sin(\theta(t)) \tag{3.1.2}$$

$$z(t) = a\,\cos(\theta(t)) \tag{3.1.3}$$

This assumption satisfies Jacobi's integral equation. Further, upon integrating Jacobi's integral equation again, the period is obtained in closed-form which uses the complete elliptic integral of the first kind K(k), where k is the modulus of the elliptic functions. Angular velocity $\dot{\theta}(t)$ is also analytically obtained as a function of the time. These findings from Reference 9 are

$$T = \frac{4kK(k)}{\omega} \tag{3.1.4}$$

$$\dot{\theta}(t) = \frac{\omega}{k}\,\mathrm{dn}\left(-\frac{\omega}{k}(t-t_0)+F\left(\frac{\pi}{2}-\theta_0\,,k\right),k\right) \tag{3.1.5}$$

$$\cos(\theta(t)) = \mathrm{sn}\left(-\frac{\omega}{k}(t-t_0)+F\left(\frac{\pi}{2}-\theta_0\,,k\right),k\right) \tag{3.1.6}$$

$$\sin(\theta(t)) = \mathrm{cn}\left(-\frac{\omega}{k}(t-t_0)+F\left(\frac{\pi}{2}-\theta_0\,,k\right),k\right) \tag{3.1.7}$$

The motion obtained after integrating Jacobi's integral equation roughly captures the non-uniform speed characteristic exhibited by periodic halo orbits obtained though numerical integration.[9] The base solution was shown to satisfy the third body equation of motion in the x axis in the bounded and averaged sense, while the other two motion equations are approximately satisfied. The tangential equation of motion was shown to be exactly satisfied. These findings and progress inspired the hypothesis that the incorporation of non-uniform speed behavior in the base solution at the initial step of the construction would induce more accurate behavior in the base and corrected solutions. In the thesis research, Jacobi elliptic functions sn(·) and cn(·) having arguments as linear functions of time, are utilized in the base construction. This step is a distinguishing feature of the thesis work when compared with Reference 9.

3.2 Vertical Circular Orbit

Consider Figure 10 for the CRTBP, with center of mass at the origin of the right-handed rotating coordinate system xyz, and larger primary mass m_1 in the positive direction of the x axis for consistency of analysis. A new plane y'z' perpendicular to the x axis at a distance d_x from the yz plane is constructed. Let the third body exactly traverse a circle in this new y'z' plane. This

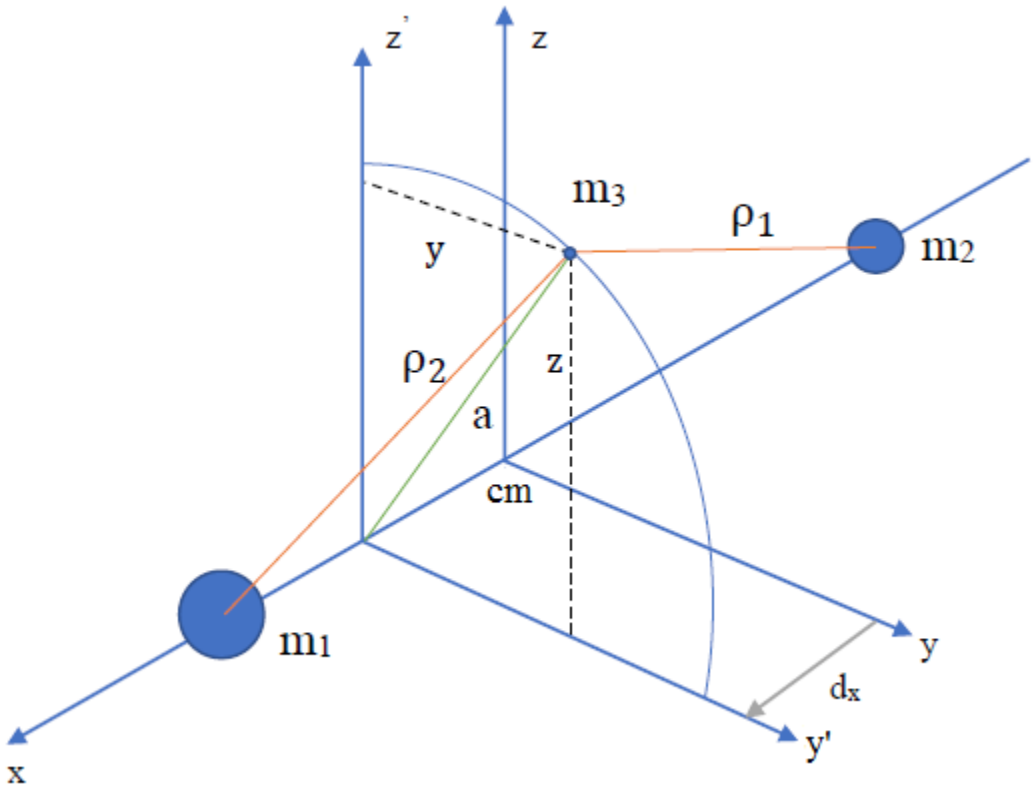

Figure 10 Suppositional Vertical Circular Orbit

type of motion is not exactly allowed by the third body governing dynamics in the CRTBP, but, it is hoped that a higher order correction or perturbation technique in the form[9] of Fourier series can approximate closely the exact numerical solution of the governing three-body equations. The radius of this circle is denoted by "a", while x_1, x_2, ρ_1, ρ_2 have their usual meaning.

The suppositional circular motion is defined as

$$x(t) = d_x \tag{3.2.1}$$

$$y(t) = a\ sn(\lambda\tau, k) \tag{3.2.2}$$

$$z(t) = a\ cn(\lambda\tau, k) \tag{3.2.3}$$

where $\tau = t-\phi$ is the transformed time and t is the actual time of the motion. Note there is no physical angle in the argument of the elliptic functions, in contrast to the Reference 9 assumptions. Also note parameter ϕ plays the role of a phase angle offset, while λ is a frequency of motion. Parameters a, λ, and ϕ are all constants and k is the modulus of the elliptic functions. An important characteristic of this motion is that the sum squares of the varying y and z coordinates is constant and is shown from an elliptic function identity.

$$\left(sn(\lambda\tau, k)\right)^2+\left(cn(\lambda\tau, k)\right)^2= 1 \tag{3.2.4}$$

$$\left(y(t)\right)^2+\left(z(t)\right)^2= a^2\left(\left(sn(\lambda\tau, k)\right)^2+\left(cn(\lambda\tau, k)\right)^2\right) = a^2 \tag{3.2.5}$$

These relations show that the locus of the third body is a circle of radius a lying in the plane y'z'. The relative distances to the third body ρ_1 and ρ_2 are given by

$$\rho_1 = \{(d_x-x_1)^2+a^2\}^{\frac{1}{2}} \tag{3.2.6}$$

$$\rho_2 = \{(d_x-x_2)^2+a^2\}^{\frac{1}{2}} \tag{3.2.7}$$

In other words, ρ_1 and ρ_2 both are constants and independent of time for the supposed motion.

As $\tau = t-\phi$, and ϕ being a constant,

$$d\tau = dt \tag{3.2.8}$$

Differentiating Equations (3.2.1)-(3.2.3) with respect to the actual time of the motion t and noting $d\tau = dt$, yields

$$\dot{x}(t) = 0 \tag{3.2.9}$$

$$\dot{y}(t) = a\lambda\, cn(\lambda\tau, k)\, dn(\lambda\tau, k) \tag{3.2.10}$$

$$\dot{z}(t) = -a\lambda\, sn(\lambda\tau, k)\, dn(\lambda\tau, k) \tag{3.2.11}$$

Now, from Jacobi's integral equation,

$$C = 2J - V^2 \tag{3.2.12}$$

For the suppositional motion, the Jacobi constant is

$$C = \omega^2\left(d_x{}^2 + a^2\left(sn(\lambda\tau, k)\right)^2\right) + 2\frac{\mu_1}{\rho_1} + 2\frac{\mu_2}{\rho_2} - V^2 \tag{3.2.13}$$

where ρ_1 and ρ_2 are given by Equations (3.2.6) and (3.2.7), and the quantity V^2 is

$$V^2 = \left(\dot{x}(t)\right)^2 + \left(\dot{y}(t)\right)^2 + \left(\dot{z}(t)\right)^2 = a^2\lambda^2\left(dn(\lambda\tau, k)\right)^2 \tag{3.2.14}$$

Hence, the Jacobi constant can now be written as,

$$C = \omega^2\left(d_x{}^2 + a^2\left(sn(\lambda\tau, k)\right)^2\right) + 2\frac{\mu_1}{\rho_1} + 2\frac{\mu_2}{\rho_2} - a^2\lambda^2\left(dn(\lambda\tau, k)\right)^2 \tag{3.2.15}$$

The value of C at time $t = \phi$, i.e. when $\tau = 0$ is given as

$$C_{\tau=0} = \omega^2\left(d_x{}^2\right) + 2\frac{\mu_1}{\rho_1} + 2\frac{\mu_2}{\rho_2} - a^2\lambda^2 \tag{3.2.16}$$

Since C is constant throughout the motion,

$$C_{\tau=0} = C_{\tau=\tau} = C \tag{3.2.17}$$

Thus, equating Equation (3.2.15) and Equation (3.2.16) yields

$$\omega^2\left(d_x{}^2 + a^2\left(sn(\lambda\tau, k)\right)^2\right) + 2\frac{\mu_1}{\rho_1} + 2\frac{\mu_2}{\rho_2} - a^2\lambda^2\left(dn(\lambda\tau, k)\right)^2 = \omega^2\left(d_x{}^2\right) + 2\frac{\mu_1}{\rho_1} + 2\frac{\mu_2}{\rho_2} - a^2\lambda^2 \tag{3.2.18}$$

Cancelling out common terms on both sides,

$$\omega^2 a^2\left(sn(\lambda\tau, k)\right)^2 - a^2\lambda^2\left(dn(\lambda\tau, k)\right)^2 = -a^2\lambda^2 \tag{3.2.19}$$

Inserting the relation,[21] $k^2\left(sn(\lambda\tau, k)\right)^2 + \left(dn(\lambda\tau, k)\right)^2 = 1$, into Equation (3.2.19) yields

$$\omega^2 a^2 \left(sn(\lambda\tau, k)\right)^2 + k^2 a^2 \lambda^2 \left(sn(\lambda\tau, k)\right)^2 = 0 \tag{3.2.20}$$

or

$$a^2 \left(sn(\lambda\tau, k)\right)^2 \left(\omega^2 + k^2\lambda^2\right) = 0 \tag{3.2.21}$$

Now, in Equation (3.2.21), $a^2 \neq 0$ and $\left(sn(\lambda\tau, k)\right)^2 \neq 0$ (since, a finite radius circle is assumed and the y coordinate is assumed to be a function of time). This observation gives

$$\omega^2 + k^2\lambda^2 = 0 \tag{3.2.22}$$

$$k = \pm \frac{\omega}{\lambda} i \tag{3.2.23}$$

where "i" is the imaginary number $i = \sqrt{-1}$.

Thus, to satisfy Jacobi's integral equation, the elliptic modulus in the suppositional base solution should be taken as an imaginary number given by Equation (3.2.23). The negative complex value for k is theoretically consistent, but in applications to engineering and physics, positive roots are conventionally selected, and this choice would match the usual case where $0 < k < 1$ for real modulus frameworks. So, retaining only the positive complex number value for k in Equation (3.2.23) gives

$$k = \frac{\omega}{\lambda} i \tag{3.2.24}$$

Now, starting the suppositional process again with the base solution having k taken as $\frac{\omega}{\lambda} i$ yields

$$x(t) = d_x \tag{3.2.25}$$

$$y(t) = a\, sn\left(\lambda\tau, \frac{\omega}{\lambda} i\right) \tag{3.2.26}$$

$$z(t) = a\ cn\left(\lambda\tau,\ \frac{\omega}{\lambda}i\right) \tag{3.2.27}$$

Satisfaction of Jacobi's integral equation by this new but equivalent form of the supposition can be verified. This result may sound like an obvious fact but it is not, because now an imaginary modulus is present in the analysis. However, all the formulas and derivatives for real modulus elliptic functions remain valid for imaginary modulus arguments also.[21]

Conversion of the imaginary modulus formulation to an equivalent real modulus formulation is possible and considered next. Re-express the above suppositional equations in terms of a real modulus by using the transformation equations from imaginary modulus to real modulus as[21]

$$sn(u, ik) = k_1^{'}\ sd\left(u\sqrt{1+k^2}\ ,\ k_1\right) \tag{3.2.28}$$

$$cn(u, ik) = cd\left(u\sqrt{1+k^2}\ ,\ k_1\right) \tag{3.2.29}$$

Thus, elliptic functions sn(·) and cn(·) with imaginary modulus ik get transformed to elliptic functions sd(·) and cd(·) with real modulus k_1 where k_1 is given by

$$k_1 = \frac{k}{\sqrt{1+k^2}} \tag{3.2.30}$$

and $k_1^{'}$ is the complementary modulus of k_1 defined by

$$k_1^{'} = \sqrt{1-k_1^{\ 2}} = \frac{1}{\sqrt{1+k^2}} \tag{3.2.31}$$

Now, the base solution given by Equations (3.2.1)-(3.2.3) can be expressed in the form of elliptic functions sd(·) and cd(·) using the above format.

Using Equations (3.2.28)-(3.2.31),

$$u = \lambda\tau$$

$$k = \frac{\omega}{\lambda}$$

(3.2.32)

$$k_1=\frac{\frac{\omega}{\lambda}}{\sqrt{1+\left(\frac{\omega}{\lambda}\right)^2}}=\frac{\omega}{\sqrt{\lambda^2+\omega^2}} \quad \text{and} \quad k_1^{'}=\frac{1}{\sqrt{1+\left(\frac{\omega}{\lambda}\right)^2}}=\frac{\lambda}{\sqrt{\lambda^2+\omega^2}}$$

The transformed base solution is thus obtained as follows.

$$x(t) = d_x \tag{3.2.33}$$

$$y(t) = a\ sn(u, ik\ ) \tag{3.2.34}$$

$$= ak_1^{'} sd\left(u\sqrt{1+k^2}\ , k_1\right) \tag{3.2.35}$$

$$=\frac{a\lambda}{\sqrt{\lambda^2+\omega^2}}\ sd\left(\lambda\tau\ \sqrt{1+\left(\frac{\omega}{\lambda}\right)^2}\ , \frac{\omega}{\sqrt{\lambda^2+\omega^2}}\right) \tag{3.2.36}$$

$$=\frac{a\lambda}{\sqrt{\lambda^2+\omega^2}}\ sd\left(\tau\ \sqrt{\lambda^2+\omega^2}\ , \frac{\omega}{\sqrt{\lambda^2+\omega^2}}\right) \tag{3.2.37}$$

$$z(t) = a\ cn(u, ik\ ) \tag{3.2.38}$$

$$= a\ cd\left(u\sqrt{1+k^2}\ , k_1\right) \tag{3.2.39}$$

$$= a\ cd\left(\lambda\tau\ \sqrt{1+\left(\frac{\omega}{\lambda}\right)^2}\ , \frac{\omega}{\sqrt{\lambda^2+\omega^2}}\right) \tag{3.2.40}$$

$$= a\ cd\left(\tau\ \sqrt{\lambda^2+\omega^2}\ , \frac{\omega}{\sqrt{\lambda^2+\omega^2}}\right) \tag{3.2.41}$$

Now, using an identity for elliptic functions[21]

$$\left(y(t)\right)^2+\left(z(t)\right)^2=a^2\left(\left(k_1^{'}\right)^2\left(sd\left(u\sqrt{1+k^2}\ , k_1\right)\right)^2+\left(cd\left(u\sqrt{1+k^2}\ , k_1\ \right)\right)^2\right)=a^2 \tag{3.2.42}$$

This relation confirms the same suppositional circle is present. To be consistent with analysis, re-verify that this formulation satisfies the Jacobi integral equation.

Differentiating Equations (3.2.33), (3.2.37), and (3.2.41) with respect to time t.

$$\dot{x}(t) = 0 \tag{3.2.43}$$

$$\dot{y}(t) = \frac{d}{dt}\left[\frac{a\lambda}{\sqrt{\lambda^2+\omega^2}} \ \mathrm{sd}\left(\tau \ \sqrt{\lambda^2+\omega^2} \, , \ \frac{\omega}{\sqrt{\lambda^2+\omega^2}} \right) \right] \tag{3.2.44}$$

$$= \frac{a\lambda}{\sqrt{\lambda^2+\omega^2}} \ \mathrm{cn}\left(\tau \ \sqrt{\lambda^2+\omega^2} \, , \ \frac{\omega}{\sqrt{\lambda^2+\omega^2}} \right) \left(\mathrm{nd}\left(\tau \ \sqrt{\lambda^2+\omega^2} \, , \ \frac{\omega}{\sqrt{\lambda^2+\omega^2}} \right) \right)^2 \sqrt{\lambda^2+\omega^2} \ \frac{d\tau}{dt} \tag{3.2.45}$$

$$= a\lambda \ \mathrm{cn}\left(\tau \ \sqrt{\lambda^2+\omega^2} \, , \ \frac{\omega}{\sqrt{\lambda^2+\omega^2}} \right) \left(\mathrm{nd}\left(\tau \ \sqrt{\lambda^2+\omega^2} \, , \ \frac{\omega}{\sqrt{\lambda^2+\omega^2}} \right) \right)^2 \tag{3.2.46}$$

$$\dot{z}(t) = \frac{d}{dt}\left[a \ \mathrm{cd}\left(\tau \ \sqrt{\lambda^2+\omega^2} \, , \ \frac{\omega}{\sqrt{\lambda^2+\omega^2}} \right) \right] \tag{3.2.47}$$

$$= -a\left(k_1^{'}\right)^2 \ \mathrm{sn}\left(\tau \ \sqrt{\lambda^2+\omega^2} \, , \ \frac{\omega}{\sqrt{\lambda^2+\omega^2}} \right) \left(\mathrm{nd}\left(\tau \ \sqrt{\lambda^2+\omega^2} \, , \ \frac{\omega}{\sqrt{\lambda^2+\omega^2}} \right) \right)^2 \sqrt{\lambda^2+\omega^2} \ \frac{d\tau}{dt} \tag{3.2.48}$$

$$= \frac{-a\lambda^2}{\lambda^2+\omega^2} \ \mathrm{sn}\left(\tau \ \sqrt{\lambda^2+\omega^2} \, , \ \frac{\omega}{\sqrt{\lambda^2+\omega^2}} \right) \left(\mathrm{nd}\left(\tau \ \sqrt{\lambda^2+\omega^2} \, , \ \frac{\omega}{\sqrt{\lambda^2+\omega^2}} \right) \right)^2 \sqrt{\lambda^2+\omega^2} \ \frac{d\tau}{dt} \tag{3.2.49}$$

$$= \frac{-a\lambda^2}{\sqrt{\lambda^2+\omega^2}} \ \mathrm{sn}\left(\tau \ \sqrt{\lambda^2+\omega^2} \, , \ \frac{\omega}{\sqrt{\lambda^2+\omega^2}} \right) \left(\mathrm{nd}\left(\tau \ \sqrt{\lambda^2+\omega^2} \, , \ \frac{\omega}{\sqrt{\lambda^2+\omega^2}} \right) \right)^2 \tag{3.2.50}$$

The quantity V^2 becomes,

$$V^2 = \left(\dot{x}(t)\right)^2 + \left(\dot{y}(t)\right)^2 + \left(\dot{z}(t)\right)^2 \tag{3.2.51}$$

$$= 0+a^2\lambda^2\left[\mathrm{cn}\left(\tau\sqrt{\lambda^2+\omega^2}, \frac{\omega}{\sqrt{\lambda^2+\omega^2}}\right)\right]^2\left[\mathrm{nd}\left(\tau\sqrt{\lambda^2+\omega^2}, \frac{\omega}{\sqrt{\lambda^2+\omega^2}}\right)\right]^4$$

$$+\frac{a^2\lambda^4}{\lambda^2+\omega^2}\left[\mathrm{sn}\left(\tau\sqrt{\lambda^2+\omega^2}, \frac{\omega}{\sqrt{\lambda^2+\omega^2}}\right)\right]^2\left[\mathrm{nd}\left(\tau\sqrt{\lambda^2+\omega^2}, \frac{\omega}{\sqrt{\lambda^2+\omega^2}}\right)\right]^4 \qquad (3.2.52)$$

The Jacobi constant is

$$C = \omega^2\left(d_x{}^2+\left[\frac{a\lambda}{\sqrt{\lambda^2+\omega^2}}\ \mathrm{sd}\left(\tau\sqrt{\lambda^2+\omega^2}, \frac{\omega}{\sqrt{\lambda^2+\omega^2}}\right)\right]^2\right)+2\frac{\mu_1}{\rho_1}+2\frac{\mu_2}{\rho_2}$$

$$-a^2\lambda^2\left[\mathrm{cn}\left(\tau\sqrt{\lambda^2+\omega^2}, \frac{\omega}{\sqrt{\lambda^2+\omega^2}}\right)\right]^2\left[\mathrm{nd}\left(\tau\sqrt{\lambda^2+\omega^2}, \frac{\omega}{\sqrt{\lambda^2+\omega^2}}\right)\right]^4$$

$$-\frac{a^2\lambda^4}{\lambda^2+\omega^2}\left[\mathrm{sn}\left(\tau\sqrt{\lambda^2+\omega^2}, \frac{\omega}{\sqrt{\lambda^2+\omega^2}}\right)\right]^2\left[\mathrm{nd}\left(\tau\sqrt{\lambda^2+\omega^2}, \frac{\omega}{\sqrt{\lambda^2+\omega^2}}\right)\right]^4 \qquad (3.2.53)$$

The value of C at the time $t = \phi$, i.e., when $\tau = 0$, is given by

$$C_{\tau=0} = \omega^2\left(d_x{}^2\right)+2\frac{\mu_1}{\rho_1}+2\frac{\mu_2}{\rho_2}-a^2\lambda^2 \qquad (3.2.54)$$

Now, to show that the Jacobi's integral equation is satisfied, the condition $C_{\tau=0} = C_{\tau=\tau} = C$ must be satisfied, i.e., it must be shown that the value of C at any time is equal to the one given by Equation (3.2.54). Simplifying the expression for C given by Equation (3.2.53)

$$C = \omega^2\left(d_x{}^2+\left[\frac{a\lambda}{\sqrt{\lambda^2+\omega^2}}\ \mathrm{sd}\left(\tau\sqrt{\lambda^2+\omega^2}, \frac{\omega}{\sqrt{\lambda^2+\omega^2}}\right)\right]^2\right)+2\frac{\mu_1}{\rho_1}+2\frac{\mu_2}{\rho_2}$$

$$-a^2\lambda^2\left[\mathrm{nd}\left(\tau\sqrt{\lambda^2+\omega^2},\frac{\omega}{\sqrt{\lambda^2+\omega^2}}\right)\right]^4\left(\begin{array}{c}\left[\mathrm{cn}\left(\tau\sqrt{\lambda^2+\omega^2},\frac{\omega}{\sqrt{\lambda^2+\omega^2}}\right)\right]^2\\+\frac{\lambda^2}{\lambda^2+\omega^2}\left[\mathrm{sn}\left(\tau\sqrt{\lambda^2+\omega^2},\frac{\omega}{\sqrt{\lambda^2+\omega^2}}\right)\right]^2\end{array}\right) \tag{3.2.55}$$

Now, the last bracketed term on the right-hand side of Equation (3.2.55) can be simplified using the relations[21]

$$\left(k_1^{'}\right)^2\mathrm{sn}^2(\cdot)+\mathrm{cn}^2(\cdot)=\mathrm{dn}^2(\cdot) \tag{3.2.56}$$

$$\mathrm{nd}(\cdot)=\frac{1}{\mathrm{dn}(\cdot)} \tag{3.2.57}$$

C now becomes

$$C=\omega^2\left(d_x{}^2+\left[\frac{a\lambda}{\sqrt{\lambda^2+\omega^2}}\ \mathrm{sd}\left(\tau\sqrt{\lambda^2+\omega^2},\frac{\omega}{\sqrt{\lambda^2+\omega^2}}\right)\right]^2\right)+2\frac{\mu_1}{\rho_1}+2\frac{\mu_2}{\rho_2}$$

$$-a^2\lambda^2\left[\mathrm{nd}\left(\tau\sqrt{\lambda^2+\omega^2},\frac{\omega}{\sqrt{\lambda^2+\omega^2}}\right)\right]^2 \tag{3.2.58}$$

Also, simplifying further using the relation[21]

$$(k_1)^2\mathrm{sd}^2(\cdot)+1=\mathrm{nd}^2(\cdot) \tag{3.2.59}$$

The final value for C is obtained as

$$C=\omega^2\left(d_x{}^2\right)+2\frac{\mu_1}{\rho_1}+2\frac{\mu_2}{\rho_2}-a^2\lambda^2 \tag{3.2.60}$$

Thus, the new formulation given by Equations (3.2.33)-(3.2.41) with real elliptic modulus satisfies the Jacobi integral equation.

3.3 Determination of Constants from Initial Conditions

Rewrite the base solution and its derivative with respect to time.

$$x(t) = d_x \tag{3.3.1}$$

$$y(t) = \frac{a\lambda}{\sqrt{\lambda^2+\omega^2}}\ \mathrm{sd}\left(\tau\ \sqrt{\lambda^2+\omega^2}\ ,\ \frac{\omega}{\sqrt{\lambda^2+\omega^2}}\right) \tag{3.3.2}$$

$$z(t) = a\ \mathrm{cd}\left(\tau\ \sqrt{\lambda^2+\omega^2}\ ,\ \frac{\omega}{\sqrt{\lambda^2+\omega^2}}\right) \tag{3.3.3}$$

$$\dot{x}(t) = 0 \tag{3.3.4}$$

$$\dot{y}(t) = a\lambda\ \mathrm{cn}\left(\tau\ \sqrt{\lambda^2+\omega^2}\ ,\ \frac{\omega}{\sqrt{\lambda^2+\omega^2}}\right)\left(\mathrm{nd}\left(\tau\ \sqrt{\lambda^2+\omega^2}\ ,\ \frac{\omega}{\sqrt{\lambda^2+\omega^2}}\right)\right)^2 \tag{3.3.5}$$

$$\dot{z}(t) = \frac{-a\lambda^2}{\sqrt{\lambda^2+\omega^2}}\ \mathrm{sn}\left(\tau\ \sqrt{\lambda^2+\omega^2}\ ,\ \frac{\omega}{\sqrt{\lambda^2+\omega^2}}\right)\left(\mathrm{nd}\left(\tau\ \sqrt{\lambda^2+\omega^2}\ ,\ \frac{\omega}{\sqrt{\lambda^2+\omega^2}}\right)\right)^2 \tag{3.3.6}$$

The constants a, λ, and ϕ are to be determined from the initial conditions, i.e., when $t = 0$ or $\tau = -\phi$. Denoting $\tau_0 = -\phi$, initial condition now corresponds to $t = 0$ or $\tau = \tau_0$. Suppose, a set of initial coordinates and velocities of the third body are provided as

$$x(0) = x_0 \tag{3.3.7}$$

$$y(0) = y_0 \tag{3.3.8}$$

$$z(0) = z_0 \tag{3.3.9}$$

$$\dot{x}(0) = \dot{x}_0 \tag{3.3.10}$$

$$\dot{y}(0) = \dot{y}_0 \tag{3.3.11}$$

$$\dot{z}(0) = \dot{z}_0 \tag{3.3.12}$$

These six conditions are not completely arbitrary. Some restrictions exist on choosing the initial conditions. The third body cannot have velocity in x direction. So $\dot{x}$ must be zero initially, although initial x can be chosen arbitrarily, which remains constant throughout the motion on the suppositional circle.

Also, from Equations (3.3.2), (3.3.3), (3.3.5), and (3.3.6), the following relation is obtained

$$\frac{y(t)}{z(t)} = -\frac{\dot{z}(t)}{\dot{y}(t)} \tag{3.3.13}$$

which also holds true for initial conditions.

$$\frac{y(0)}{z(0)} = -\frac{\dot{z}(0)}{\dot{y}(0)} \quad \text{or} \quad \frac{y_0}{z_0} = -\frac{\dot{z}_0}{\dot{y}_0} \tag{3.3.14}$$

Thus, any three initial values out of y_0, z_0, $\dot{y}_0$, and $\dot{z}_0$ can be chosen with freedom while the fourth initial condition gets automatically fixed, which is a restriction on the choice.

If the base solution and its derivatives are considered only for the y and z coordinates, and when considering Equation (3.3.14), there are only three independent equations with three constants a, λ, and ϕ. This observation indicates the values of all the constants can be derived from the three independent initial conditions. This outcome is necessarily true if the equations are linear, but in the case of nonlinear equations, constants are not always obtainable in analytic form. However, in this problem, the constants are obtainable in closed-form.

Substituting $\tau = \tau_0$ and initial values given by Equations (3.3.7)-(3.3.12) into Equations (3.3.1) - (3.3.6), yields

$$x_0 = d_x \tag{3.3.15}$$

$$y_0 = \frac{a\lambda}{\sqrt{\lambda^2+\omega^2}}\ \mathrm{sd}\left(\tau_0\sqrt{\lambda^2+\omega^2}\,,\ \frac{\omega}{\sqrt{\lambda^2+\omega^2}}\right) \tag{3.3.16}$$

$$z_0 = a\ \mathrm{cd}\left(\tau_0\ \sqrt{\lambda^2+\omega^2}\,,\ \frac{\omega}{\sqrt{\lambda^2+\omega^2}}\right) \tag{3.3.17}$$

$$\dot{x}_0 = 0 \tag{3.3.18}$$

$$\dot{y}_0 = a\lambda\ \mathrm{cn}\left(\tau_0\sqrt{\lambda^2+\omega^2}\,,\ \frac{\omega}{\sqrt{\lambda^2+\omega^2}}\right)\left(\mathrm{nd}\left(\tau_0\ \sqrt{\lambda^2+\omega^2}\,,\ \frac{\omega}{\sqrt{\lambda^2+\omega^2}}\right)\right)^2 \tag{3.3.19}$$

$$\dot{z}_0 = \frac{-a\lambda^2}{\sqrt{\lambda^2+\omega^2}}\ \mathrm{sn}\left(\tau_0\sqrt{\lambda^2+\omega^2}\,,\ \frac{\omega}{\sqrt{\lambda^2+\omega^2}}\right)\left(\mathrm{nd}\left(\tau_0\sqrt{\lambda^2+\omega^2}\,,\ \frac{\omega}{\sqrt{\lambda^2+\omega^2}}\right)\right)^2 \tag{3.3.20}$$

Circle radius a can be obtained as follows.

$$a^2 = {y_0}^2+{z_0}^2 \tag{3.3.21}$$

To obtain frequency λ,

$$\left(\frac{\dot{y}_0}{z_0}\right)^2 = \lambda^2\left(\mathrm{nd}\left(\tau_0\ \sqrt{\lambda^2+\omega^2}\,,\ \frac{\omega}{\sqrt{\lambda^2+\omega^2}}\right)\right)^2 \tag{3.3.22}$$

$$\left(\frac{\omega y_0}{a}\right)^2 = \frac{\omega^2\lambda^2}{\lambda^2+\omega^2}\left(\mathrm{sd}\left(\tau_0\sqrt{\lambda^2+\omega^2}\,,\ \frac{\omega}{\sqrt{\lambda^2+\omega^2}}\right)\right)^2 \tag{3.3.23}$$

$$\left(\frac{\dot{y}_0}{z_0}\right)^2 - \left(\frac{\omega y_0}{a}\right)^2 = \lambda^2\left(\mathrm{nd}\left(\tau_0\ \sqrt{\lambda^2+\omega^2}\,,\ \frac{\omega}{\sqrt{\lambda^2+\omega^2}}\right)\right)^2$$

$$-\frac{\omega^2\lambda^2}{\lambda^2+\omega^2}\left(\mathrm{sd}\left(\tau_0\sqrt{\lambda^2+\omega^2},\frac{\omega}{\sqrt{\lambda^2+\omega^2}}\right)\right)^2 \tag{3.3.24}$$

Using the relation written in Equation (3.2.59),

$$\left(\frac{\dot{y}_0}{z_0}\right)^2-\left(\frac{\omega y_0}{a}\right)^2=\lambda^2\left(\frac{\omega^2}{\lambda^2+\omega^2}\left(\mathrm{sd}\left(\tau_0\sqrt{\lambda^2+\omega^2},\frac{\omega}{\sqrt{\lambda^2+\omega^2}}\right)\right)^2+1\right)$$

$$-\frac{\omega^2\lambda^2}{\lambda^2+\omega^2}\left(\mathrm{sd}\left(\tau_0\sqrt{\lambda^2+\omega^2},\frac{\omega}{\sqrt{\lambda^2+\omega^2}}\right)\right)^2 \tag{3.3.25}$$

$$=\lambda^2 \tag{3.3.26}$$

Hence, frequency λ is given by

$$\lambda=\pm\sqrt{\left(\frac{\dot{y}_0}{z_0}\right)^2-\left(\frac{\omega y_0}{a}\right)^2} \tag{3.3.27}$$

The remaining constant $\tau_0 = -\phi$ can be calculated using

$$z_0=a\,\mathrm{cd}\left(\tau_0\sqrt{\lambda^2+\omega^2},\frac{\omega}{\sqrt{\lambda^2+\omega^2}}\right) \tag{3.3.28}$$

3.4 Constraints on Frequency and Elliptic Modulus

Two values for λ with opposite signs were obtained in Equation (3.3.27). The constant τ_0 obtained from z_0 in Equation (3.3.28) can also take two values, because cd(·) is an even function. On the other hand sd(·) is an odd function and in the expression for y_0 in Equation (3.3.16), λ is a multiplier. Thus, there are four combinations of choices for λ and τ_0 out of which two are valid depending on the sign of y_0. The following table is provided for clarity.

Table 1 Possible Values of λ and τ_0

τ_0	λ	y_0
+	+	+P
-	+	-P
+	-	-P
-	-	+P

Three observations are made.

1. Depending on whether the provided value for y_0 is +P or -P where P is the magnitude of y_0 , there are two choices for selecting the combination of λ and τ_0 . In the case where $\tau_0 = 0$, then $\dot{y}_b(0) = a\lambda$. So, the value of $\dot{y}(0)$ determines the sign of λ.

2. Frequency λ cannot be a complex number, because in that case, the motion outputs are obtained as complex numbers. Therefore, the quantity $\left(\frac{\dot{y}_0}{z_0}\right)^2 - \left(\frac{\omega y_0}{a}\right)^2$ should always be a positive number, i.e.,

$$\left(\frac{\dot{y}_0}{z_0}\right)^2 > \left(\frac{\omega y_0}{a}\right)^2$$

which is another constraint on the initial conditions. The equality condition is excluded to avoid zero frequency.

3. Also, frequency λ cannot be zero, because then $k_1 = 1$ and $K(1) = \infty$, which means the solution for period (see Section 3.5) T is infinite.

3.5 Periodicity

The period of the elliptic functions sd (u, k_1) and cd (u, k_1) is $4K(k_1)$. Equations (3.3.16) and (3.3.17) for the base solution indicate argument u is given by $\tau\sqrt{\lambda^2+\omega^2}$

Thus, the period T of the base solution is

$$T = \frac{4K(k_1)}{\sqrt{\lambda^2+\omega^2}} \qquad (3.5.1)$$

If k and λ are used interchangeably, i.e., $k = \frac{\omega}{\lambda}$, then the period T can also be written as

$$T = \frac{4kK(k_1)}{\omega\sqrt{1+k^2}} \tag{3.5.2}$$

Although Equation (3.5.2) is a valid expression, it may not be fully appropriate here because elliptic modulus, usually denoted by symbol k, lies between 0 and 1. However, in this development k equals $\frac{\omega}{\lambda}$ which can be greater than 1. Remember that k does not really play a role in this development nor it is required because the actual modulus is k_1, which always is between 0 and 1 as mentioned before. Modulus k_1 depends only on λ for a specific CRTBP according to Equation (3.2.32). So, λ seems to be the sole important parameter for determining period T.

Figure 11 demonstrates the non-dimensional period T against various values of λ. Considering non-dimensional forms for the equations of motion and taking the value of ω equal to one, the plot obtained is true for any case of the circular restricted three-body problem. As the value of λ (which is dependent on the initial condition) increases, the non-dimensional time for the third body to complete one revolution on the suppositional circle decreases. Likewise, as λ decreases, the T increases.

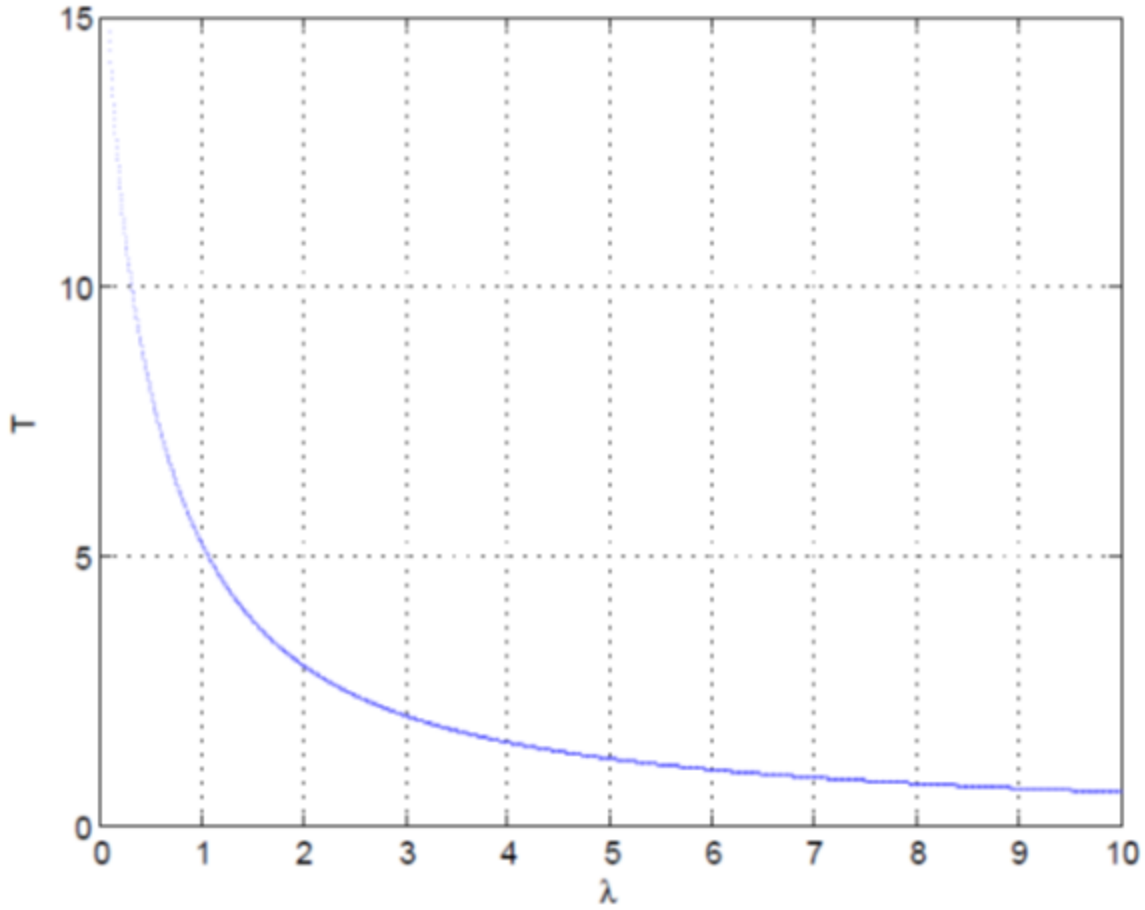

Figure 11 Period T of Base Solution Against frequency λ

3.6 Base Solution Accuracy

The base solution is now substituted into the third body equations of motion. For that, the second order derivatives of the base solution are needed and writing them and substituting in real modulus form becomes overly complicated. So, the complex modulus form of the base solution is considered when taking the first and second order derivatives.

$$x(t) = d_x \tag{3.6.1}$$

$$y(t) = a\ sn\left(\lambda\tau, \frac{\omega}{\lambda} i\ \right) \tag{3.6.2}$$

$$z(t) = a\ cn\left(\lambda\tau, \frac{\omega}{\lambda} i\right) \tag{3.6.3}$$

From the Section 3.4, λ can be any real number except zero. The first derivatives are

$$\dot{x}(t) = 0 \tag{3.6.4}$$

$$\dot{y}(t) = a\lambda \, cn\left(\lambda\tau, \frac{\omega}{\lambda}i\right) dn\left(\lambda\tau, \frac{\omega}{\lambda}i\right) \tag{3.6.5}$$

$$\dot{z}(t) = -a\lambda \, sn\left(\lambda\tau, \frac{\omega}{\lambda}i\right) dn\left(\lambda\tau, \frac{\omega}{\lambda}i\right) \tag{3.6.6}$$

And the second order derivatives are

$$\ddot{x}(t) = 0 \tag{3.6.7}$$

$$\ddot{y}(t) = a\lambda^2 \left(\begin{array}{c} cn\left(\lambda\tau, \frac{\omega}{\lambda}i\right)\left(\left(\frac{\omega}{\lambda}\right)^2 sn\left(\lambda\tau, \frac{\omega}{\lambda}i\right) cn\left(\lambda\tau, \frac{\omega}{\lambda}i\right)\right) \\ +dn\left(\lambda\tau, \frac{\omega}{\lambda}i\right)\left(-sn\left(\lambda\tau, \frac{\omega}{\lambda}i\right) dn\left(\lambda\tau, \frac{\omega}{\lambda}i\right)\right) \end{array} \right) \tag{3.6.8}$$

$$\ddot{z}(t) = -a\lambda^2 \left(\begin{array}{c} sn\left(\lambda\tau, \frac{\omega}{\lambda}i\right)\left(\left(\frac{\omega}{\lambda}\right)^2 sn\left(\lambda\tau, \frac{\omega}{\lambda}i\right) cn\left(\lambda\tau, \frac{\omega}{\lambda}i\right)\right) \\ +dn\left(\lambda\tau, \frac{\omega}{\lambda}i\right)\left(cn\left(\lambda\tau, \frac{\omega}{\lambda}i\right) dn\left(\lambda\tau, \frac{\omega}{\lambda}i\right)\right) \end{array} \right) \tag{3.6.9}$$

Using shorthand notations "sn", "cn", "dn" and substituting these into third-body equations of motion

$$0-\omega^2 d_x - 2\omega a\lambda \, cn \, dn + \frac{\mu_1}{((d_x-x_1)^2+a^2)^{\frac{3}{2}}}(d_x-x_1) + \frac{\mu_2}{((d_x-x_2)^2+a^2)^{\frac{3}{2}}}(d_x-x_2) = 0 \tag{3.6.10}$$

$$a\lambda^2\left(cn\left(\left(\frac{\omega}{\lambda}\right)^2 sn \, cn\right) + dn\,(-sn\, dn)\right) - \omega^2 a \, sn + \frac{\mu_1 a \, sn}{((d_x-x_1)^2+a^2)^{\frac{3}{2}}} + \frac{\mu_2 a \, sn}{((d_x-x_2)^2+a^2)^{\frac{3}{2}}} = 0 \tag{3.6.11}$$

$$-a\lambda^2\left(sn\left(\left(\frac{\omega}{\lambda}\right)^2 sn \, cn\right) + dn\,(cn\, dn)\right) + \frac{\mu_1 a \, cn}{((d_x-x_1)^2+a^2)^{\frac{3}{2}}} + \frac{\mu_2 a \, cn}{((d_x-x_2)^2+a^2)^{\frac{3}{2}}} = 0 \tag{3.6.12}$$

Multiplying Equation (3.6.11) by cn and Equation (3.6.12) by sn and subtracting yields

$$a\lambda^2\left(cn\left(\left(\frac{\omega}{\lambda}\right)^2 sn\right)\right)-\omega^2 a\ sn\ cn = 0$$

or

$$0 = 0 \tag{3.6.13}$$

This result shows that suppositional motion satisfies the combination of second and third equations of motion (i.e., the transverse equation of motion). However, the y and z motion equations might not get satisfied individually. The first equation can also be written as

$$-2\omega a\lambda\ cn\ dn = -\frac{\mu_1}{((d_x-x_1)^2+a^2)^{\frac{3}{2}}}(d_x-x_1)-\frac{\mu_2}{((d_x-x_2)^2+a^2)^{\frac{3}{2}}}(d_x-x_2)+\omega^2 d_x \tag{3.6.14}$$

In Equation (3.6.14), the left-hand side represents a term variable with time while the right-hand side is a constant, which implies this relation cannot be correct for a finite segment of time as cn(·) and dn(·) are continuously changing in value.

However, Equation (3.6.14) can be shown to be satisfied in an averaged sense if the plane y'z' is selected to pass through one of the collinear Lagrange points.If d_x = representing Lagrange points L_1, L_2, L_3 and $a \ll (d_x-x_i)_{,\ \text{for i=1,2,}}$ then the radius can be neglected and the right-hand term in Equation (3.6.14) becomes zero, approximately. Now the left-hand side term $-2\omega a\lambda\ cn\ dn$ is a finite zero mean oscillating perturbation. To show this, the term is averaged by integrating with respect to time over a general whole orbit.

$$[-2\omega\dot{y}]_{avg} = \frac{-2\omega a\lambda}{T}\int_{\tau_0}^{\tau_0+T} cn\ dn\ d\tau = \frac{-2\omega a\lambda}{T}[sn]_{\tau_0}^{\tau_0+T} = 0 \tag{3.6.15}$$

$$[-2\omega\dot{y}]_{avg} = \frac{-2\omega a\lambda}{T}\int_{\tau_0}^{\tau_0+T} cn\ dn\ d\tau = \frac{-2\omega a\lambda}{T}\left[\frac{\lambda}{\sqrt{\lambda^2+\omega^2}}\ sd\left(\tau\ \sqrt{\lambda^2+\omega^2}\ ,\ \frac{\omega}{\sqrt{\lambda^2+\omega^2}}\right)\right]_{\tau_0}^{\tau_0+T} = 0$$

(3.6.16)

Both the sn(·) and sd(·) functions are periodic and when evaluated at the indicated limits produce a value of zero.

Also, the term -2ωaλ cn dn is bounded and this property can be shown by differentiating the term and equating it to zero to find maxima and minima and the time corresponding to them.

$$\frac{d}{dt}[-2\omega\dot{y}] = -2\omega\ddot{y}$$

$$= -2\omega a\lambda^2 \begin{pmatrix} \mathrm{cn}\left(\lambda\tau, \frac{\omega}{\lambda} i\right)\left(\left(\frac{\omega}{\lambda}\right)^2 \mathrm{sn}\left(\lambda\tau, \frac{\omega}{\lambda} i\right) \mathrm{cn}\left(\lambda\tau, \frac{\omega}{\lambda} i\right)\right) \\ +\mathrm{dn}\left(\lambda\tau, \frac{\omega}{\lambda} i\right)\left(-\mathrm{sn}\left(\lambda\tau, \frac{\omega}{\lambda} i\right) \mathrm{dn}\left(\lambda\tau, \frac{\omega}{\lambda} i\right)\right) \end{pmatrix}$$

$$= -2\omega a\lambda^2 \mathrm{sn}\left(\lambda\tau, \frac{\omega}{\lambda} i\right) \left(\left(\mathrm{cn}\left(\lambda\tau, \frac{\omega}{\lambda} i\right)\right)^2 \left(\frac{\omega}{\lambda}\right)^2 - \left(\mathrm{dn}\left(\lambda\tau, \frac{\omega}{\lambda} i\right)\right)^2\right) \quad (3.6.17)$$

Using the relation, $dn^2 = 1-k^2sn^2 = 1-k^2+k^2cn^2$ and putting $k = \frac{\omega}{\lambda} i$

$$\frac{d}{dt}[-2\omega\dot{y}] = -2\omega a\lambda^2 \mathrm{sn}\left(\lambda\tau, \frac{\omega}{\lambda} i\right) \left(2\left(\mathrm{cn}\left(\lambda\tau, \frac{\omega}{\lambda} i\right)\right)^2 \left(\frac{\omega}{\lambda}\right)^2 -1- \left(\frac{\omega}{\lambda}\right)^2\right) \quad (3.6.18)$$

Applying the condition for an extremum results in

$$\frac{d}{dt}[-2\omega\dot{y}] = 0 \Rightarrow \mathrm{sn}\left(\lambda\tau, \frac{\omega}{\lambda} i\right) = 0 \quad (3.6.19)$$

Or equivalently

$$\frac{\lambda}{\sqrt{\lambda^2+\omega^2}} \mathrm{sd}\left(\tau \sqrt{\lambda^2+\omega^2}, \frac{\omega}{\sqrt{\lambda^2+\omega^2}}\right) = 0 \quad (3.6.20)$$

This condition occurs i.e when $\tau = 0$ or $t = \phi$. The other condition for extremum is

$$\left(2\left(\mathrm{cn}\left(\lambda\tau, \frac{\omega}{\lambda} i\right)\right)^2 \left(\frac{\omega}{\lambda}\right)^2 -1- \left(\frac{\omega}{\lambda}\right)^2\right) = 0 \Rightarrow \quad \mathrm{cn}\left(\lambda\tau, \frac{\omega}{\lambda} i\right) = \pm\frac{\sqrt{\lambda^2+\omega^2}}{\sqrt{2}\omega} \quad (3.6.21)$$

or

$$\mathrm{cd}\left(\tau\ \sqrt{\lambda^2+\omega^2}\ ,\ \frac{\omega}{\sqrt{\lambda^2+\omega^2}}\right)=\pm\frac{\sqrt{\lambda^2+\omega^2}}{\sqrt{2}\omega} \tag{3.6.22}$$

This second condition occurs when $\tau=\frac{1}{\sqrt{\lambda^2+\omega^2}}\ \mathrm{cd}^{-1}\left(\pm\frac{\sqrt{\lambda^2+\omega^2}}{\sqrt{2}\omega}\ ,\ \frac{\omega}{\sqrt{\lambda^2+\omega^2}}\right)$

Since, cn(·) and dn(·) are actually cd(·) and nd(·) functions with real modulus, then at $\tau = 0$, both of them are equal to unity. Evaluating the term $-2\omega\dot{y}$ at $\tau = 0$ gives the maximum and minimum for the first condition, or

$$[-2\omega\dot{y}]_{\tau=0} = -2\omega a\lambda \tag{3.6.23}$$

Now consider the relation,

$$(k_1)^2\mathrm{cd}^2+\left(k_1^{'}\right)^2\mathrm{nd}^2 = 1 \tag{3.6.24}$$

If the value for cd(·) is known from Equation (3.6.22), then the value for nd(·) can be obtained as

$$\mathrm{nd}\left(\tau\ \sqrt{\lambda^2+\omega^2}\ ,\ \frac{\omega}{\sqrt{\lambda^2+\omega^2}}\right)=\pm\frac{\sqrt{\lambda^2+\omega^2}}{\sqrt{2}\lambda} \tag{3.6.25}$$

Hence,

$$[-2\omega\dot{y}]_{\tau=\frac{1}{\sqrt{\lambda^2+\omega^2}}\mathrm{cd}^{-1}\left(\frac{\sqrt{\lambda^2+\omega^2}}{\sqrt{2}\omega},\frac{\omega}{\sqrt{\lambda^2+\omega^2}}\right)} = -2\omega a\lambda\left(\pm\frac{\sqrt{\lambda^2+\omega^2}}{\sqrt{2}\omega}\right)\left(\pm\frac{\sqrt{2}\lambda}{\sqrt{\lambda^2+\omega^2}}\right)$$

$$= \pm\ 2a\lambda^2 \tag{3.6.26}$$

Thus, the maximum and minimum values for the term $-2\omega\dot{y}$ are finite and equal to $+2a\lambda^2$ and $-2a\lambda^2$ respectively.

In summary, the first equation of motion (x) is satisfied in an averaged and bounded sense when the suppositional circle lies in the y'z' plane passing through the collinear libration points. Further, a combination of the second (y) and third (z) equations of motion are satisfied precisely, but not individually. Thus, the base solution , though exactly not correct, partially satisfies the second and third equations of motion and the first equation can be approximately correct in the special case of halo orbits around L_1, L_2, L_3 in the indicated sense. To improve on accuracy, a correction process is considered in the next chapter.

CHAPTER 4

FIRST ORDER CORRECTION TO THE BASE SOLUTION

The correction procedure in this chapter is similar to that in Ghazy and Newman.[9] The third body equations of motion (2.2.41)-(2.2.43) can be used to correct the suppositional motion results using an iterative analytic approximate procedure. Assuming a motion for the x axis, motion in the y and z axes is solved using the second and third equations of motion respectively. These results constitute the base solution: x_b, $y_b(t)$, $z_b(t)$. Now, the base solutions in the y and z axes are used to solve for a correction to the x axis base solution, i.e., $x_{c1}(t)$. The total solution can now be expanded as the base plus first correction, some approximations being invoked in doing so. Then for a first order correction in the y and z axes, i.e., $y_{c1}(t)$ and $z_{c1}(t)$, the x axis first correction is used in equations for the y and z axes. The procedure can be iterated for higher order corrections. This correction procedure outlined in this chapter is also general and does not pertain to any specific three-body problem. Table 2 outlines the correction procedure.

Table 2 Outline of Higher Order Correction to Base Solution.

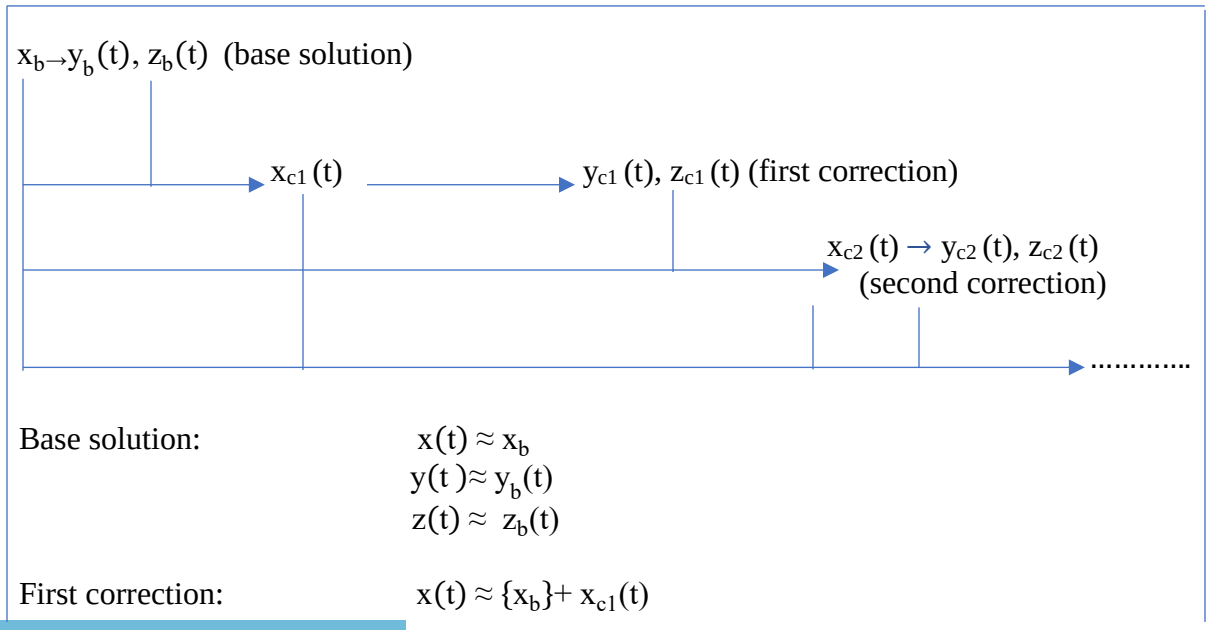

	$y(t) \approx \{y_b(t)\} + y_{c1}(t)$ $z(t) \approx \{z_b(t)\} + z_{c1}(t)$
Second correction:	$x(t) \approx \{x_b + x_{c1}(t)\} + x_{c2}(t)$ $y(t) \approx \{y_b(t) + y_{c1}(t)\} + y_{c2}(t)$ $z(t) \approx \{z_b(t) + z_{c1}(t)\} + z_{c2}(t)$

First, a correction to x_b is discussed. Substituting $x(t) = x_b + x_{c1}(t)$, $y(t) = y_b(t)$, and $z(t) = z_b(t)$ into Equation (2.2.41) yields

$$\ddot{x}_{c1}(t) - 2\omega\dot{y}_b(t) = \omega^2[x_b + x_{c1}(t)] - \frac{Gm_1}{\left[(x_b + x_{c1}(t) - x_1)^2 + \left(y_b(t)\right)^2 + (z_b(t))^2\right]^{3/2}}(x_b + x_{c1}(t) - x_1)$$

$$- \frac{Gm_2}{\left[(x_b + x_{c1}(t) - x_2)^2 + \left(y_b(t)\right)^2 + (z_b(t))^2\right]^{3/2}}(x_b + x_{c1}(t) - x_2) \qquad (4.1)$$

Expanding the nonlinear gravitational terms about the base solution in Equation (4.1), yields

$$\ddot{x}_{c1}(t) - 2\omega\dot{y}_b(t) = \omega^2[x_b + x_{c1}(t)] - Gm_1\left[\frac{x_b - x_1}{\rho_1^3} + \left\{\frac{1}{\rho_1^3} - \frac{3(x_b - x_1)^2}{\rho_1^5}\right\}x_{c1}(t) + \ldots\right]$$

$$- Gm_2\left[\frac{x_b - x_2}{\rho_2^3} + \left\{\frac{1}{\rho_2^3} - \frac{3(x_b - x_2)^2}{\rho_2^5}\right\}x_{c1}(t) + \ldots\right] \qquad (4.2)$$

Selecting d_x as one of the collinear libration points, i.e., $d_x = \xi_1$, ξ_2, or ξ_3 and cancelling out the embedded (approximate bounded averaged) base solution ($a \ll (d_x - x_i)$, $i = 1,2$) and deleting higher-order terms in $x_{c1}(t)$ $\left(|x_{c1}(t)| \ll \rho_i \text{ for } i = 1,2\right)$, one finds

$$\ddot{x}_{c1}(t) + \left[-\omega^2 + G\left\{m_1\left(\frac{1}{\rho_1^3} - \frac{3(x_b - x_1)^2}{\rho_1^5}\right) + m_2\left(\frac{1}{\rho_2^3} - \frac{3(x_b - x_2)^2}{\rho_2^5}\right)\right\}\right]x_{c1}(t) = 2\omega\dot{y}_b(t) \qquad (4.3)$$

$$\ddot{x}_{c1}(t) + G\left\{m_1\left(\frac{1}{\rho_1^3} - \frac{3(x_b - x_1)^2}{\rho_1^5} - \frac{1}{r_{12}^3}\right) + m_2\left(\frac{1}{\rho_2^3} - \frac{3(x_b - x_2)^2}{\rho_2^5} - \frac{1}{r_{12}^3}\right)\right\}x_{c1}(t) = 2\omega\dot{y}_b(t) \qquad (4.4)$$

Depending on the sign of the gravitational coefficient, Equation (4.4) represents a stable-unstable forced second order linear time invariant dynamic system. Only the unstable case is considered further.

$$\ddot{x}_{c1}(t)-\lambda_{c1}^2\, x_{c1}(t) = 2\omega\dot{y}_b(t) \tag{4.5}$$

$$\lambda_{c1}^2 = \omega^2-G\left\{m_1\left(\frac{1}{\rho_1^3}-\frac{3(x_b-x_1)^2}{\rho_1^5}\right)+ m_2\left(\frac{1}{\rho_2^3}-\frac{3(x_b-x_2)^2}{\rho_2^5}\right)\right\}> 0 \tag{4.6}$$

The forcing function in Equation (4.5) is

$$2\omega\dot{y}_b(t) = 2\omega a\lambda\, cn\left(\tau\ \sqrt{\lambda^2+\omega^2}\ ,\ \frac{\omega}{\sqrt{\lambda^2+\omega^2}}\right)\left(nd\left(\tau\ \sqrt{\lambda^2+\omega^2}\ ,\ \frac{\omega}{\sqrt{\lambda^2+\omega^2}}\right)\right)^2 \tag{4.7}$$

This forcing can also be written as

$$2\omega\dot{y}_b(t) = 2\omega a\lambda\, cd\left(\tau\ \sqrt{\lambda^2+\omega^2}\ ,\ \frac{\omega}{\sqrt{\lambda^2+\omega^2}}\right)\left(nd\left(\tau\ \sqrt{\lambda^2+\omega^2}\ ,\ \frac{\omega}{\sqrt{\lambda^2+\omega^2}}\right)\right) \tag{4.8}$$

In terms of the nome expansion, the forcing function becomes

$$2\omega\dot{y}_b(t) = 2\omega a\lambda\left[\frac{2\pi}{k_1K(k_1)}\sum_{m=0}^{\infty}(-1)^m\frac{q^{m+\frac{1}{2}}}{1-q^{2m+1}}\cos\left\{\frac{(2m+1)\pi}{2K(k_1)}\tau\sqrt{\lambda^2+\omega^2}\right\}\right]\bullet$$

$$\left[\frac{\pi}{2K(k_1)k_1^{'}}+\frac{2\pi}{K(k_1)k_1^{'}}\sum_{p=0}^{\infty}(-1)^{p+1}\frac{q^{p+1}}{1+q^{2(p+1)}}\cos\left\{\frac{(p+1)\pi}{K(k_1)}\tau\ \sqrt{\lambda^2+\omega^2}\right\}\right] \tag{4.9}$$

where

$$k_1=\frac{\omega}{\sqrt{\lambda^2+\omega^2}}\ ,\ k_1^{'}=\frac{\lambda}{\sqrt{\lambda^2+\omega^2}}\ ,\quad q=e^{\frac{-\pi K^{'}}{K}} \tag{4.10}$$

In the above expressions , $K(k_1)$ is the is the complete elliptic integral of the first kind corresponding to elliptic modulus k_1, $K'(k_1^{'})$ the complete elliptic integral of the first kind

corresponding to elliptic modulus k_1' and $q = e^{\frac{-\pi K'}{K}}$ is the nome. Substituting the expressions of k_1 and k_1' into Equation (4.9), forcing term $2\omega\dot{y}_b(t)$ can also be written as

$$2\omega\dot{y}_b(t) = 2\omega a\lambda\left[\frac{2\pi\sqrt{\lambda^2+\omega^2}}{\omega K(k_1)}\sum_{m=0}^{\infty}(-1)^m\frac{q^{m+\frac{1}{2}}}{1-q^{2m+1}}\cos\left\{\frac{(2m+1)\pi}{2K(k_1)}\tau\sqrt{\lambda^2+\omega^2}\right\}\right]\bullet$$
$$\left[\frac{\pi\sqrt{\lambda^2+\omega^2}}{2\lambda K(k_1)}+\frac{2\pi\sqrt{\lambda^2+\omega^2}}{\lambda K(k_1)}\sum_{p=0}^{\infty}(-1)^{p+1}\frac{q^{p+1}}{1+q^{2(p+1)}}\cos\left\{\frac{(p+1)\pi}{K(k_1)}\tau\ \sqrt{\lambda^2+\omega^2}\right\}\right] \qquad (4.11)$$

Simplifying further,

$$2\omega\dot{y}_b(t) = c_Q\left[\sum_{m=0}^{\infty}Q_m\cos\{\omega_m\tau\}+4\sum_{m=0}^{\infty}\sum_{p=0}^{\infty}Q_{mp}\cos\{\omega_m\tau\}\cos\{\omega_p\tau\}\right] \qquad (4.12)$$

where

$$c_Q=\frac{2\pi^2 a\,(\lambda^2+\omega^2)}{\left(K(k_1)\right)^2}$$

$$Q_m=(-1)^m\frac{q^{m+\frac{1}{2}}}{1-q^{2m+1}}\ ,\qquad Q_{mp}=(-1)^{m+p+1}\frac{q^{m+\frac{1}{2}}}{1-q^{2m+1}}\ \frac{q^{p+1}}{1+q^{2(p+1)}} \qquad (4.13)$$

$$\omega_m=\frac{(2m+1)\pi}{2K(k_1)}\sqrt{\lambda^2+\omega^2}\ ,\quad \omega_p=\frac{(p+1)\pi}{K(k_1)}\sqrt{\lambda^2+\omega^2}$$

The homogeneous solution to Equation (4.5) is

$$x_{c1H}(t) = A_1e^{\lambda_{c1}t}+A_2e^{-\lambda_{c1}t} \qquad (4.14)$$

whereas the non-homogeneous solution can be written as

$$x_{c1NH}(t) = c_Q\sum_{m=0}^{\infty}\frac{Q_m}{-\omega_m{}^2-\lambda_{c1}^2}\cos\{\omega_m\tau\}$$
$$+\,4c_Q\sum_{m=0}^{\infty}\sum_{p=0}^{\infty}\frac{Q_{mp}}{2\left[-\left(\omega_m-\omega_p\right)^2-\lambda_{c1}^2\right]}\cos\{(\omega_m-\omega_p)\tau\}$$

$$+ 4c_Q \sum_{m=0}^{\infty}\sum_{p=0}^{\infty} \frac{Q_{mp}}{2\left[-(\omega_m+\omega_p)^2-\lambda_{c1}^2\right]} \cos\{(\omega_m+\omega_p)\tau\} \tag{4.15}$$

So, the complete solution for the x axis first correction is

$$\begin{aligned} x_{c1}(t) = A_1 e^{\lambda_{c1}t} + A_2 e^{-\lambda_{c1}t} &+ c_Q \sum_{m=0}^{\infty} \frac{Q_m}{-\omega_m^2-\lambda_{c1}^2} \cos\{\omega_m\tau\} \\ &+ 4c_Q \sum_{m=0}^{\infty}\sum_{p=0}^{\infty} \frac{Q_{mp}}{2\left[-(\omega_m-\omega_p)^2-\lambda_{c1}^2\right]} \cos\{(\omega_m-\omega_p)\tau\} \\ &+ 4c_Q \sum_{m=0}^{\infty}\sum_{p=0}^{\infty} \frac{Q_{mp}}{2\left[-(\omega_m+\omega_p)^2-\lambda_{c1}^2\right]} \cos\{(\omega_m+\omega_p)\tau\} \end{aligned} \tag{4.16}$$

Determining A_1 and A_2 requires the initial values for x_{c1} and $\dot{x}_{c1}$.

So, differentiating $x_{c1}(t)$ with respect to time t gives

$$\begin{aligned} \dot{x}_{c1}(t) = \lambda_{c1}A_1 e^{\lambda_{c1}t} - \lambda_{c1}A_2 e^{-\lambda_{c1}t} &+ c_Q \sum_{m=0}^{\infty} \frac{Q_m\omega_m}{-\omega_m^2-\lambda_{c1}^2} (-\sin\{\omega_m\tau\}) \\ &+ 4c_Q \sum_{m=0}^{\infty}\sum_{p=0}^{\infty} \frac{Q_{mp}(\omega_m-\omega_p)}{2\left[-(\omega_m-\omega_p)^2-\lambda_{c1}^2\right]} (-\sin\{(\omega_m-\omega_p)\tau\}) \\ &+ 4c_Q \sum_{m=0}^{\infty}\sum_{p=0}^{\infty} \frac{Q_{mp}(\omega_m+\omega_p)}{2\left[-(\omega_m+\omega_p)^2-\lambda_{c1}^2\right]} (-\sin\{(\omega_m+\omega_p)\tau\}) \end{aligned} \tag{4.17}$$

Let the initial conditions be

$$x_{c1}(0) = x_{c10} \quad \text{and } \dot{x}_{c1}(0) = \dot{x}_{c10} \tag{4.18}$$

Substituting these values into Equation (4.16) and (4.17) respectively and noting at $t = 0$, or $\tau = \tau_0$

$$x_{c1}(0) = x_{c10} = A_1 + A_2 + c_Q \sum_{m=0}^{\infty} \frac{Q_m}{-\omega_m^2-\lambda_{c1}^2} \cos\{\omega_m\tau_0\}$$

$$+4c_Q\sum_{m=0}^{\infty}\sum_{p=0}^{\infty}\frac{Q_{mp}}{2\left[-(\omega_m-\omega_p)^2-\lambda_{c1}^2\right]}\cos\{(\omega_m-\omega_p)\tau_0\}$$

$$+4c_Q\sum_{m=0}^{\infty}\sum_{p=0}^{\infty}\frac{Q_{mp}}{2\left[-(\omega_m+\omega_p)^2-\lambda_{c1}^2\right]}\cos\{(\omega_m+\omega_p)\tau_0\}$$

$$=A_1+A_2+\beta_x \tag{4.19}$$

$$\dot{x}_{c1}(0)=\dot{x}_{c10}=\lambda_{c1}A_1-\lambda_{c1}A_2+c_Q\sum_{m=0}^{\infty}\frac{Q_m\omega_m}{-\omega_m^2-\lambda_{c1}^2}(-\sin\{\omega_m\tau_0\})$$

$$+4c_Q\sum_{m=0}^{\infty}\sum_{p=0}^{\infty}\frac{Q_{mp}(\omega_m-\omega_p)}{2\left[-(\omega_m-\omega_p)^2-\lambda_{c1}^2\right]}(-\sin\{(\omega_m-\omega_p)\tau_0\})$$

$$+4c_Q\sum_{m=0}^{\infty}\sum_{p=0}^{\infty}\frac{Q_{mp}(\omega_m+\omega_p)}{2\left[-(\omega_m+\omega_p)^2-\lambda_{c1}^2\right]}(-\sin\{(\omega_m+\omega_p)\tau_0\})$$

$$=\lambda_{c1}A_1-\lambda_{c1}A_2+\beta_{\dot{x}} \tag{4.20}$$

Now, from Equations (4.19) and (4.20), A_1 and A_2 can be obtained as follows

$$A_1=\frac{\lambda_{c1}x_{c10}+\dot{x}_{c10}-\lambda_{c1}\beta_x-\beta_{\dot{x}}}{2\lambda_{c1}}\quad,\quad A_2=\frac{\lambda_{c1}x_{c10}-\dot{x}_{c10}-\lambda_{c1}\beta_x+\beta_{\dot{x}}}{2\lambda_{c1}} \tag{4.21}$$

For a general set of initial conditions, and when $x_{c1}(t)$ is added to x_b, the third body will deviate from the suppositional y'z' plane with a combined multi-frequency oscillatory and aperiodic nature,[9] at least initially, when the variation from the plane is not excessive according to Equation (4.16). A special class of solution of Equation (4.16) giving unstable periodic orbits is also possible for certain initial conditions sets, for example libration point halo orbits. To do so, homogeneous coefficients A_1 and A_2 are to be nulled. An initial condition set satisfying this requirement from Equation (4.22) is

$$x_{c10}=\beta_x\,,\quad \dot{x}_{c10}=\beta_{\dot{x}} \tag{4.22}$$

Corrections to $y_b(t)$ and $z_b(t)$ will be discussed now assuming the form of the solutions as

$$x(t) = x_b + x_{c1}(t) \qquad y(t) = y_b(t) + y_{c1}(t) \qquad z(t) = z_b(t) + z_{c1}(t) \tag{4.23}$$

Substituting this form into Equations (2.2.42) and (2.2.43)

$$\ddot{y}_b(t)+\ddot{y}_{c1}(t)+2\omega\dot{x}_{c1}(t) = \omega^2\left[y_b(t)+ y_{c1}(t)\right]$$

$$- \frac{Gm_1\left(y_b(t)+y_{c1}(t)\right)}{\left[(x_b+ x_{c1}(t) - x_1)^2 + \left(y_b(t)+y_{c1}(t)\right)^2 + \left(z_b(t)+ z_{c1}(t)\right)^2\right]^{\frac{3}{2}}}$$

$$- \frac{Gm_2\left(y_b(t)+y_{c1}(t)\right)}{\left[(x_b+ x_{c1}(t) - x_2)^2 + \left(y_b(t) + y_{c1}(t)\right)^2 + \left(z_b(t)+ z_{c1}(t)\right)^2\right]^{3/2}} \tag{4.24}$$

$$\ddot{z}_b(t) + \ddot{z}_{c1}(t) = - \frac{Gm_1\left(z_b(t)+z_{c1}(t)\right)}{\left[(x_b+ x_{c1}(t)-x_1)^2+ \left(y_b(t)+y_{c1}(t)\right)^2 + \left(z_b(t)+ z_{c1}(t)\right)^2\right]^{\frac{3}{2}}}$$

$$- \frac{Gm_2\left(z_b(t)+z_{c1}(t)\right)}{\left[(x_b+ x_{c1}(t)-x_2)^2+ \left(y_b(t)+y_{c1}(t)\right)^2 + \left(z_b(t)+ z_{c1}(t)\right)^2\right]^{3/2}} \tag{4.25}$$

Gravitational expansion of these relations about the base solution provides

$$\ddot{y}_b(t)+\ddot{y}_{c1}(t)+2\omega\dot{x}_{c1}(t) = \omega^2\left[y_b(t)+ y_{c1}(t)\right]$$

$$- Gm_1\left[\frac{y_b(t)}{\rho_1^3} - \frac{3(x_b-x_1)y_b(t)}{\rho_1^5} x_{c1}(t) + \left\{\frac{1}{\rho_1^3} - \frac{3y_b^2(t)}{\rho_1^5}\right\} y_{c1}(t) - \frac{3y_b(t)z_b(t)}{\rho_1^5} z_{c1}(t) + \ldots\right]$$

$$- Gm_2\left[\frac{y_b(t)}{\rho_2^3} - \frac{3(x_b-x_2)y_b(t)}{\rho_2^5} x_{c1}(t) + \left\{\frac{1}{\rho_2^3} - \frac{3y_b^2(t)}{\rho_2^5}\right\} y_{c1}(t) - \frac{3y_b(t)z_b(t)}{\rho_2^5} z_{c1}(t) + \ldots\right] \tag{4.26}$$

$$\ddot{z}_b(t)+\ddot{z}_{c1}(t) = -Gm_1\left[\frac{z_b(t)}{\rho_1^3} - \frac{3(x_b-x_1)z_b(t)}{\rho_1^5} x_{c1}(t) + \left\{\frac{1}{\rho_1^3} - \frac{3z_b^2(t)}{\rho_1^5}\right\} z_{c1}(t) - \frac{3y_b(t)z_b(t)}{\rho_1^5} y_{c1}(t) + \ldots\right]$$

$$- Gm_2 \left[\frac{z_b(t)}{\rho_2^3} - \frac{3(x_b - x_2) z_b(t)}{\rho_2^5} x_{c1}(t) + \left\{ \frac{1}{\rho_2^3} - \frac{3 z_b^2(t)}{\rho_2^5} \right\} z_{c1}(t) - \frac{3 y_b(t) z_b(t)}{\rho_2^5} y_{c1}(t) + \ldots \right] \tag{4.27}$$

Proceed analytically by canceling out the embedded (approximate banded) base solution and delete higher order terms in $x_{c1}(t),\ y_{c1}(t),\ z_{c1}(t)$ $\left(|x_{c1}(t)|, |y_{c1}(t)|, |z_{c1}(t)| \ll \rho_i \text{ for } i = 1,2\right)$.[9]

$$\ddot{y}_{c1}(t) + \left[-\omega^2 + G \left\{ m_1 \left(\frac{1}{\rho_1^3} - \frac{3 y_b^2(t)}{\rho_1^5} \right) + m_2 \left(\frac{1}{\rho_2^3} - \frac{3 y_b^2(t)}{\rho_2^5} \right) \right\} \right] y_{c1}(t)$$

$$+ \left[-3G \left\{ m_1 \frac{y_b(t) z_b(t)}{\rho_1^5} + m_2 \frac{y_b(t) z_b(t)}{\rho_2^5} \right\} \right] z_{c1}(t)$$

$$= -2\omega \dot{x}_{c1}(t) + \left[3G \left\{ m_1 \frac{(x_b - x_1) y_b(t)}{\rho_1^5} + m_2 \frac{(x_b - x_2) y_b(t)}{\rho_2^5} \right\} \right] x_{c1}(t) \tag{4.28}$$

$$\ddot{z}_{c1}(t) + \left[G \left\{ m_1 \left(\frac{1}{\rho_1^3} - \frac{3 z_b^2(t)}{\rho_1^5} \right) + m_2 \left(\frac{1}{\rho_2^3} - \frac{3 z_b^2(t)}{\rho_2^5} \right) \right\} \right] z_{c1}(t)$$

$$+ \left[-3G \left\{ m_1 \frac{y_b(t) z_b(t)}{\rho_1^5} + m_2 \frac{y_b(t) z_b(t)}{\rho_2^5} \right\} \right] y_{c1}(t)$$

$$= \left[3G \left\{ m_1 \frac{(x_b - x_1) z_b(t)}{\rho_1^5} + m_2 \frac{(x_b - x_2) z_b(t)}{\rho_2^5} \right\} \right] x_{c1}(t) \tag{4.29}$$

Equations (4.29) and (4.30) represent two coupled forced second order linear time varying dynamic systems. Assuming y and z axis base solutions are small in comparison to the third body relative position magnitudes $\left(|y_b(t)|, |z_b(t)| \ll \rho_i^{5/2} \text{ for } i = 1,2\right)$, Equations (4.29) and (4.30) simplify to uncoupled time invariant systems.[9]

$$\ddot{y}_{c1}(t) + \left[-\omega^2 + G \left\{ \frac{m_1}{\rho_1^3} + \frac{m_2}{\rho_2^3} \right\} \right] y_{c1}(t) = -2\omega \dot{x}_{c1}(t)$$

or

$$\ddot{y}_{c1}(t) + G \left\{ m_1 \left(\frac{1}{\rho_1^3} - \frac{1}{r_{12}^3} \right) + m_2 \left(\frac{1}{\rho_2^3} - \frac{1}{r_{12}^3} \right) \right\} y_{c1}(t) = -2\omega \dot{x}_{c1}(t) \tag{4.30}$$

$$\ddot{z}_{c1}(t)+G\left\{\frac{m_1}{\rho_1^3}+\frac{m_2}{\rho_2^3}\right\}z_{c1}(t)=0 \tag{4.31}$$

The sign of the gravitational coefficient in Equation (4.31) decides whether the y axis system is stable or unstable.[9] The coefficient is positive when $\omega^2 y < -\frac{\partial U}{\partial y}$, i.e., the gravitational acceleration component in the y direction is greater than the centripetal component in the y direction (assuming $y > 0$). Small radius orbits located between the primary and secondary bodies tend to be y axis stable, such as small L_1 halo orbits. Small radius orbits lying well outside the CRTBP system (small L_2, L_3 halo orbits) or large radius orbits located anywhere along the x axis tend to be unstable. Only the stable y axis case is explored further. The z axis system in Equation (4.32) is always stable. Further note the z axis system is Coriolis unforced. Equations (4.31) and (4.32) can be rewritten as

$$\ddot{y}_{c1}(t)+\omega_{c1y}^2 y_{c1}(t)=-2\omega\dot{x}_{c1}(t) \tag{4.32}$$

$$\omega_{c1y}^2=-\omega^2+G\left\{\frac{m_1}{\rho_1^3}+\frac{m_2}{\rho_2^3}\right\}>0 \tag{4.33}$$

$$\ddot{z}_{c1}(t)+\omega_{c1z}^2 z_{c1}(t)=0 \tag{4.34}$$

$$\omega_{c1z}^2=G\left\{\frac{m_1}{\rho_1^3}+\frac{m_2}{\rho_2^3}\right\}>0 \tag{4.35}$$

Finally, the forcing function in Equation (4.33), making use of the x axis first correction in Equation (4.16), is

$$-2\omega\dot{x}_{c1}(t) = -2\omega\left\{\lambda_{c1}A_1e^{\lambda_{c1}t}-\lambda_{c1}A_2e^{-\lambda_{c1}t}+c_Q\left[\sum_{m=0}^{\infty}\frac{Q_m\omega_m}{-\omega_m{}^2-\lambda_{c1}^2}(-\sin\{\omega_m\tau\}) + 4\sum_{m=0}^{\infty}\sum_{p=0}^{\infty}\frac{Q_{mp}(\omega_m-\omega_p)}{2\left[-(\omega_m-\omega_p)^2-\lambda_{c1}^2\right]}\right.\right.$$
$$\left.\left.(-\sin\{(\omega_m-\omega_p)\tau\})+4\sum_{m=0}^{\infty}\sum_{p=0}^{\infty}\frac{Q_{mp}(\omega_m+\omega_p)}{2\left[-(\omega_m+\omega_p)^2-\lambda_{c1}^2\right]}(-\sin\{(\omega_m+\omega_p)\tau\})\right]\right\} \tag{4.36}$$

The homogeneous solution to Equation (4.32) is

$$y_{c1H}(t) = C_1\sin(\omega_{c1y}t) + C_2\cos(\omega_{c1y}t) \tag{4.37}$$

whereas the non-homogeneous solution is

$$= -2\omega\left\{\frac{\lambda_{c1}A_1}{\lambda_{c1}^2+\omega_{c1y}^2}e^{\lambda_{c1}t} - \frac{\lambda_{c1}A_2}{\lambda_{c1}^2+\omega_{c1y}^2}e^{-\lambda_{c1}t}+c_Q\left(\sum_{m=0}^{\infty}\frac{Q_m\omega_m}{-\omega_m{}^2-\lambda_{c1}^2}\left(\frac{-\sin\{\omega_m\tau\}}{-\omega_m{}^2+\omega_{c1y}^2}\right)\right.\right.$$
$$+4\sum_{m=0}^{\infty}\sum_{p=0}^{\infty}\frac{Q_{mp}(\omega_m-\omega_p)}{2\left[-(\omega_m-\omega_p)^2-\lambda_{c1}^2\right]}\left(\frac{-\sin\{(\omega_m-\omega_p)\tau\}}{-(\omega_m-\omega_p)^2+\omega_{c1y}^2}\right)$$
$$\left.\left.+4\sum_{m=0}^{\infty}\sum_{p=0}^{\infty}\frac{Q_{mp}(\omega_m+\omega_p)}{2\left[-(\omega_m+\omega_p)^2-\lambda_{c1}^2\right]}\left(\frac{-\sin\{(\omega_m+\omega_p)\tau\}}{-(\omega_m+\omega_p)^2+\omega_{c1y}^2}\right)\right)\right\} \tag{4.38}$$

Introduce constants D1 and D_2

$$D_1 = \frac{-2\omega\lambda_{c1}A_1}{\lambda_{c1}^2+\omega_{c1y}^2} \quad \text{and} \quad D_2 = \frac{2\omega\lambda_{c1}A_2}{\lambda_{c1}^2+\omega_{c1y}^2} \tag{4.39}$$

so that $y_{c1NH}(t)$ can also be represented as

$$= D_1e^{\lambda_{c1}t}+D_2e^{-\lambda_{c1}t} -2\omega c_Q\left(\sum_{m=0}^{\infty}\frac{Q_m\omega_m}{-\omega_m{}^2-\lambda_{c1}^2}\left(\frac{-\sin\{\omega_m\tau\}}{-\omega_m{}^2+\omega_{c1y}^2}\right)\right.$$
$$+4\sum_{m=0}^{\infty}\sum_{p=0}^{\infty}\frac{Q_{mp}(\omega_m-\omega_p)}{2\left[-(\omega_m-\omega_p)^2-\lambda_{c1}^2\right]}\left(\frac{-\sin\{(\omega_m-\omega_p)\tau\}}{-(\omega_m-\omega_p)^2+\omega_{c1y}^2}\right)$$
$$\left.+4\sum_{m=0}^{\infty}\sum_{p=0}^{\infty}\frac{Q_{mp}(\omega_m+\omega_p)}{2\left[-(\omega_m+\omega_p)^2-\lambda_{c1}^2\right]}\left(\frac{-\sin\{(\omega_m+\omega_p)\tau\}}{-(\omega_m+\omega_p)^2+\omega_{c1y}^2}\right)\right) \tag{4.40}$$

Thus, the complete solution to $y_{c1}(t)$ is

$$y_{c1}(t) = C_1 \sin(\omega_{c1y}t) + C_2 \cos(\omega_{c1y}t) + D_1 e^{\lambda_{c1}t} + D_2 e^{-\lambda_{c1}t} - 2\omega c_Q \left(\sum_{m=0}^{\infty} \frac{Q_m \omega_m}{-\omega_m{}^2 - \lambda_{c1}^2} \left(\frac{-\sin\{\omega_m \tau\}}{-\omega_m{}^2 + \omega_{c1y}^2} \right) \right.$$
$$+ 4 \sum_{m=0}^{\infty} \sum_{p=0}^{\infty} \frac{Q_{mp}(\omega_m - \omega_p)}{2\left[-(\omega_m - \omega_p)^2 - \lambda_{c1}^2\right]} \left(\frac{-\sin\{(\omega_m - \omega_p)\tau\}}{-(\omega_m - \omega_p)^2 + \omega_{c1y}^2} \right)$$
$$\left. + 4 \sum_{m=0}^{\infty} \sum_{p=0}^{\infty} \frac{Q_{mp}(\omega_m + \omega_p)}{2\left[-(\omega_m + \omega_p)^2 - \lambda_{c1}^2\right]} \left(\frac{-\sin\{(\omega_m + \omega_p)\tau\}}{-(\omega_m + \omega_p)^2 + \omega_{c1y}^2} \right) \right) \tag{4.41}$$

Note that in Equation (4.42), the values of D_1 and D_2 are already known, because they depend on A_1 and A_2 whose values are known from the initial values of x_{c10} and $\dot{x}_{c10}$.

To calculate C_1 and C_2 , two equations with two initial values of y_{c1} and $\dot{y}_{c1}$ are required. Hence differentiating Equation (4.42) with respect to time t gives

$$\dot{y}_{c1}(t) = C_1 \omega_{c1y} \cos(\omega_{c1y}t) -$$
$$C_2 \omega_{c1y} \sin(\omega_{c1y}t) + D_1 \lambda_{c1} e^{\lambda_{c1}t} - \lambda_{c1} D_2 e^{-\lambda_{c1}t}$$
$$-2\omega c_Q \left(\sum_{m=0}^{\infty} \frac{Q_m \omega_m{}^2}{-\omega_m{}^2 - \lambda_{c1}^2} \left(\frac{-\cos\{\omega_m \tau\}}{-\omega_m{}^2 + \omega_{c1y}^2} \right) \right.$$
$$+ 4 \sum_{m=0}^{\infty} \sum_{p=0}^{\infty} \frac{Q_{mp}(\omega_m - \omega_p)^2}{2\left[-(\omega_m - \omega_p)^2 - \lambda_{c1}^2\right]} \left(\frac{-\cos\{(\omega_m - \omega_p)\tau\}}{-(\omega_m - \omega_p)^2 + \omega_{c1y}^2} \right)$$
$$\left. + 4 \sum_{m=0}^{\infty} \sum_{p=0}^{\infty} \frac{Q_{mp}(\omega_m + \omega_p)^2}{2\left[-(\omega_m + \omega_p)^2 - \lambda_{c1}^2\right]} \left(\frac{-\cos\{(\omega_m + \omega_p)\tau\}}{-(\omega_m + \omega_p)^2 + \omega_{c1y}^2} \right) \right) \tag{4.42}$$

Let the initial conditions be

$$y_{c1}(0) = y_{c10} \quad \text{and} \quad \dot{y}_{c1}(0) = \dot{y}_{c10} \tag{4.43}$$

Substituting these values into Equation (4.41) and (4.42) respectively and noting at $t = 0$, or $\tau = \tau_0$ yields

$$y_{c1}(0) = y_{c10} = C_2+D_1+D_2$$
$$-2\omega c_Q\left(\sum_{m=0}^{\infty}\frac{Q_m\omega_m}{-\omega_m{}^2-\lambda_{c1}^2}\left(\frac{-\sin\{\omega_m\tau_0\}}{-\omega_m{}^2+\omega_{c1y}^2}\right)\right.$$
$$+4\sum_{m=0}^{\infty}\sum_{p=0}^{\infty}\frac{Q_{mp}(\omega_m-\omega_p)}{2\left[-(\omega_m-\omega_p)^2-\lambda_{c1}^2\right]}\left(\frac{-\sin\{(\omega_m-\omega_p)\tau_0\}}{-(\omega_m-\omega_p)^2+\omega_{c1y}^2}\right)$$
$$\left.+4\sum_{m=0}^{\infty}\sum_{p=0}^{\infty}\frac{Q_{mp}(\omega_m+\omega_p)}{2\left[-(\omega_m+\omega_p)^2-\lambda_{c1}^2\right]}\left(\frac{-\sin\{(\omega_m+\omega_p)\tau_0\}}{-(\omega_m+\omega_p)^2+\omega_{c1y}^2}\right)\right)$$

$$= C_2+D_1+D_2+\delta_y \tag{4.44}$$

$$\dot{y}_{c1}(0) = \dot{y}_{c10} = C_1\omega_{c1y}+D_1\lambda_{c1}-\lambda_{c1}D_2 -2\omega c_Q\left(\sum_{m=0}^{\infty}\frac{Q_m\omega_m{}^2}{-\omega_m{}^2-\lambda_{c1}^2}\left(\frac{-\cos\{\omega_m\tau_0\}}{-\omega_m{}^2+\omega_{c1y}^2}\right)\right.$$
$$+4\sum_{m=0}^{\infty}\sum_{p=0}^{\infty}\frac{Q_{mp}(\omega_m-\omega_p)^2}{2\left[-(\omega_m-\omega_p)^2-\lambda_{c1}^2\right]}\left(\frac{-\cos\{(\omega_m-\omega_p)\tau_0\}}{-(\omega_m-\omega_p)^2+\omega_{c1y}^2}\right)$$
$$\left.+4\sum_{m=0}^{\infty}\sum_{p=0}^{\infty}\frac{Q_{mp}(\omega_m+\omega_p)^2}{2\left[-(\omega_m+\omega_p)^2-\lambda_{c1}^2\right]}\left(\frac{-\cos\{(\omega_m+\omega_p)\tau_0\}}{-(\omega_m+\omega_p)^2+\omega_{c1y}^2}\right)\right)$$

$$= C_1\omega_{c1y}+D_1\lambda_{c1}-\lambda_{c1}D_2+\delta_{\dot{y}} \tag{4.45}$$

Now, from Equations (4.44) and (4.45), C_1 and C_2 can be obtained as follows

$$C_1 = \frac{\dot{y}_{c10}-D_1\lambda_{c1}+\lambda_{c1}D_2-\delta_{\dot{y}}}{\omega_{c1y}} \quad ; \; C_2 = y_{c10}-D_1-D_2-\delta_y \tag{4.46}$$

Thus, the values of C_1 and C_2 are known from the initial conditions, which when substituted into Equation (4.41), the complete solution for $y_{c1}(t)$ is known.

For a general set of initial conditions, and when $y_{c1}(t)$ is added to $y_b(t)$, the third body will deviate from the suppositional y'z' circle with a combined multi-frequency oscillatory and

aperiodic nature,[9] at least initially when the variation from the circle is not excessive according to Equation (4.41). A special class of solution of Equation (4.41) giving unstable periodic orbits is again possible for certain initial conditions. This motion is possible when the non-homogeneous coefficients D_1 and D_2 are zero, i.e., when A_1 and A_2 are zero. This condition is achieved by Equation (4.23). Finally, a further special class of unstable periodic orbits with no homogeneous frequency content occurs when C_1 and C_2 are zero. This condition is achieved when

$$y_{c10} = \delta_y \quad , \dot{y}_{c10} = \delta_{\dot{y}} \tag{4.47}$$

Being unforced in the Coriolis sense, the z axis first correction solution is much simpler, having only the homogeneous component, or

$$z_{c1}(t) = F_1 \sin(\omega_{c1z}t) + F_2 \cos(\omega_{c1z}t) \tag{4.48}$$

where

$$\omega_{c1z}^2 = G\left\{\frac{m_1}{\rho_1^3} + \frac{m_2}{\rho_2^3}\right\} \tag{4.49}$$

Differentiating Equation (4.48) with respect to time,

$$\dot{z}_{c1}(t) = F_1\omega_{c1z}\cos(\omega_{c1z}t) - F_2\omega_{c1z}\sin(\omega_{c1z}t) \tag{4.50}$$

Substituting the initial conditions $z_{c1}(0) = z_{c10}$ and $\dot{z}_{c1}(0) = \dot{z}_{c10}$ into Equations (4.48) and (4.50) respectively, F_1 and F_2 can be obtained as follows.

$$F_1 = \frac{\dot{z}_{c10}}{\omega_{c1z}} \quad , \quad F_2 = z_{c10} \tag{4.51}$$

For a given set of initial conditions, and when $z_{c1}(t)$ is added to $z_b(t)$, the third body will again move off from the supposition circle but with a single frequency oscillatory nature, [9] assuming the

initial conditions are not excessively large, according to Equation (4.48). This homogeneous motion is the only motion allowed in the z axis first correction under the stated assumptions.

This iterative procedure can be extended in a systematic fashion for higher orders, but a solution through the first correction will be sufficient here. The overall analytical approximate solution for the third body motion is thus

$$x(t) = x_b(t) + x_{c1}(t), \qquad y(t) = y_b(t) + y_{c1}(t), \qquad z(t) = z_b(t) + z_{c1}(t) \tag{4.52}$$

where $x_b(t), y_b(t), z_b(t)$ are listed in Equations (3.2.33)-(3.2.41) and $x_{c1}(t), y_{c1}(t), z_{c1}(t)$ are listed in Equations (4.16), (4.41), and (4.48).

CHAPTER 5

COMPARISON TO NUMERICAL SOLUTIONS

The analytical base and first order correction solutions developed so far are evaluated numerically and compared with the exact numerical solutions in this chapter. One periodic halo orbit around the L_1 point is used as the test case. Initially, the base orbit is compared with the true orbit and errors are evaluated. Following this, a similar analysis is carried out for the first order corrected solution. A truncated version of the x axis forcing function is considered and validated to simplify analysis. Further, an updated process to determine the frequency parameter is considered. This process is different from that studied in Reference 9, and provided improved orbital accuracy. Finally, a more careful analysis and comparison between the thesis base solution and that used in Reference 9 revealed the two suppositional orbits are exactly equivalent.

5.1 Comparison of Base and True Orbits

A periodic L_1 halo orbit with the mass ratio $\mu_2 = 0.04$ in Reference 15 is considered for comparison. The same orbit was mentioned in Section 2.7. The coordinate system used in Reference 15 is used throughout Chapter 5. The initial conditions for position and velocity of the third body in orbit are given below. The non-dimensional formulation is used in Reference 15 (similar to the one discussed in Section 2.6). The dimensional values can be obtained by multiplying the non-dimensional values for position coordinates by r_{12} , for velocity coordinates by ωr_{12} , for the period by $\frac{1}{\omega}$, and for the Jacobi constant by $\omega^2 r_{12}^2$. Subscript "h" denotes values for the exact halo orbit to be distinguished from subscript "b" denoting base solution values.

$$
\begin{aligned}
&x_{h0} = 0.723268\ r_{12} \qquad && \dot{x}_{h0} = 0 \\
&y_{h0} = 0 && \dot{y}_{h0} = 0.198019\ \omega r_{12} \\
&z_{h0} = 0.039993891964\ r_{12} && \dot{z}_{h0} = 0
\end{aligned}
\tag{5.1.1}
$$

$$T = 2.600354/\omega \qquad C = 3.329168\ \omega^2 r_{12}^2$$

With these initial conditions, the nonlinear simulation of the third body equations of motion gives an exact or true periodic orbit symmetric about xz plane, which is computationally generated in the same manner as described in Section 2.7.

This orbit is compared now with the orbit of the base solution. The initial conditions for the exact numerical orbit in Equation (5.1.1) are mapped into the initial conditions for the base solution. The d_x value of the base solution is not x_{h0} but taken as the x coordinate of the L_1 point, as this value provides a correct averaged x axis motion as discussed in the Section 3.6. The other five initial state values are identical to the corresponding true halo orbit values. All values are indicated below, along with base solution parameters a, λ, $\phi = -\tau_0$, k_1, $K(k_1)$, k and T.

$$x_{b0} = d_x = 0.74090984286\ r_{12} \qquad y_{b0} = 0 \qquad z_{b0} = 0.039993891964\ r_{12}$$

$$\dot{x}_{b0} = 0 \qquad \dot{y}_{b0} = 0.198019\ \omega r_{12} \qquad \dot{z}_{b0} = 0$$

$$a = \left(y_{b0}^2 + z_{b0}^2\right)^{\frac{1}{2}} = 0.039993891964\ r_{12}$$

$$\lambda = \pm\sqrt{\left(\frac{\dot{y}_{b0}}{z_{b0}}\right)^2 - \left(\frac{\omega y_{b0}}{a}\right)^2} = \pm 4.95123\ \omega \qquad (5.1.2)$$

$$\tau_0 = 0, \text{ i.e., } t = \tau \text{ and } \phi = 0$$

$$k_1 = \frac{\omega}{\sqrt{\lambda^2+\omega^2}} = \frac{1}{\sqrt{(\pm 4.95123)^2+1}} = 0.198\ , \quad K(k_1)=1.5865$$

$$k = \frac{\omega}{\lambda} = \pm 0.202$$

$$T = \frac{4K(k_1)}{\sqrt{\lambda^2+\omega^2}} = 1.2566/\omega$$

Note the base solution period is 1.2566/ω, which is only approximately half of the true solution period of 2.6003/ω. Out of the two values for λ , the positive value of 4.95123ω gives the proper matching of the initial time rate of change of y (See Figure 14). Recall $\dot{y}_b(0) = a\lambda$ and since $\dot{y}_b(0)$ and a are positive, then should be chosen as positive.

The figures 12-17 show the overlay plots of the x, y, and z axis motion against time for base and exact solutions. Also, the deviations from the exact motion against time are shown. The motion is plotted for one complete orbital period of the exact solution.

In Figure 12, the two-dimensional suppositional motion lying in the plane passing through libration point L_1 is exhibited by the constant base solution. From Figure 13, the maximum x positional error magnitude is $0.0274\ r_{12}$. The y and z motions in Figures 14 and 16 exhibit significant differences from the exact motions regarding frequency of oscillation, originating from the period differences. The maximum y and z position error magnitudes are $0.10125\ r_{12}$ and $0.0753\ r_{12}$, respectively, from Figures 15 and 17. Table 3 summarizes these differences between the base and true solutions for x, y, z, T and give a percent difference also. These differences clearly indicate the need for the correction solution.

Table 3 Comparison between the True and Base Orbits

	True	Base	Percentage
Maximum x Axis Error	0	$0.0274\ r_{12}$	2.74
Maximum y Axis Error	0	$0.10125\ r_{12}$	10.125
Maximum z Axis Error	0	$0.0753\ r_{12}$	7.53
Period	$2.603/\omega$	$1.2566/\omega$	51.725

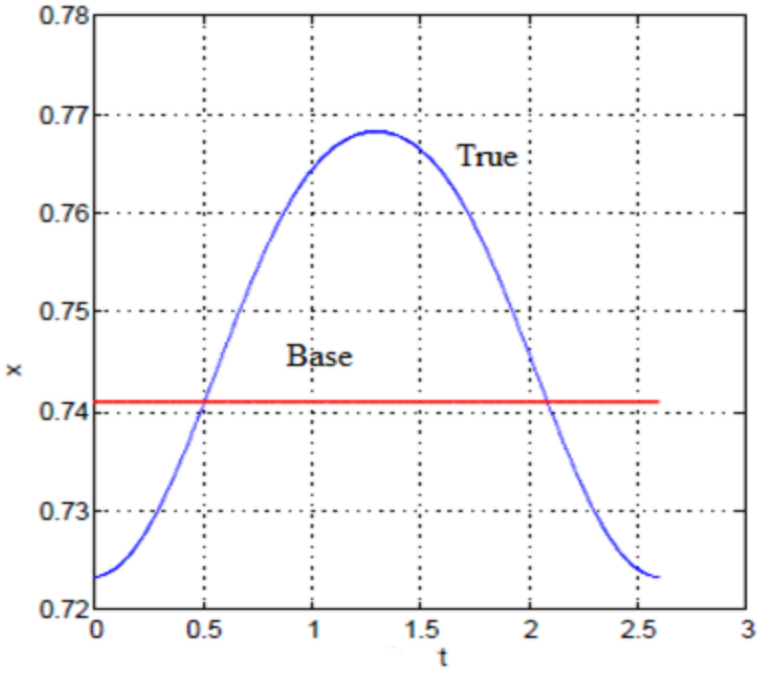

Figure 12 x Motion Against Time t, Base vs. True

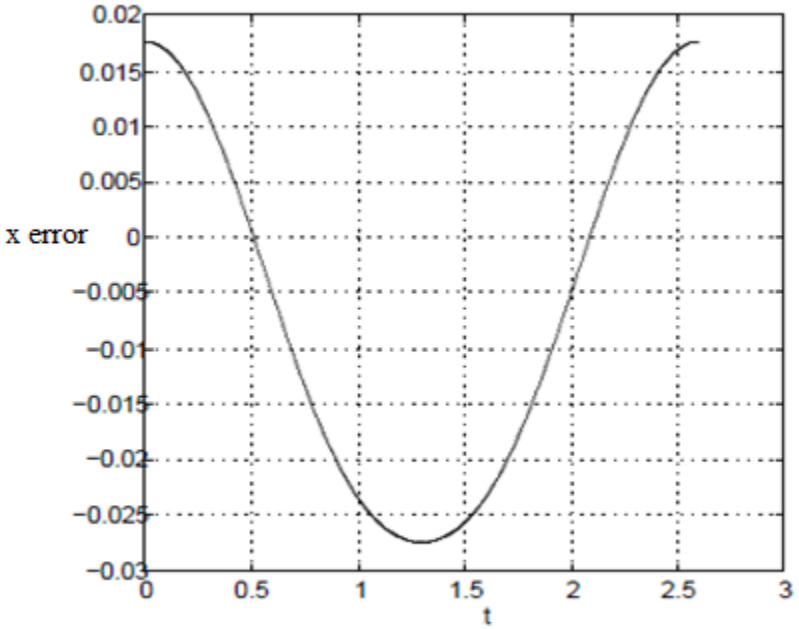

Figure 13 x Error Against Time t, Base vs. True

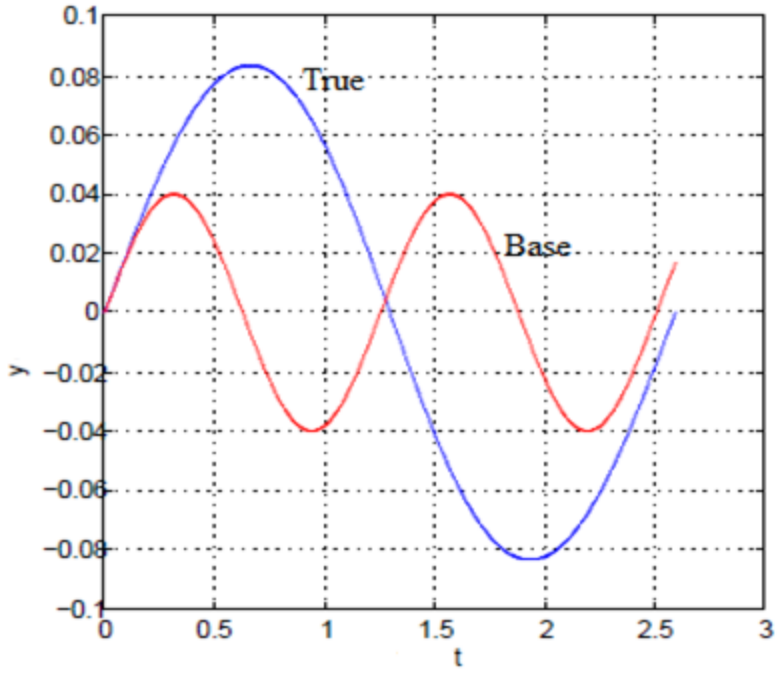

Figure 14 y Motion Against Time t, Base vs. True

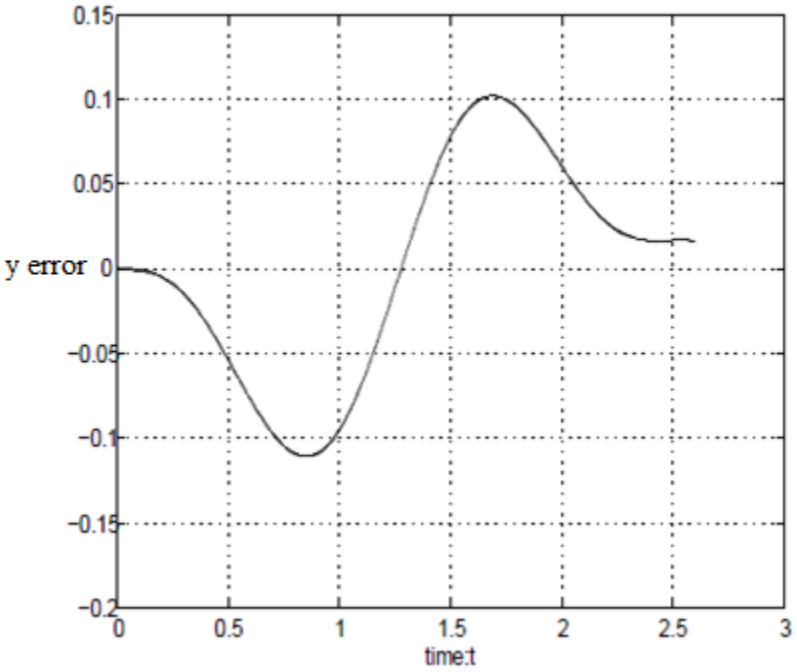

Figure 15 y Error Against Time t, Base vs. True

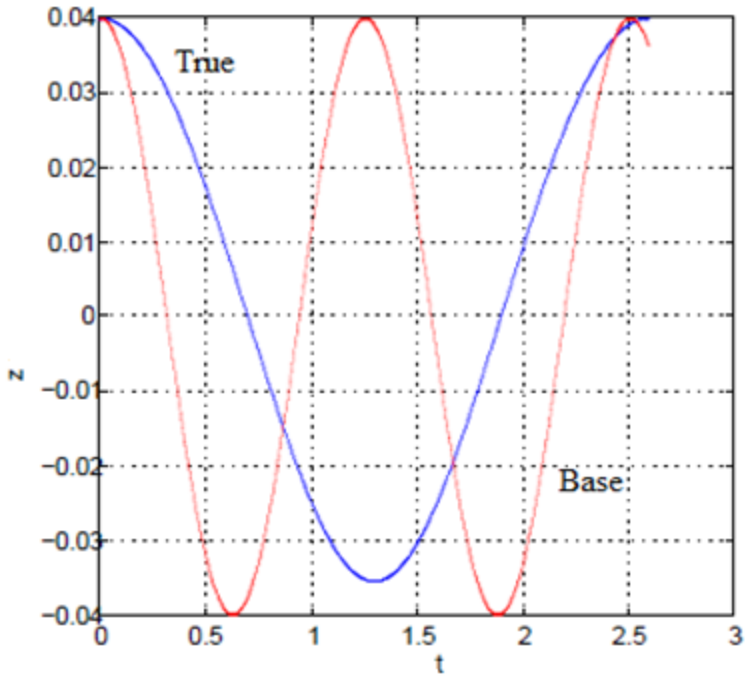

Figure 16 z Motion Against Time t, Base vs. True

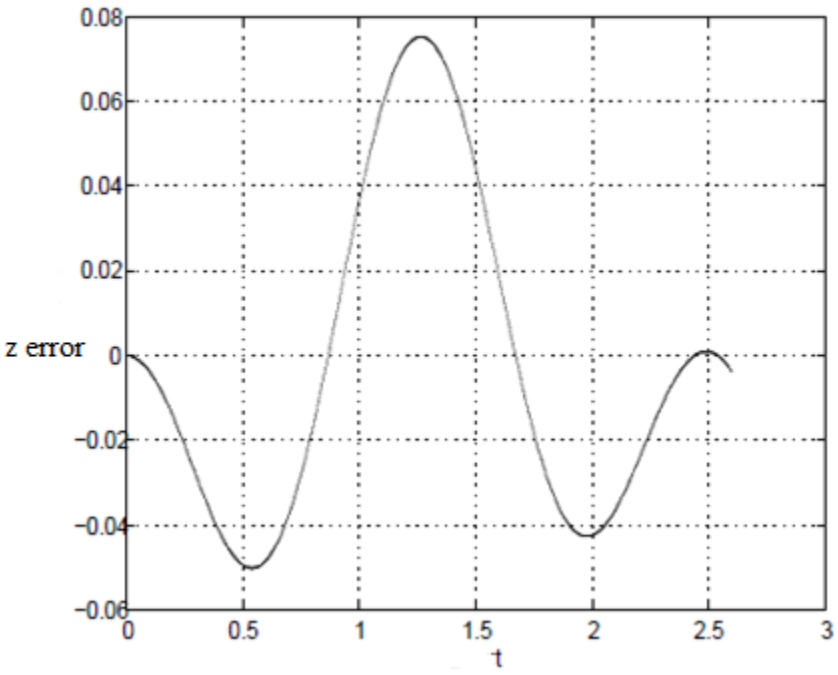

Figure 17 z Error Against Time t, Base vs. True

For additional insights, both true and base orbits are shown in three-dimensional and two-dimensional views in Figures 18-21. Remember that these x, y, and z coordinates with respect to the rotating frame. The orbital tracks clearly show the base solution must be modified to include out-of-plane motion (See Figure 20) and an expanded amplitude in the y axis (See Figure 21), without corrupting the z axis amplitude (see Figures 20, 21).

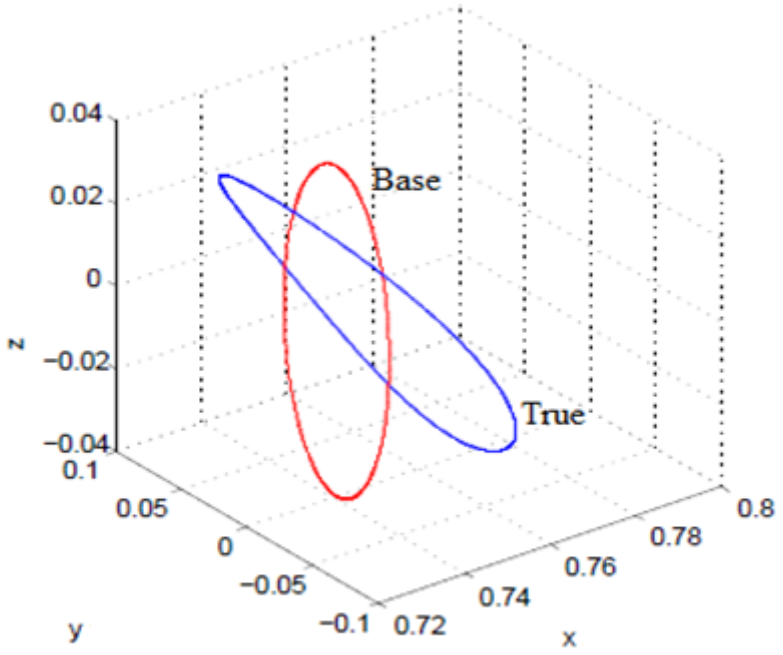

Figure 18 Perspective View, Base vs. True

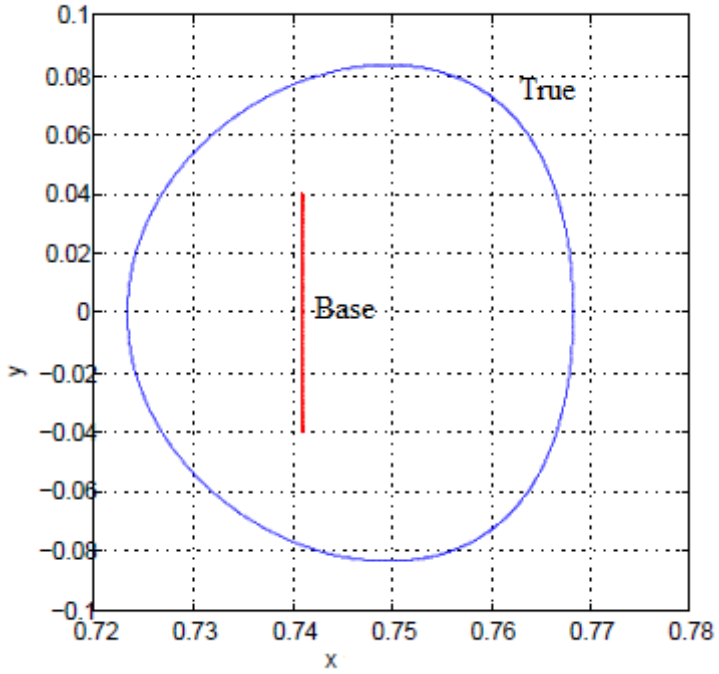

Figure 19 xy Sectional View, Base vs. True

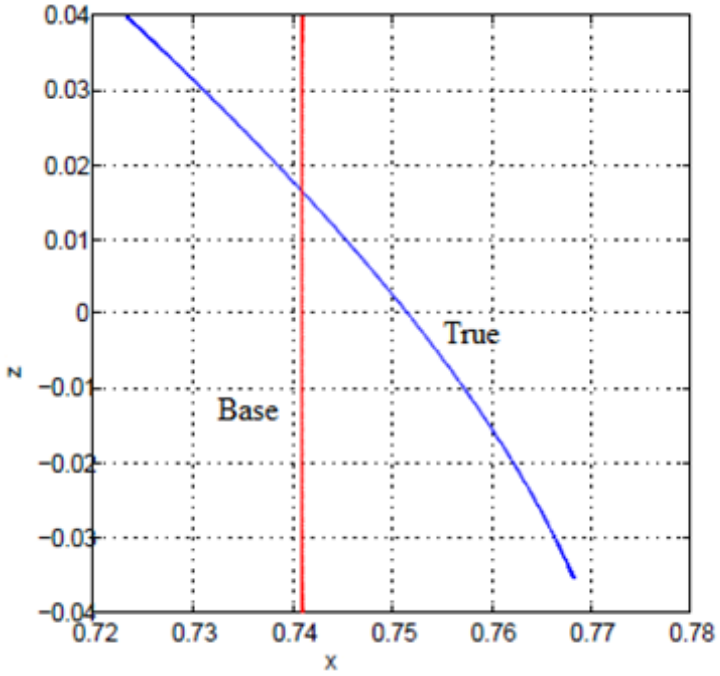

Figure 20 xz Sectional View, Base vs. True

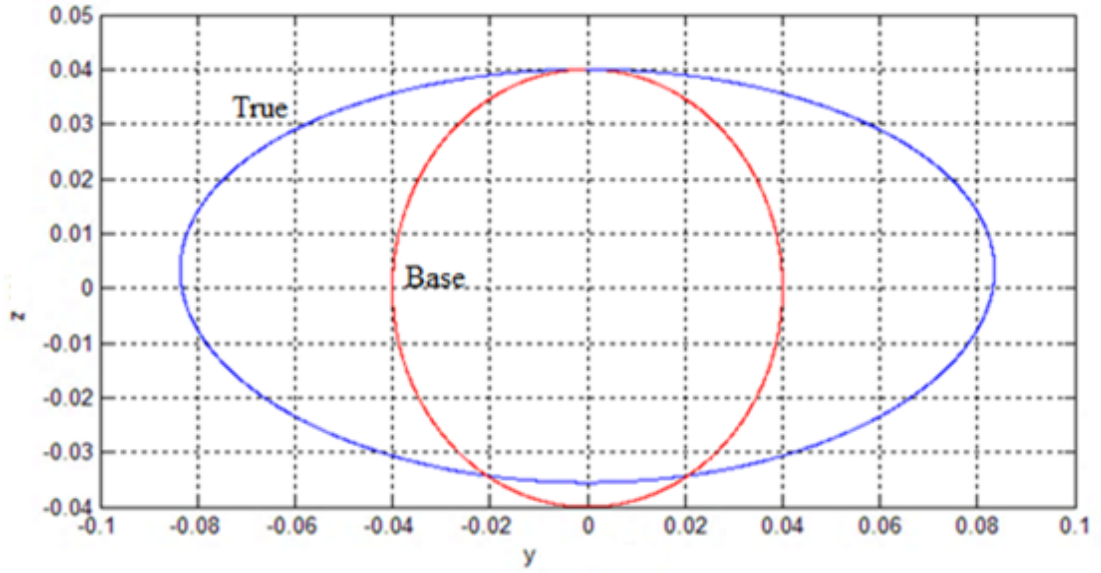

Figure 21 yz Sectional View, Base vs. True

Non-dimensional acceleration errors in the three differantial equations of motion after substituting the base solution are shown in Figures 22-24. Note the errors are plotted for one period of the base solution, i.e.,1.2566/ω. As discussed in Section 3.6, the first equation of motion gets

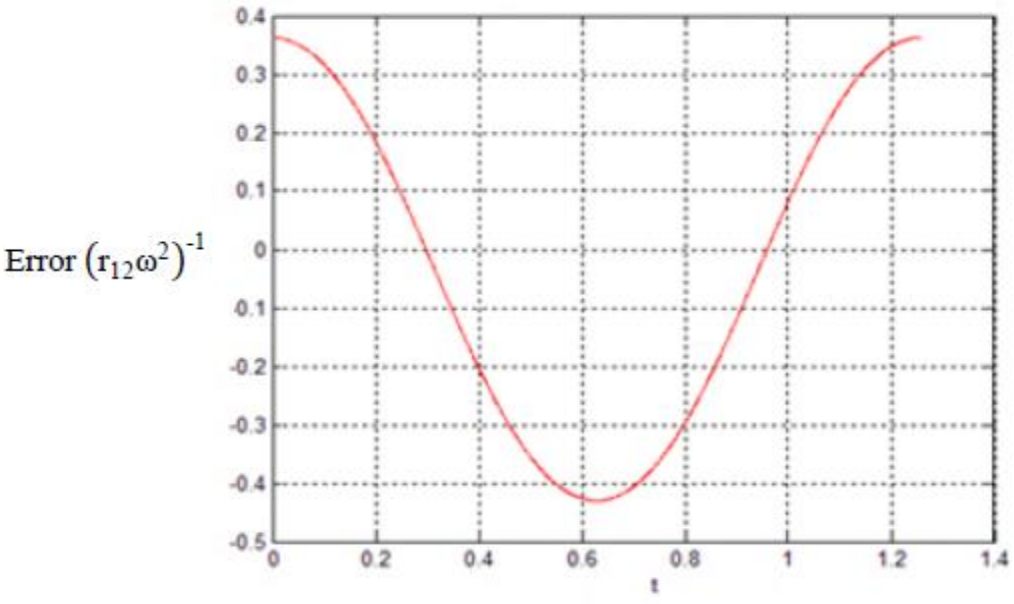

Figure 22 First Equation of Motion Error

satisfied in the averaged and bounded sense when the suppositional plane is taken at one of the collinear libration points. Figure 22 shows that the first equation of motion residual is averaged and bounded. The average error is approximately zero, meaning the area under the curve accounting for positive and negative values, equals zero approximately. Further, the residuals are bounded. The maximum positive error occurs at t = 0, which is consistent with the analysis in section 3.6. The magnitude of error at t = 0 should be approximately $2\omega a\lambda = 0.396$, see Section 3.6, which is roughly the value seen in Figure 22. Errors in the second and third equation of motion are shown in Figures 23 and 24.

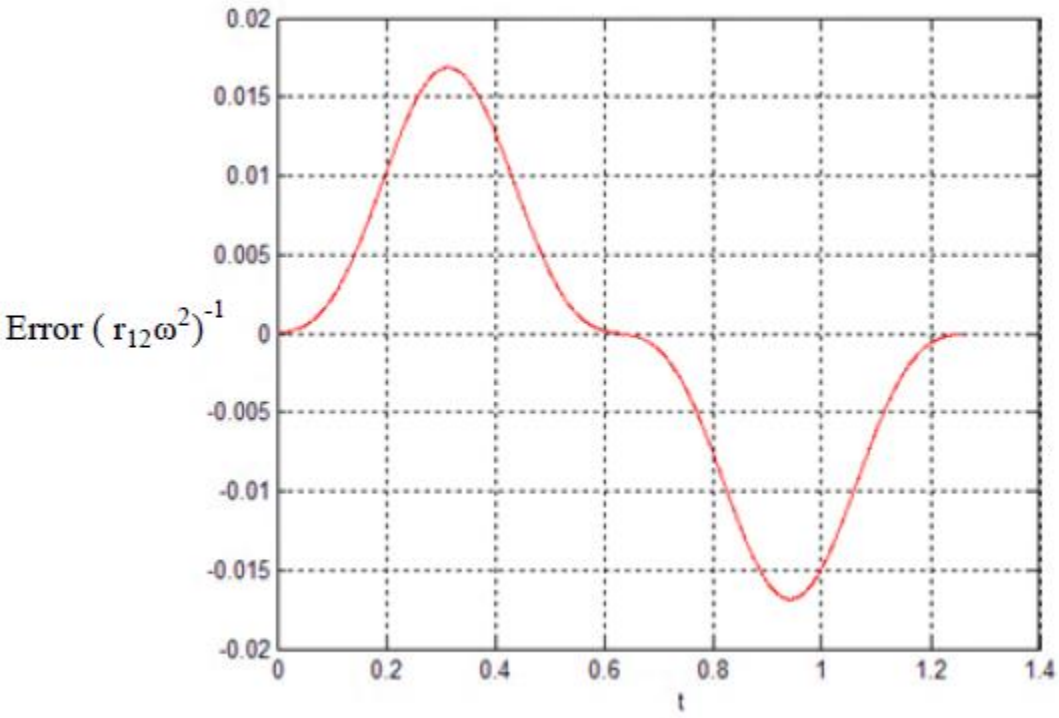

Figure 23 Second Equation of Motion Error

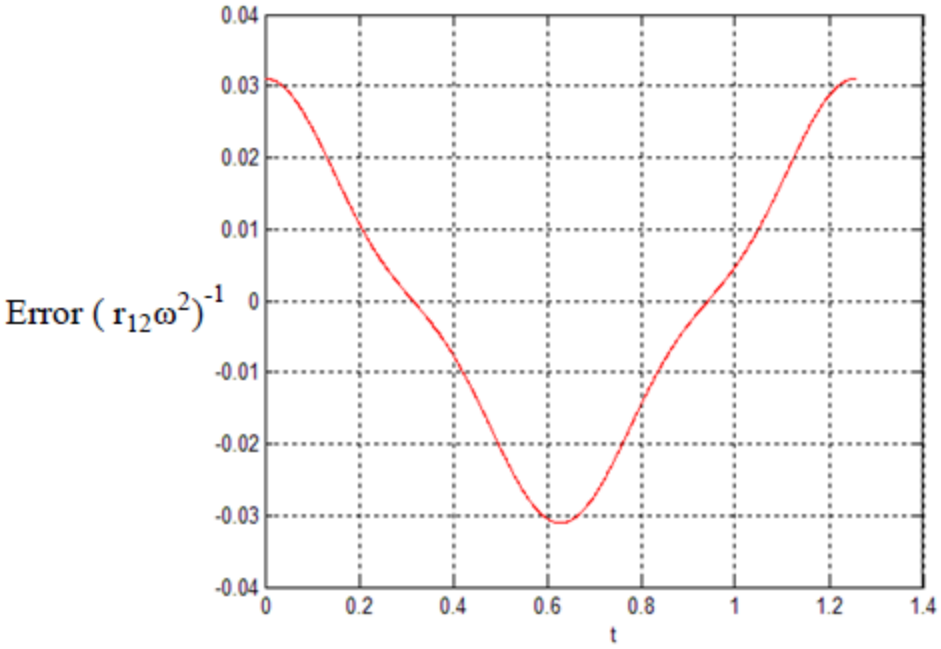

Figure 24 Third Equation of Motion Error

5.2 Excitation Simplification and Frequency Update

This section addresses two objectives. First, the coriolis forcing term $2\omega\dot{y}_b(t)$ in the x axis correction analysis is an infinite series but only the first few terms are significant. Simplification of this forcing term is the first objective. Second, the base solution frequency parameter predicted by Equation (3.3.27) requires improved accuracy. Procedure for updating tha value of λ within the framework of the three-body problem analytic solution is the second objective.

The coriolis forcing term $2\omega\dot{y}_b(t)$ given by Equation (4.9) will not be considered in the full form, rather a truncated version consisting of nome terms for m = 0, 1 and p = 0 will be expanded for further analysis. Thus,

$$2\omega\dot{y}_b(t) = \frac{2\pi^2 a\left(\lambda^2+\omega^2\right)}{\left(K(k_1)\right)^2}\left[\frac{q^{\frac{1}{2}}}{1-q}\cos\left\{\frac{\pi\sqrt{\lambda^2+\omega^2}\,\tau}{2K(k_1)}\right\}+\frac{q^{\frac{3}{2}}}{q^3-1}\cos\left\{\frac{3\pi\sqrt{\lambda^2+\omega^2}\,\tau}{2K(k_1)}\right\}\right.$$
$$+\frac{4\,q^{\frac{3}{2}}}{(q-1)(1+q^2)}\cos\left\{\frac{\pi\sqrt{\lambda^2+\omega^2}\,\tau}{2K(k_1)}\right\}\cos\left\{\frac{\pi\sqrt{\lambda^2+\omega^2}\,\tau}{K(k_1)}\right\}$$
$$\left.+\frac{4\,q^{\frac{5}{2}}}{(1-q^3)(1+q^2)}\cos\left\{\frac{3\pi\sqrt{\lambda^2+\omega^2}\,\tau}{2K(k_1)}\right\}\cos\left\{\frac{\pi\sqrt{\lambda^2+\omega^2}\,\tau}{K(k_1)}\right\}\right] \tag{5.2.1}$$

Introduce the simplifying term

$$\frac{\pi\sqrt{\lambda^2+\omega^2}\,\tau}{2K(k_1)} = \upsilon(t) \tag{5.2.2}$$

so that

$$2\omega\dot{y}_b(t) = \frac{2\pi^2 a\left(\lambda^2+\omega^2\right)}{\left(K(k_1)\right)^2}\left[\frac{q^{\frac{1}{2}}}{1-q}\cos\{\upsilon(t)\}+\frac{q^{\frac{3}{2}}}{q^3-1}\cos\{3\upsilon(t)\}+\frac{4\,q^{\frac{3}{2}}}{(q-1)(1+q^2)}\cos\{\upsilon(t)\}\cos\{2\upsilon(t)\}\right.$$
$$\left.+\frac{4\,q^{\frac{5}{2}}}{(1-q^3)(1+q^2)}\cos\{3\upsilon(t)\}\cos\{2\upsilon(t)\}\right] \tag{5.2.3}$$

Using the trigonemetric identities,

$$\cos\{\upsilon(t)\}\cos\{2\upsilon(t)\} = \frac{1}{2}[\cos\{\upsilon(t)\}+\cos\{3\upsilon(t)\}]$$
$$\cos\{3\upsilon(t)\}\cos\{2\upsilon(t)\} = \frac{1}{2}[\cos\{\upsilon(t)\}+\cos\{5\upsilon(t)\}] \tag{5.2.4}$$

Equation (5.2.3) becomes

$$2\omega\dot{y}_b(t) = \frac{2\pi^2 a\left(\lambda^2+\omega^2\right)}{\left(K(k_1)\right)^2}\left[\frac{q^{\frac{1}{2}}}{1-q}\cos\{\upsilon(t)\}+\frac{q^{\frac{3}{2}}}{q^3-1}\cos\{3\upsilon(t)\}+\frac{2\,q^{\frac{3}{2}}}{(q-1)(1+q^2)}[\cos\{\upsilon(t)\}+\cos\{3\upsilon(t)\}]\right.$$
$$\left.+\frac{2\,q^{\frac{5}{2}}}{(1-q^3)(1+q^2)}[\cos\{\upsilon(t)\}+\cos\{5\upsilon(t)\}]\right] \tag{5.2.5}$$

Finally , $2\omega\dot{y}_b(t)$ can be written as

$$2\omega\dot{y}_b(t) = \frac{2\pi^2 a\left(\lambda^2+\omega^2\right)}{\left(K(k_1)\right)^2}\left[\left(\frac{q^{\frac{1}{2}}}{1-q}+\frac{2\,q^{\frac{3}{2}}}{(q-1)(1+q^2)}+\frac{2\,q^{\frac{5}{2}}}{(1-q^3)(1+q^2)}\right)\cos\{\upsilon(t)\}\right.$$
$$\left.+\left(\frac{q^{\frac{3}{2}}}{q^3-1}+\frac{2\,q^{\frac{3}{2}}}{(q-1)(1+q^2)}\right)\cos\{3\upsilon(t)\}+\left(\frac{2\,q^{\frac{5}{2}}}{(1-q^3)(1+q^2)}\right)\cos\{5\upsilon(t)\}\right] \qquad (5.2.6)$$

This truncated version of the Fourier series for the forcing function is an accurate representation of the exact signal if the value of λ is equal to or greater than one. As value of λ decreases below one , the deviation from the exact signal begins to increase. Figure 24 shows the forcing signal $\frac{2\omega\dot{y}_b(t)}{2\pi^2 a}$ plotted against the dimensionless time for various values of λ. The red curves represent the forcing approxiamation while blue ones represent the exact forcing. For the halo orbit example with λ = 4.95123, there is no apparent difference beetween the exact and approxiamate forcing. In general, for any *L1* halo orbit whose initial conditions allow the value of λ to go beyond one, the simplified expression for the forcing signal given by Equation (5.2.6) will suffice instead of the full form. One reason behind using Equation (5.2.6) is to simplify orbit propogation calculations. Another reason is to simplify calculations reagrding update to the value of λ for thr first order correction, which is considered next.

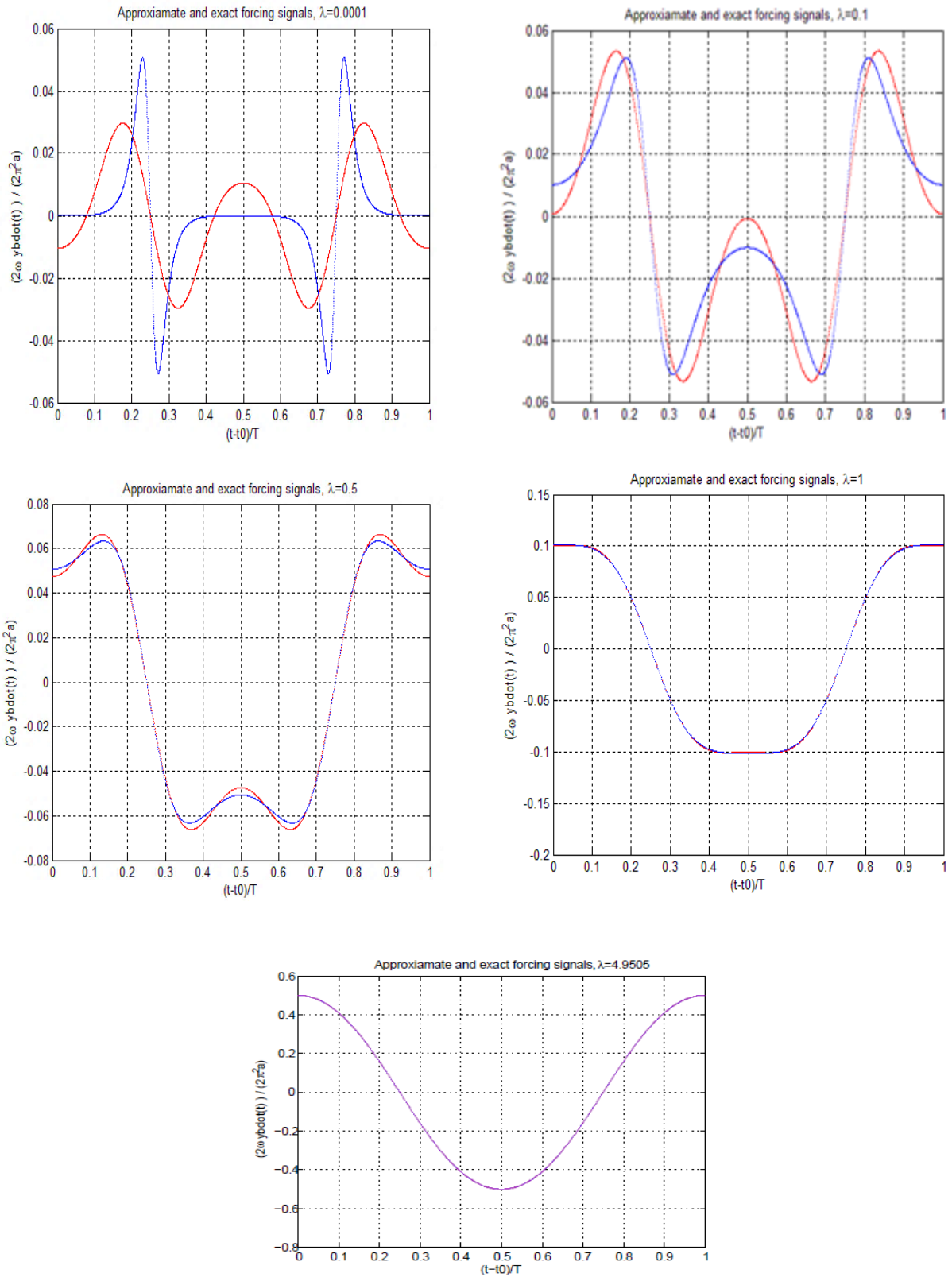

Figure 25 Approximate and Exact Forcing Signals for Family of Frequency Values

As the forcing function $2\omega\dot{y}_b(t)$ now consists of finite number of terms, the non-homogeneous parts of the first order corrections to the base solution in x axis will also consist of finite number of terms. This can be readily seen from the analysis done in chapter 4. First order correction to the x axis base solution is written in Equation (5.2.7). In Equation (5.2.7), the terms having coefficients A_1 and A_2 are homogeneous part of the correction while terms consisting of coefficients D_x , E_x , F_x are non-homogeneous part of the correction.

$$x_{c1}(t)=A_1e^{\lambda_{c1}t}+A_2e^{-\lambda_{c1}t}+D_x\cos\{\upsilon(t)\}+E_x\cos\{3\upsilon(t)\}+F_x\cos\{5\upsilon(t)\} \tag{5.2.7}$$

where

$$D_x = \frac{2\pi^2 a\left(\lambda^2+\omega^2\right)}{\left(K(k_1)\right)^2}\left[\frac{q^{\frac{1}{2}}}{1-q}+\frac{2\,q^{\frac{3}{2}}}{(q-1)(1+q^2)}+\frac{2\,q^{\frac{5}{2}}}{(1-q^3)(1+q^2)}\right]\left[\frac{1}{-\left(\frac{\pi\sqrt{\lambda^2+\omega^2}}{2K(k_1)}\right)^2-\lambda_{c1}^2}\right] \tag{5.2.8}$$

$$E_x = \frac{2\pi^2 a\left(\lambda^2+\omega^2\right)}{\left(K(k_1)\right)^2}\left[\frac{q^{\frac{3}{2}}}{q^3-1}+\frac{2\,q^{\frac{3}{2}}}{(q-1)(1+q^2)}\right]\left[\frac{1}{-\left(\frac{3\pi\sqrt{\lambda^2+\omega^2}}{2K(k_1)}\right)^2-\lambda_{c1}^2}\right] \tag{5.2.9}$$

$$F_x = \frac{2\pi^2 a\left(\lambda^2+\omega^2\right)}{\left(K(k_1)\right)^2}\left[\frac{2\,q^{\frac{5}{2}}}{(1-q^3)(1+q^2)}\right]\left[\frac{1}{-\left(\frac{5\pi\sqrt{\lambda^2+\omega^2}}{2K(k_1)}\right)^2-\lambda_{c1}^2}\right] \tag{5.2.10}$$

& λ_{c1}^2 is given by Equation (4.6). Since the periodic orbit is of interest, the non-periodic terms containing A_1 and A_2 should be eliminated. i.e., $A_1 = A_2 = 0$

The expression for $x_{c1}(t)$ is now written as

$$x_{c1}(t) = D_x\cos\{\upsilon(t)\}+E_x\cos\{3\upsilon(t)\}+F_x\cos\{5\upsilon(t)\} \tag{5.2.11}$$

Differentiating Equation (5.2.11) with respect to time

$$\dot{x}_{c1}(t) = -\frac{\pi\sqrt{\lambda^2+\omega^2}}{2K(k_1)} D_x \sin\{\upsilon(t)\}-3\frac{\pi\sqrt{\lambda^2+\omega^2}}{2K(k_1)}E_x\sin\{3\upsilon(t)\} -5\frac{\pi\sqrt{\lambda^2+\omega^2}}{2K(k_1)}F_x \sin\{5\upsilon(t)\} \tag{5.2.12}$$

Multiplying Equation (5.2.12) by -2ω

$$-2\omega\dot{x}_{c1}(t) = \frac{2\omega\pi\sqrt{\lambda^2+\omega^2}}{2K(k_1)} D_x \sin\{\upsilon(t)\}+\frac{6\omega\pi\sqrt{\lambda^2+\omega^2}}{2K(k_1)} E_x \sin\{3\upsilon(t)\} + \frac{10\omega\pi\sqrt{\lambda^2+\omega^2}}{2K(k_1)} F_x \sin\{5\upsilon(t)\} \tag{5.2.13}$$

Forcing function $-2\omega\dot{x}_{c1}(t)$ given by Equation (5.2.13) also consists of finite number of terms, hence the non-homogeneous parts of the first order corrections to the base solution in y axis will also consist of finite number of terms (see Chapter 4) . First order correction to the y axis base solution is written in Equation (5.2.14). In Equation (5.2.14), the terms having coefficients C_1 and C_2 are homogeneous part of the correction while terms consisting of coefficients D_y , E_y , F_y are non-homogeneous part of the correction.

$$y_{c1}(t) = C_1 \sin(\omega_{c1y}t) +C_2 \cos(\omega_{c1y}t) +D_y \sin\{\upsilon(t)\}+E_y \sin\{3\upsilon(t)\}+F_y \sin\{5\upsilon(t)\} \tag{5.2.14}$$

Considering a further special class of periodic orbits in which C_1 and C_2 are equated to zero, Equation (5.2.14) can be written as

$$y_{c1}(t) = \frac{2\omega\pi\sqrt{\lambda^2+\omega^2}}{2K(k_1)} \frac{1}{\omega_{c1y}^2-\left(\frac{\pi\sqrt{\lambda^2+\omega^2}}{2K(k_1)}\right)^2} D_x \sin\{\upsilon(t)\}$$

$$+\frac{6\omega\pi\sqrt{\lambda^2+\omega^2}}{2K(k_1)}\ \frac{1}{\omega_{c1y}^2-\left(\frac{3\pi\sqrt{\lambda^2+\omega^2}}{2K(k_1)}\right)^2}\ E_x\sin\{3\upsilon(t)\}+$$

$$\frac{10\omega\pi\sqrt{\lambda^2+\omega^2}}{2K(k_1)}\ \frac{1}{\omega_{c1y}^2-\left(\frac{5\pi\sqrt{\lambda^2+\omega^2}}{2K(k_1)}\right)^2}\ F_x\sin\{5\upsilon(t)\} \qquad (5.2.15)$$

In Equation (5.2.15), the coefficients of terms $\sin\{\upsilon(t)\}, \sin\{3\upsilon(t)\}, \sin\{5\upsilon(t)\}$ are D_y, E_y, F_y respectively. Equation (5.2.15) is now written as

$$y_{c1}(t) = D_y\sin\{\upsilon(t)\}+E_y\sin\{3\upsilon(t)\}+F_y\sin\{5\upsilon(t)\} \qquad (5.2.16)$$

Differentiating Equation (5.2.15) with respect to time

$$\dot{y}_{c1}(t) = \frac{\pi\sqrt{\lambda^2+\omega^2}}{2K(k_1)}\ D_y\cos\{\upsilon(t)\} + 3\frac{\pi\sqrt{\lambda^2+\omega^2}}{2K(k_1)}\ E_y\cos\{3\upsilon(t)\} \quad + 5\frac{\pi\sqrt{\lambda^2+\omega^2}}{2K(k_1)}\ F_y\cos\{5\upsilon(t)\} \qquad (5.2.17)$$

The primary inaccuracy noted from the comparison of the base and true solutions lies in the period T, which is ultimately determined by the frequency λ. Currently the value of λ is determined by Equation (3.3.27), which is founded entirely on the base solution. Fortunately, the corrected solution provides two options to explore for the purpose of updating the λ value.

Recall the exact halo orbit solution is defined by the six initial values x_{h0}, y_{h0}, z_{h0} , $\dot{x}_{h0}$, $\dot{y}_{h0}$, $\dot{z}_{h0}$ given in Equation (5.1.1). Note only three of these values are non-trivial being x_{h0} , $\dot{y}_{h0}$, z_{h0} . Also recall the base halo orbit solution is defined by the non-trivial values $x_b(0) = d_x \neq x_{h0}$, $\dot{y}_b(0) = \dot{y}_{h0}$, $z_{b0} = z_{h0}$. In some sense, the corrected solution adds several degrees of freedom to the initial condition analysis, specifically, the initial values x_{c10} , $\dot{y}_{c10}$, z_{c10} . However, since F_2 from Equation (4.52) is not a function of λ and $F_2 = 0$ implying $z_{c10} = 0$, this leaves only the non-trivial terms x_{c10} and $\dot{y}_{c10}$ for frequency updating.

The first option for frequency updating is based on x_{c10}. Equation (4.22) requires

$$x_{c10} = \beta_x \tag{5.2.18}$$

where $x_{c10} = x_{h0} - x_{b0} = -0.0176418\, r_{12}$ and β_x is defined from Equation (4.19) and depends on the value of λ. The equality in Equation (5.2.18) is not satisfied numerically for $\lambda = 4.95123\omega$. Therefore, the first option is to calculate a new value for λ that satisfies the equality numerically. Using the simplified nome expression, β_x is obtained by substituting t = 0 in Equation (5.2.11).

$$\beta_x = D_x + E_x + F_x \tag{5.2.19}$$

where D_x,E_x, and F_x are given by Equation (5.2.8), (5.2.9), and (5.2.10) respectively.

The updated values of λ is then computed from the expression

$$f(\lambda) = x_{c10} - \beta_x(\lambda) = 0 \tag{5.2.20}$$

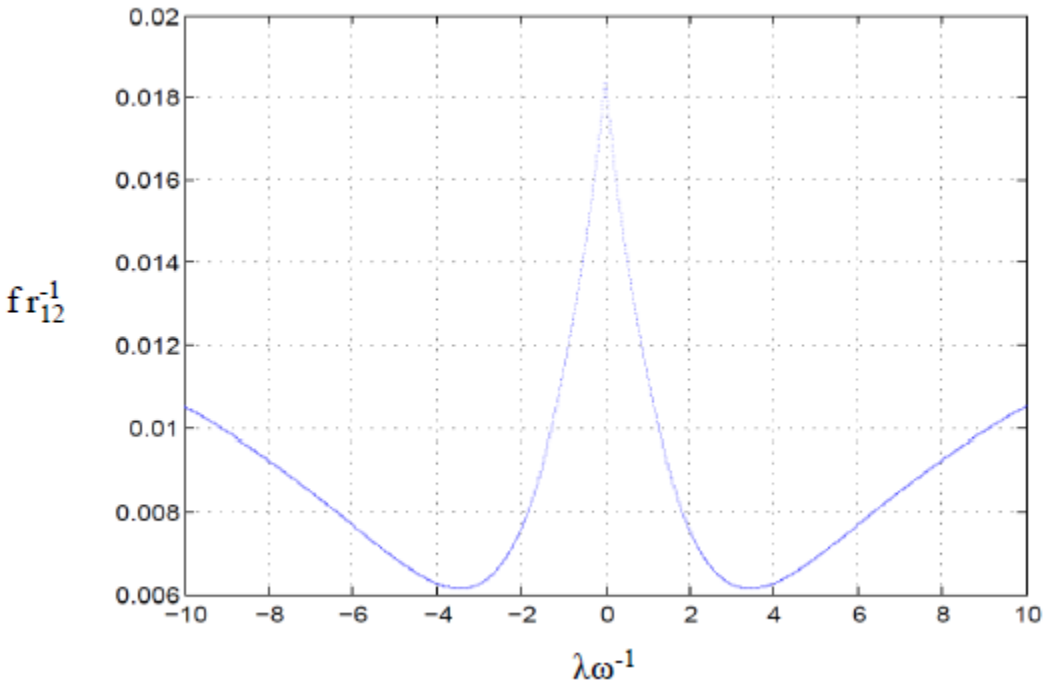

Figure 26 First Option Function Behavior

Note the determined λ may satisfy Equation (5.2.20) exactly or it may only minimize the residual of Equation (5.2.20). Figure 26 shows function f (λ) plotted against λ. There is no value of λ that achieves f (λ) = 0. However, the value of $\lambda = \pm 3.44\omega$ minimizes f (λ). The updated positive value is an improvement in that the period T will be larger, but the accuracy is still considered insufficient. Note this correction was considered in Reference 9. The second option for frequency updating is based on $\dot{y}_{c10}$. Equation (4.47) requires

$$\dot{y}_{c10} = \delta_{\dot{y}} \tag{5.2.21}$$

where $\dot{y}_{c10} = \dot{y}_{h0} - \dot{y}_{b0}$ and $\delta_{\dot{y}}$ is defined from Equation (4.45) and depends on the value of λ. Currently, $\dot{y}_{b0}$ is selected to equal $\dot{y}_{h0}$ (See Equation (5.1.2)) or $\dot{y}_{h0} = \dot{y}_{b0} = 0.198019\omega r_{12}$ leading to $\dot{y}_{c10} = 0$. The equality in Equation (5.2.21) is not satisfied numerically for $\lambda = 4.95123\omega$. Therefore, the second option is to calculate a new value for λ that satisfies the equality numerically. A slightly modified approach will be considered, however. Returning to Equation (3.3.19) for $\tau_0 = 0$, a new selection for $\dot{y}_{b0} = a\lambda$. Therefore, the corrected initial rate to be used in Equation (5.2.21) is $\dot{y}_{c10} = 0.198019\omega r_{12} - a\lambda$ where a equals the value given in Equation (5.1.2). After using the simplified nome expression to compute $\dot{x}_{c1}(t)$ which determines $y_{c1}(t)$ i.e., substituting t = 0 in Equation (5.2.17), $\delta_{\dot{y}}$ is given by

$$\delta_{\dot{y}} = \frac{\pi\sqrt{\lambda^2+\omega^2}}{2K(k_1)} D_y + 3\frac{\pi\sqrt{\lambda^2+\omega^2}}{2K(k_1)} E_y + 5\frac{\pi\sqrt{\lambda^2+\omega^2}}{2K(k_1)} F_y \tag{5.2.22}$$

The updated value of λ is then computed from the expression

$$g(\lambda) = \dot{y}_{c10}(\lambda) - \delta_{\dot{y}}(\lambda) = 0 \tag{5.2.23}$$

Again, the determined value of λ may satisfy Equation (5.2.23) or it may only minimize the residual of Equation (5.2.23). Figure 26 shows function g(λ) plotted against λ. Several values of λ can be found that achieve g(λ) = 0 and include $\lambda = -2.1252\omega$, -0.4199ω , $+0.4190\omega$, $+0.1036\omega$,

+2.3082ω, +4.1910ω. Of these six values, λ = +2.3082ω is the best choice. This update value significantly improves the period T and the corrected orbit accuracy. This correction process was not considered in Reference 9 and is a distinguishing feature of the thesis research.

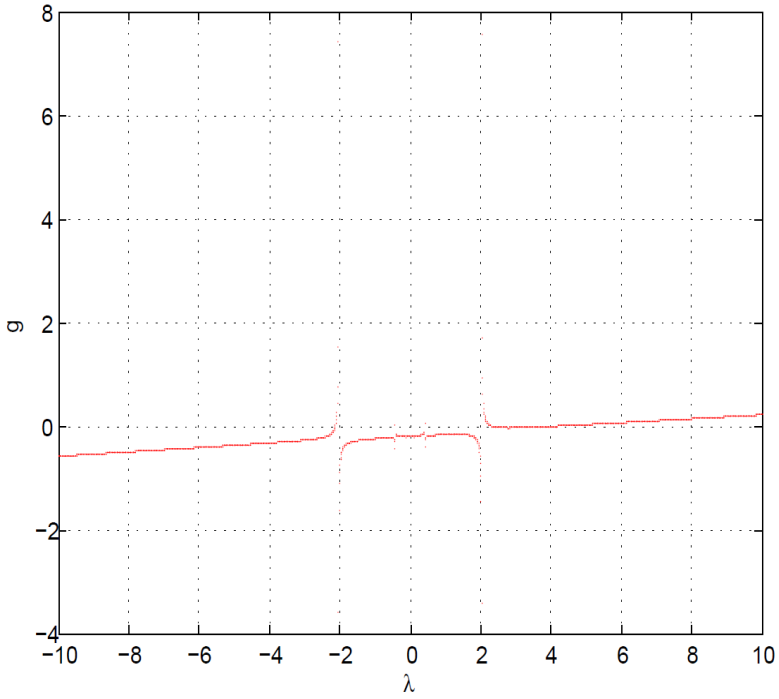

Figure 27 Second Option Function Behavior

5.3 Comparison of Corrected and True Orbits

When $\lambda = 2.3082$ is substituted into $x_{c1}(t)$, $y_b(t)$, $y_{c1}(t)$, and $z_b(t)$, first order corrected orbit reaches closer to the true orbit. The period of corrected motion is 2.603/ω. Thus, the error in period gets reduced to zero. The corrected and true motion plots for x, y, and z coordinates against time are shown in figures 28, 29, and 30 respectively. The blue curve represents true while red curve represents corrected motion. The plot of y axis motion against the time and the plot of z axis motion against time for corrected orbit are significantly similar to that of true orbit. The magnitude of maximum y positional error is 0.0025 r_{12} and that of maximum z positional error is 0.0045 r_{12}. The value of $\lambda = 2.3082$ takes the initial x coordinate of the base solution closer to the true initial

x coordinate. The error in initial x coordinate is reduced from 0.0176418 r_{12} to 0.007 r_{12} while the magnitude of maximum x positional error is 0.0167 r_{12}.These results are shown in Table 4. The percentage errors in x, y, and z axes are reduced to good extent as compared to the errors for base.

Table 4 Comparison between the True, Base, and Corrected Orbits

	True	Corrected	Percentage
Maximum x Axis Error	0	0.0167 r_{12}	1.67
Maximum y Axis Error	0	0.0025 r_{12}	0.25
Maximum z Axis Error	0	0.0045 r_{12}	0.45
Period	2.603/ω	2.603/ω	0

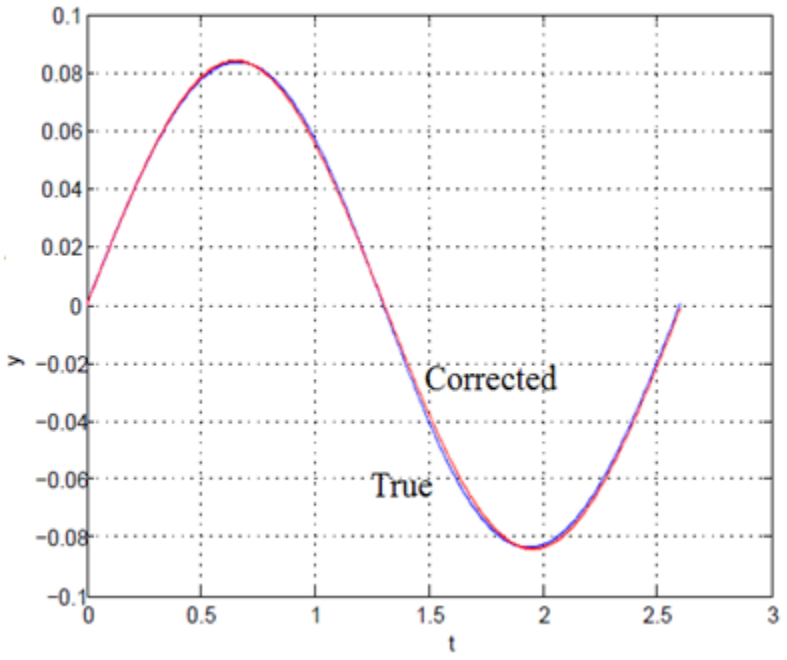

Figure 28 y Motion Against Time, True vs. Corrected

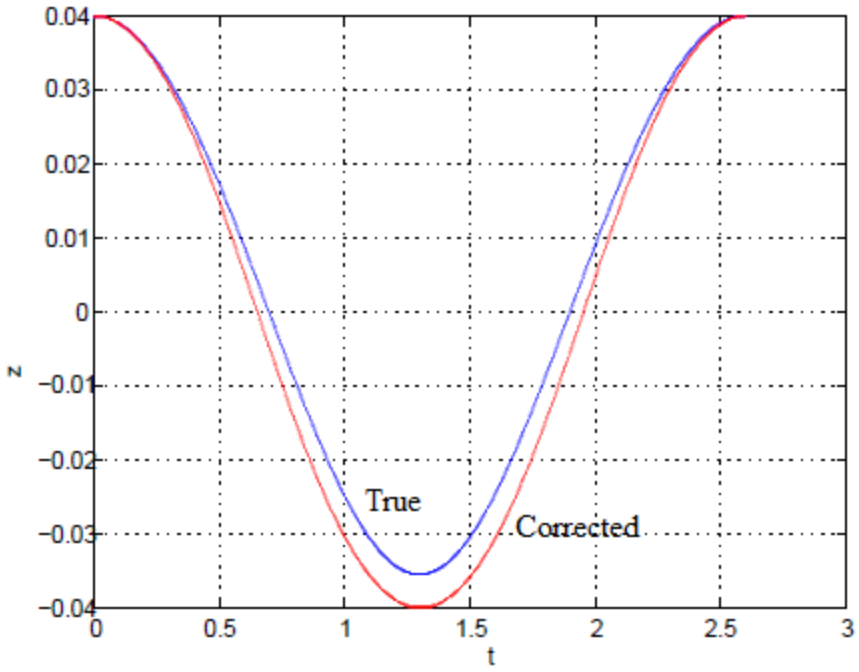

Figure 29 z Motion Against Time, True vs. Corrected

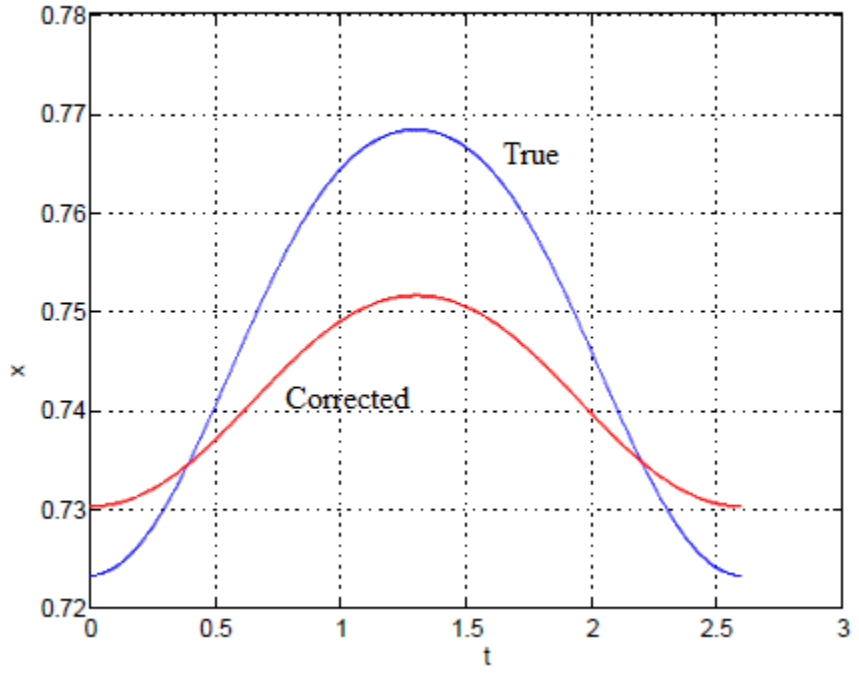

Figure 30 x Motion Against Time, True vs. Corrected

For additional insights, both true and corrected orbits are shown in three-dimensional and two-dimensional views in Figures 31-34. The orbital tracks clearly show the corrected solution is closer to the true solution as compared to the base solution. From figure 33, it can be seen the out-of-plane motion is improved and corrected xz plot is aligned in the direction of true xz plot. Figure 31 shows that amplitude in the x axis is expanded without disturbing z axis. In figure 32, the constant coordinate of x axis of base solution is expanded and the overall corrected xy plot is trying to capture true xy plot roughly. The corrected three-dimensional perspective view is in much better shape now as seen in figure 34. The quantitative data can be found in Table 4.

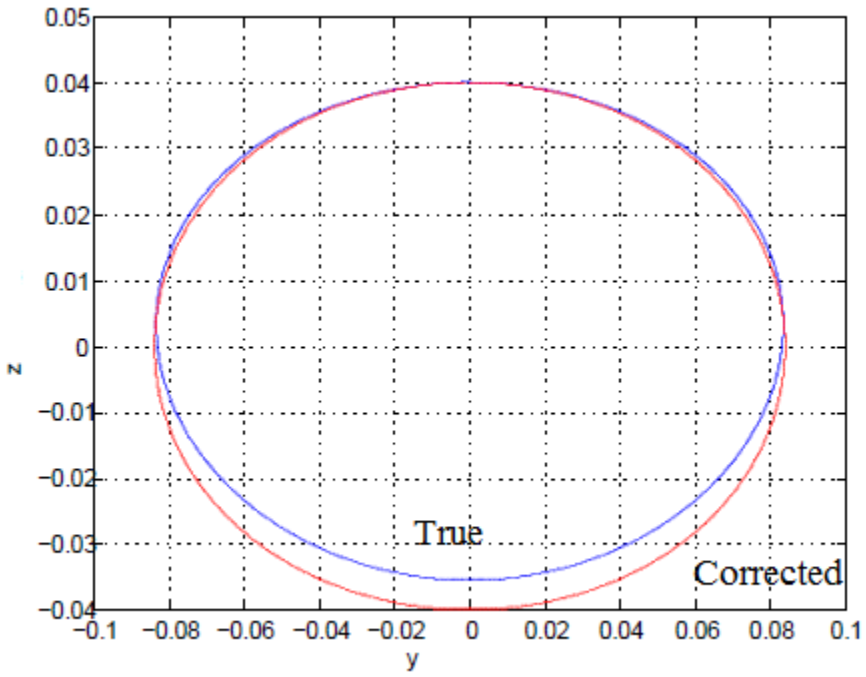

Figure 31 yz Sectional View, True vs. Corrected

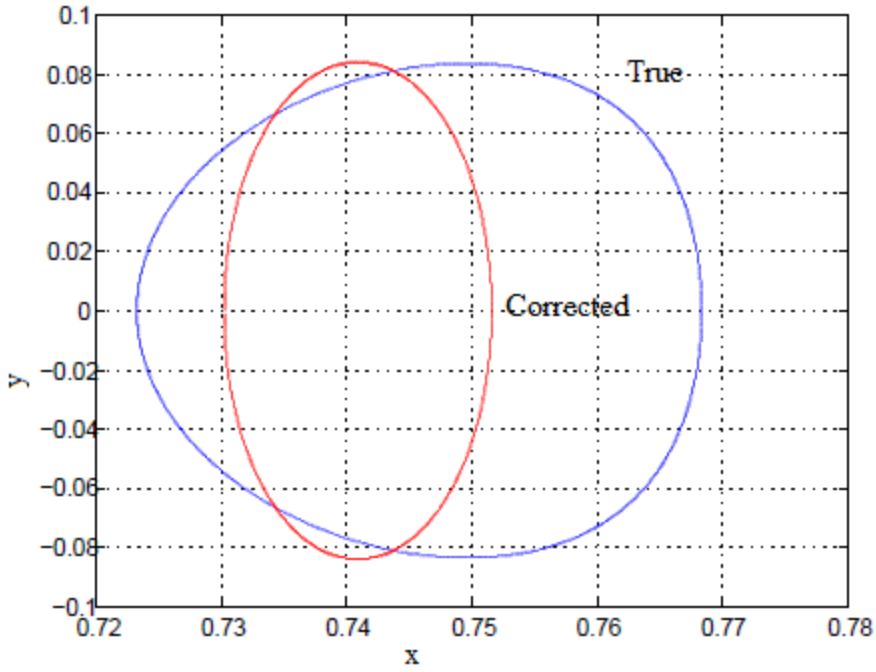

Figure 32 xy Sectional View, True vs. Corrected

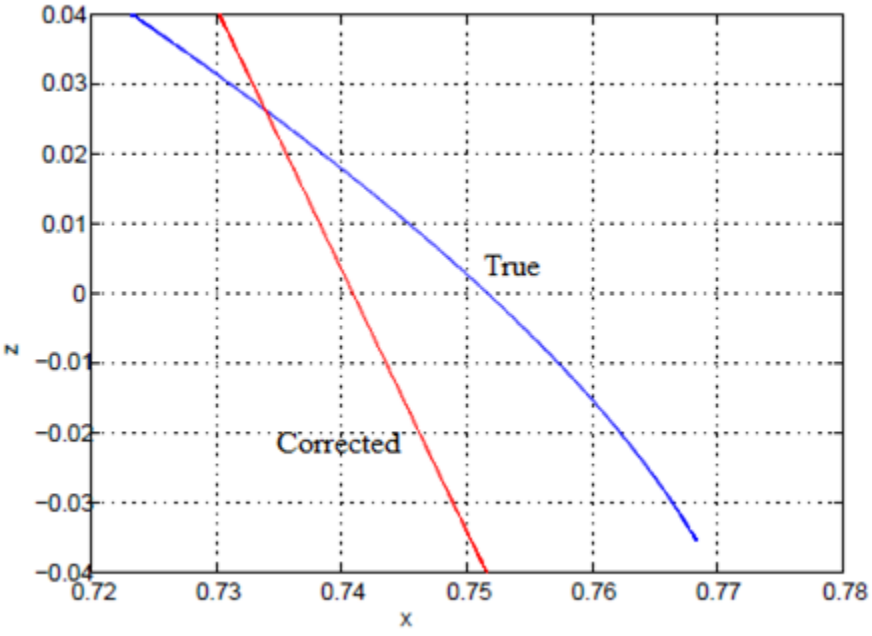

Figure 33 xz Sectional View, True vs. Corrected

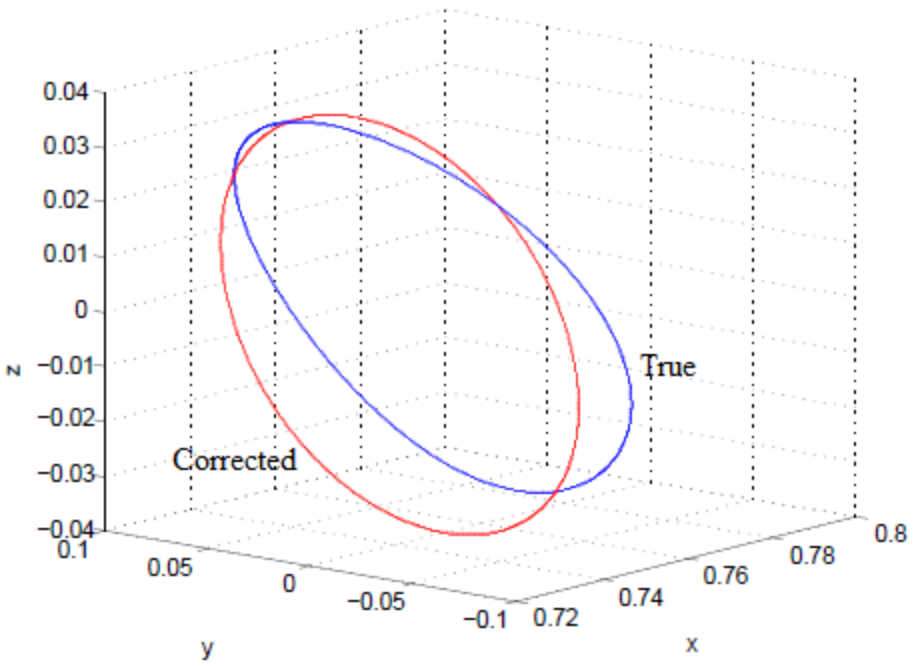

Figure 34 Perspective View, True vs. Corrected

5.4 A Further Discussion on the Base Solution

The same halo orbit test case as in Reference 9 was considered for analysis in this chapter. The updated value of the modulus of elliptic functions k in Reference 9 is chosen from the initial conditions on x coordinate, while in this thesis it is chosen from initial conditions on the derivative of y coordinate. The period of the base solution obtained for the test case is same for this thesis and for Reference 9. Also the motion in x, y and z axes with time is same in both cases. Hence, the new base solution and the base solution in Reference 9 are comparably the same in accuracy with which they are capturing non-uniform speed of the third body along halo orbits as shown in the Figure 35. It is to be remembered that the period of the base solution in both cases is approximately half of the true orbit.

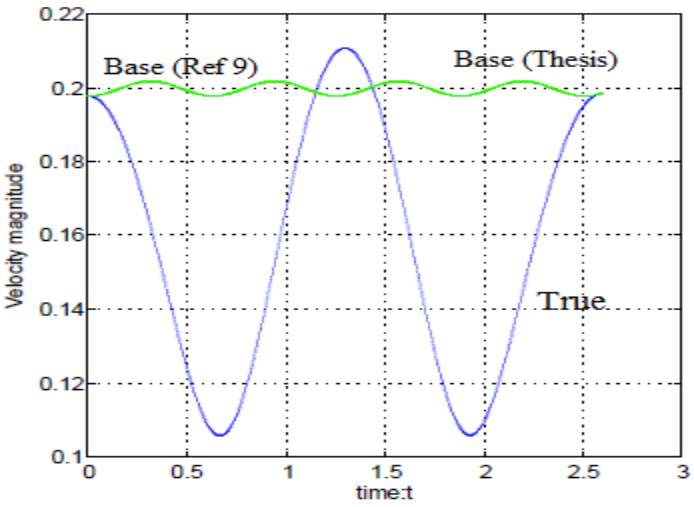

Figure 35 Velocity Magnitude against the Time

But after the first order correction, the non-uniform speed characteristic along the halo orbit is more accurately captured as seen from the Figure 36.

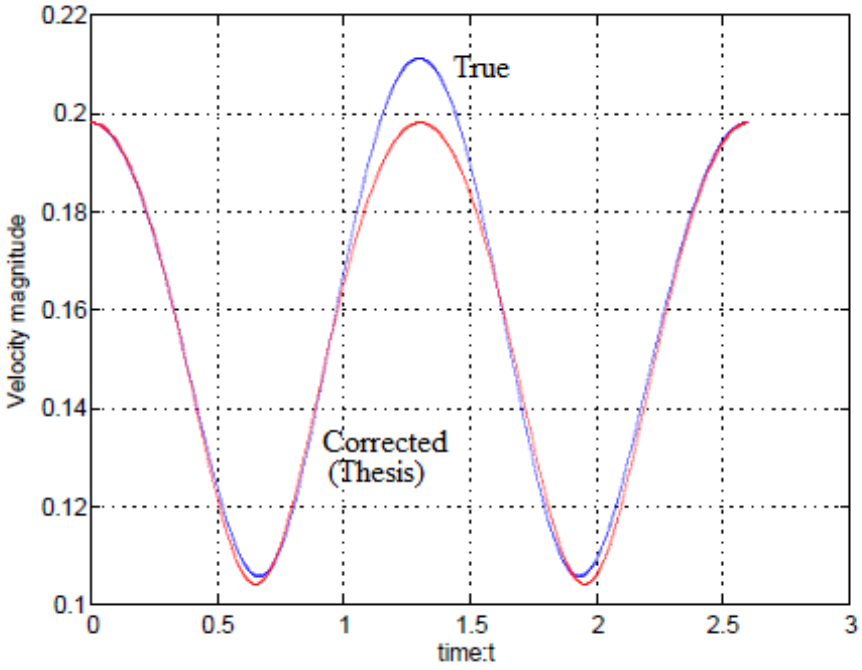

Figure 36 Velocity Magnitude against the Time

Analytical expressions for the base solution in the thesis and in Reference 9 are now compared. The modulus of elliptic functions in the thesis is

$$k_T = \frac{\omega}{\sqrt{\lambda^2+\omega^2}} \tag{5.4.1}$$

while in the reference 9, this modulus is calculated as

$$k_9 = \frac{\omega}{\sqrt{\omega^2 \cos^2(\theta_0)+\dot{\theta}_0^2}} \tag{5.4.2}$$

$$k_9 = \frac{\omega}{\sqrt{\omega^2 \left\{1- \sin^2(\theta_0)\right\}+\dot{\theta}_0^2}} \tag{5.4.3}$$

Comparing Equation (5.4.2) with Equation (5.4.3) gives

$$\lambda^2 = \dot{\theta}_0^2 - \omega^2 \sin^2(\theta_0) \tag{5.4.4}$$

From Reference 9

$$y_0 = a \sin(\theta_0) ; \quad \dot{y}_0 = a \cos(\theta_0)\, \dot{\theta}_0 ; \quad z_0 = a \cos(\theta_0) \tag{5.4.5}$$

Using Equation (5.4.5), the right-hand side of Equation (5.4.4) can also be written as

$$\dot{\theta}_0^2 - \omega^2 \sin^2(\theta_0) = \left(\frac{\dot{y}_0}{z_0}\right)^2 - \left(\frac{\omega\, y_0}{a}\right)^2 \tag{5.4.6}$$

But from Equation (3.3.27) in the thesis

$$\lambda^2 = \left(\frac{\dot{y}_0}{z_0}\right)^2 - \left(\frac{\omega\, y_0}{a}\right)^2 \tag{5.4.7}$$

This concludes

$$k_T = k_9 \tag{5.4.8}$$

Thus, for the same initial conditions, modulus of the elliptic functions k in the Reference 9 and the modulus k_1 of the thesis give same numerical value.

The y and z coordinates of the base solution in Reference 9 are

$$y(t) = a\ cn\left(-\frac{\omega}{k}(t-t_0) + F\left(\frac{\pi}{2} - \theta_0, k\right), k\right) \tag{5.4.9}$$

$$z(t) = a\ sn\left(-\frac{\omega}{k}(t-t_0) + F\left(\frac{\pi}{2} - \theta_0, k\right), k\right) \tag{5.4.10}$$

Taking $t_0 = 0$, Equations (5.4.9) and (5.4.10) can be rewritten as

$$y(t) = a\ cn\left(-\frac{\omega}{k}(t) + F\left(\frac{\pi}{2} - \theta_0, k\right), k\right) \tag{5.4.11}$$

$$z(t) = a\ sn\left(-\frac{\omega}{k}(t) + F\left(\frac{\pi}{2} - \theta_0, k\right), k\right) \tag{5.4.12}$$

The y and z coordinates of the base solution in the thesis are

$$y(t) = \frac{a\lambda}{\sqrt{\lambda^2+\omega^2}}\ sd\left((t-\phi)\sqrt{\lambda^2+\omega^2}, \frac{\omega}{\sqrt{\lambda^2+\omega^2}}\right) \tag{5.4.13}$$

$$z(t) = a\ cd\left((t-\phi)\sqrt{\lambda^2+\omega^2}, \frac{\omega}{\sqrt{\lambda^2+\omega^2}}\right) \tag{5.4.14}$$

A special set of initial conditions from Reference 15 is taken into consideration at the beginning of Chapter 5. These initial conditions when substituted into Equation (5.4.5) yields

$$\theta_0 = 0 \tag{5.4.15}$$

This value when substituted into Equations (5.4.11) and (5.4.12) gives

$$y(t) = a\ cn\left(-\frac{\omega}{k}(t) + F\left(\frac{\pi}{2}, k\right), k\right) \tag{5.4.16}$$

$$z(t) = a\ sn\left(-\frac{\omega}{k}(t) + F\left(\frac{\pi}{2}, k\right), k\right) \tag{5.4.17}$$

Since,

$$F\left(\frac{\pi}{2}, k\right) = K(k) \tag{5.4.18}$$

Equations (5.4.16) and (5.4.17) become

$$y(t) = a\,cn\left(-\frac{\omega}{k}(t) + K(k), k\right) \tag{5.4.19}$$

$$z(t) = a\,sn\left(-\frac{\omega}{k}(t) + K(k), k\right) \tag{5.4.20}$$

But from Reference 20

$$sn(u+K) = cd(-u) \tag{5.4.21}$$

$$cn(u+K) = k' sd(-u) \tag{5.4.22}$$

Hence, Equations (5.4.19) and (5.4.20) become

$$y(t) = ak' sd\left(\frac{\omega}{k}(t), k\right) \tag{5.4.23}$$

$$z(t) = a\,cd\left(\frac{\omega}{k}(t), k\right) \tag{5.4.24}$$

Now, the special set of initial conditions mentioned earlier, when substituted into Equations (5.4.13) and (5.4.14), yields

$$\phi = 0 \tag{5.4.25}$$

Using Equations (5.4.1) and (5.4.25), the y and z coordinate of the base solution in the thesis i.e. Equations (5.4.13) and (5.4.14) for these special initial conditions can be written as

$$y(t) = ak_T' sd\left(\frac{\omega}{k}(t), k_T\right) \tag{5.4.26}$$

$$z(t) = a\,cd\left(\frac{\omega}{k}(t), k_T\right) \tag{5.4.27}$$

But from Equation (5.4.8), $k_T = k_9$ which indicates

$$y_T(t) = y_9(t) \tag{5.4.28}$$

$$z_T(t) = z_9(t) \tag{5.4.29}$$

Thus, for the special initial conditions, i.e. when $\theta_0 = 0$ and $\phi = 0$, the base solution in this thesis and in the Reference 9 are mathematically the same thing.

Similarly, using numerical calculations, it can be shown that for any other set of initial conditions, the base solution used in this thesis and in Reference 9 are representing the same hypothetical motion of the third body but with different mathematical structures. For any physical non-zero angle θ_0 , there exists a non-physical and non-zero constant ϕ such that the plots of base solution are exactly the same. In the same manner, for any non-physical and non-zero constant ϕ, there exists a physical angle θ_0.

CHAPTER 6

CONCLUSIONS

A suppositional base solution satisfying the Jacobi's integral equation in circular restricted three-body problem is discussed in the thesis. The locus of this solution is a circle lying in the plane perpendicular to the line joining the primaries. The Jacobi functions sn and dn are used with the complex elliptic modulus which get transformed to sd and cd functions with real modulus. This real modulus inherently is in between 0 and 1. The period is obtained in closed form in the terms of a constant λ which acts like frequency modulator and with somewhat restricted arbitrariness, the initial conditions can be mapped into the parameters like circular orbit radius a, constant λ, the plane location d_x and reference time τ_0. The base solution satisfies the third body equation of motion in the x axis in bounded and averaged sense when plane location is at one of the collinear libration points. Also, the combination of second and third equations of motion in y and z axes is satisfied but the accuracy in individual equations is limited.

This base solution is then compared with an L_1 halo orbit example and somewhat rough similarity is observed; the period of the base solution being approximately half of the true orbit, which demands further correction in the base solution. The third body differential equations are set up in terms of correction in axes. The non-homogeneous solutions for the corrections are in the form of perturbations which are Fourier series expansions of the Jacobi's elliptic functions in the terms of nome. The development is done assuming the suppositional plane passes through one of the collinear Lagrange points. Only homogeneous correction is obtained for z axis. The modified solution now consists of base solution plus first order corrections which can be further worked out to include second and higher order corrections.

An interesting result is obtained when the trimmed version of forcing signal is compared with the exact one. When constant $\lambda \geq 1$, they both become almost identical which justifies the use of the truncated forcing function for the same L_1 halo orbit taste case.

The initial conditions for true orbit are again substituted in the modified series solution and a new value of λ is obtained using numerical computation depending on which axis it is sought. For the taste case a unique value of λ is obtained from y axis velocity initial conditions, which when employed into y and z axis complete solution gives improved motion over the true one and corrected orbit reaches closer to the true orbit. The error in the period of this corrected orbit is reduced to zero.

REFERENCES

[1] Moulton, F. R., "*An Introduction to Celestial Mechanics*", Dover, New York, New York, 1914.

[2] Brouwer, O. and Clemence, G.M., "*Methods of Celestial Mechanics",* Academic Press, New York, New York, 1961.

[3] Szebehely, V. G., "*Theory of Orbits—The Restricted Problem of Three Bodies*", Academic Press, New York, New York,1967.

[4] Robert W. Farquhar, "The Flight of ISEE-3/ICE: Origins, Mission History, and a Legacy," The Journal of the Astronautical Sciences, ISSN 0021-9142, Vol. 49, No 1, January-March 2001, pp. 23-73; and previously presented at the AIAA/AAS Astrodynamics Conference, Boston, Massachusetts, August 11, 1998 (AIAA paper 98-4464)

[5] Domingo, V., et al. "The SOHO Mission: An Overview," Solar Physics, Vol. 162, No. 1-2, December 1995, pp. 1-37.

[6] Limon, M.; et al. (March 20, 2008) "Wilkinson Microwave Anisotropy Probe (WMAP): Five–Year Explanatory Supplement"

[7] Jonathan P. Gardner; et al. (November 2006). "The James Webb Space Telescope". *Space Science Reviews*. Springer, Netherlands.

[8] Farquhar, R.W.:1968, "The Control and Use of Libration-Point Satellites", Ph.D. Dissertation, Dept. of Aeronautics and Astronautics, Stanford University, Stanford, Calif., U.S.A.

[9] Mohammed A. Ghazy and Brett Newman, "Analytic Theory for High-Inclination Orbits in the Restricted Three-Body Problem," *Journal of Guidance, Control, and Dynamics ‘’,* Vol. 33, No. 2, March–April 2010

[10] Battin, R. H., "*An Introduction to the Mathematics and Methods of Astrodynamics* ", American Institute of Aeronautics and Astronautics, New York, 1987.

[11] Valtonen, M., and Karttunen, H., "The Three-Body Problem", Cambridge Univ. Press, Cambridge, England, U.K., 2006.

[12] Lundberg, J., Szebehely, V., Nerem, R. S., and Beal, B., "*Surfaces of Zero Velocity in the Restricted Problem of Three Bodies*," Celestial Mechanics, Vol. 36, No. 2, June 1985, pp. 191–205.doi:10.1007/BF0123065

[13] Schaub, H., and Junkins, J. L., "*Analytical Mechanics of Space Systems*", American Institute of Aeronautics and Astronautics, Reston, Virginia, 2005.

[14] MacMillan, W. D., "An Integrable Case in the Restricted Problem of Three Bodies," The Astronomical Journal, Vol. 27, No. 625–626, May 1911, pp. 11–13.

[15] Howell, K. C., "Three-Dimensional, Periodic, 'Halo' Orbits,"*Celestial Mechanics*, Vol. 32, No. 1, Jan. 1984, pp. 53–71. doi:10.1007/BF01358403

[16] Farquhar, R. W., and Kamel, A. A., *"Quasi-Periodic Orbits About the Translunar Libration Point*," Celestial Mechanics, Vol. 7, No. 4, 1973, pp. 458–473.doi:10.1007/BF01227511

[17] Barden, B. T., and Howell, K. C., "*Fundamental Motions Near Collinear Libration Points and Their Transitions*,"Journal of the Astronautical Sciences, Vol. 46, No. 4, Oct.–Dec. 1998, pp. 361–378.

[18] Richardson, D. L., "Analytic Construction of Periodic Orbits about the Collinear Points," Celestial Mechanics, Vol. 22, No. 3, Oct. 1980 pp. 241–253. doi:10.1007/BF01229511

[19] Sitnikov, K., "The *Existence of Oscillatory Motions in the Three-Body Problem*," Soviet Physics Doklady, Vol. 5, No. 4, Jan. 1961, pp. 647–650.

[20] Curtis, H., *"Orbital Mechanics for Engineering Students"*, Elsevier, Butterworth Heinman, 2005.

[21] Byrd, P.F., and Friedman, M.D., *"Handbook of Elliptic Integrals for Engineers and Scientists"*, Springer-Verlag Berlin Heidelberg New York, 1971

[22] Synge, J.L., and Griffith, B.A., *"Principles of Mechanics"*, Mc-Graw Hill Book Company, New York, 1949

[23] Howell, K. C., "*Families of Orbits in the Vicinity of the Collinear Libration Points*," Journal of the Astronautical Sciences, Vol. 49, No. 1, Jan.–March, 2001, pp. 107–125

VITA

Jay Shriram Suryawanshi graduated in 2013 with Bachelor of Technology degree in Production engineering from College of Engineering, Pune, India. In 2015, he was enrolled in the Aerospace engineering program to pursue his Master's degree in Frank Batten College of Engineering and Technology of the Old Dominion University, Norfolk, Virginia, USA. There he was awarded Graduate Teaching Assistantship in 2016. He is a student member of American Institute of Aeronautics and Astronautics (AIAA).